

T - 4081

Light Hydrocarbon Microseepage Mechanism(s):

Theoretical Considerations

By:

Mahyoub Saeed

T - 4081

A thesis submitted to the Faculty and the Board of Trustees of the Colorado School of Mines in partial fulfillment of the requirements for the degree of Doctor of Philosophy in Geochemistry.

Golden, Colorado

Date: Dec. 16, 1991

Signed: Mahyoub Saeed
Mahyoub A. Saeed

Approved: Ronald W. Klusman
Ronald Klusman
Thesis Advisor

Golden, Colorado

Date: Dec. 16, 1991

Stephen R. Daniel
Stephen R. Daniel
Head of Department

ABSTRACT

Surface geochemical exploration methods for petroleum are based essentially on the premise that light hydrocarbons migrate vertically from the subsurface reservoirs to the near-surface soils and sediments. During the last 60 years, many surface and near-surface techniques, based on vertical migration of light hydrocarbons, have been developed. Although the mechanism involved in moving light hydrocarbons from the surface petroleum accumulations to the near-surface is not yet clearly understood, the evidence is available which substantiates the concept that this movement does occur.

Since vertical migration of light hydrocarbons is a required fundamental mechanism of surface and near-surface exploration methods, it must be understood in order to fully utilize the strengths, and to realize the limitations of those methods. Up to the present time, few reports dealt with the measurement of the vertical migration rates due to the experimental barriers in determining such rates.

Two computer programs were designed that simulate the vertical migration of light hydrocarbons as a gas phase or in true solution. Migration as a gas phase or in true solution are the most likely of many proposed mechanisms to explain the light hydrocarbon migration. The equations used to model the light hydrocarbon transport in water or as a gas phase are solved using the finite-difference technique.

Both models have shown that overlying rock permeability is the most important

T - 4081

parameter in determining the rate of light hydrocarbon migration. The models demonstrate that light hydrocarbon concentrations change within the overlying rocks and are found to be pronounced near the reservoir and becomes smaller towards the surface. The models also demonstrate that at a specific depth, the hydrocarbon concentration increases with time.

For the transport of light hydrocarbons dissolved in water to be considered as a microseepage mechanism, a shallow reservoir and/or higher permeability of the overlying rock is required. The light hydrocarbon movement in water is a slow process compared to flow as a gas phase and requires a long period of time to reach the surface from a reservoir. By comparing the results from the two models with data from nature, it is found that the migration as a gas phase model is the most likely mechanism to account for light hydrocarbon microseepage. This model suggests transport rates sufficiently rapid to observe the disappearance of hydrocarbon anomalies above reservoirs undergoing production.

TABLE OF CONTENTS

ABSTRACT	iii
LIST OF FIGURES	vii
LIST OF TABLES	ix
ACKNOWLEDGEMENTS	x
1.0 INTRODUCTION	1
2.0 RESEARCH OBJECTIVES	7
3.0 GROUNDWATER AND LIGHT HYDROCARBON MIGRATION	8
3.1 Numerical Solution	14
3.1.1 The Implicit Method	14
3.1.2 Strongly Implicit Procedure (SIP)	16
3.2 Initial and Boundary Conditions	22
3.3 Assumptions in the Model	22
3.4 Computer Program	23
3.4.1 Input Parameters	24
4.0 RESULTS AND DISCUSSION FOR THE WATER TRANSPORT MODEL	38
5.0 CONCLUSIONS FROM PREVIOUS DATA	49
6.0 HYDROCARBON GASES - WATER FLOW IN POROUS MEDIA	50
6.1 Derivation of the Gas-water Flow in Porous Media	52
6.1.1 Mass Conservation	53
6.2 Relative Permeability and Capillary Pressure	55
6.3 Numerical Analysis	60
7.0 RESULTS AND DISCUSSION FOR THE TWO-PHASE FLOW MODEL	62
8.0 CONCLUSIONS FOR THE TWO-PHASE TRANSPORT MODEL	76

TABLE OF CONTENTS (cont.)

9.0	COMPARISON OF RESULTS FROM THE MODELS WITH DATA FROM NATURE	78
10.0	COMPARISON OF THE TWO MODELS	88
11.0	REFERENCES	90
12.0	APPENDIX 1 - Water Transport Computer Code	94
13.0	APPENDIX 2 - Two-phase Transport Computer Code	115
14.0	APPENDIX 3 - Equations.	126

LIST OF FIGURES

Fig. 1	Solubility of Normal Alkanes in Water	9
Fig. 2	Two-dimensional Centered-block, Finite-difference Block	15
Fig. 3	Part of Finite-Difference Grid Showing Nodes in X and Z Directions and X and Z Component Velocity	18
Fig. 4	Ethane Concentration vs. Time at Different Water Velocities	39
Fig. 5	Ethane Concentration vs. Depth (10,000 years)	40
Fig. 6	Concentration of Ethane, Methane, Butane vs. Depth at 10,000 Years . . .	41
Fig. 7	Ethane Concentration vs. Depth as a Function of Porosity at 10,000 Years	42
Fig. 8	Ethane Concentration vs. Depth at Constant Water Rate and Different Permeabilities	44
Fig. 9	Methane, Butane, n-Heptane and n-Decane Concentration vs. Depth . . .	46
Fig. 10	Methane, Ethane and n-Decane Concentration vs. Depth at 500,000 Years	47
Fig. 11	Ethane Mass vs. Time	48
Fig. 12	Threshold Displacement Pressure vs. Water Permeability	51
Fig. 13	Relative Permeability Curves for Water and Hydrocarbon Gas	54
Fig. 14	Hydrocarbon Gas Potential vs. Depth at 2, 5, 10 and 27 Years Permeability = 0.001 md	66
Fig. 15	Hydrocarbon Gas Potential vs. Depth at 2, 5, 10 and 27 Years Permeability = 0.0001 md	67
Fig. 16	Gas Potential vs. Permeability at 27, 54 and 273 Years at 100 Meters Above the Reservoir	68

Fig. 17 Hydrocarbon Gas Saturation vs. Time at 100 m Above the Reservoir . . .	69
Fig. 18 Hydrocarbon Gas Saturation vs. Depth Within the 100 m Interval Above the Reservoir, at 2, 5, 10 and 27 Years	70
Fig. 19 Hydrocarbon Gas Potential vs. Time as a Function of Reservoir Potential	72
Fig. 20 Hydrocarbon Gas Potential vs. Time Near Surface as a Function of Reservoir Potential	74
Fig. 21 Pressure Change at Surface vs. Time as a Function of Reservoir Pressure	75
Fig. 22 Ethane Plus Heavier Hydrocarbon Concentration at Hastings Field, Texas, 1946	79
Fig. 23 Ethane Plus Heavier Hydrocarbon Concentration at Hastings Field, Texas, 1968	80
Fig. 24 Chromatographic Distribution of C ₂ - C ₅ Hydrocarbons Through the Stratigraphic Section of the Kumdag Field	83
Fig. 25 C ₂ + Hydrocarbons vs. Depth	84
Fig. 26 Hydrocarbon Concentration vs. Depth at Rosenberg, Fort Bend Co., Texas (producing) and at Harris Co., Texas (dry)	85
Fig. 27 Gaseous Hydrocarbon Concentrations vs. Depth near Walvis Ridge	86
Fig. 28 Hydrocarbon (C ₂ - C ₅) Concentration in the Near-surface Interval of Plienbachian Shale	87

LIST OF TABLES

Table 1	Permeability of Porous Materials to Water	26
Table 2	Diffusion Coefficients In Water $DIF(cm^2s^{-1})$ at $25^\circ C$	27
Table 3	Solubility of Selected Hydrocarbon Compounds in Water at $25^\circ C$ in PPM (wt/wt)	28
Table 4	Input Data File for the Water Transport Model	29
Table 5	Output Data File for the Water Transport Model	30
Table 6	Methane, n-Butane, n-Hexane and n-Decane Concentration vs. Depth . .	45
Table 7	Input Parameters for Gas Migration Model	63
Table 8	Output Data File for the Two-phase Flow Model	65

ACKNOWLEDGEMENTS

I would like to acknowledge and express my gratitude to my advisor, Dr. Ronald Klusman, for his guidance and support throughout the study.

Sincere appreciation is also extended to Dr. Scott Cowley, Dr. Graham Closs, Dr. Kenneth Edwards and Prof. Donald Dickinson for serving on my committee.

Special thanks are also due to the staff of both the Department of Chemistry and Geochemistry and the CSM Computing Center for their assistance and help when I needed it.

Finally, I would like to thank my family for their continuous support, encouragement, patience and understanding throughout the study.

1.0 INTRODUCTION

Macroseeps of oil and gas have been widely used in prospecting and have resulted in the discovery of more oil and gas fields than any single method. With the development of modern sensitive analytical instrumentation and procedures of modern chemistry, it has become possible to detect minute amounts of microseepage and related alteration in near-surface soils. Surface geochemical exploration methods for petroleum are based essentially on the premise that light hydrocarbons migrate vertically from the subsurface reservoirs to the near-surface soils and sediments.

The earliest recorded literature on the measurement of the near-surface effects of vertical migration of petroleum constituents can be attributed to Laubmeyer (1933). He collected soil air from shallow boreholes that were sealed for a period of 24-48 hours and measured the total gas content. He found that near-surface soil samples contained more methane over producing areas than similar soil over non-producing areas. Sokolov and Mogilevski (1933a, b) pointed out in their soil analysis that a halo-like concentration of light hydrocarbons exists in the near-surface soils and sediments, which outlines the limits of underlying reservoirs. Rosaire (1938) and Horvitz (1939) have analyzed gases adsorbed by soils and found that a direct relationship exists between adsorbed soil hydrocarbons and the subsurface petroleum accumulations at depth.

During the last 60 years, many surface and near-surface techniques based on vertical migration have been developed . Some of these techniques have been shown to

be successful in detecting petroleum deposits and others have not shown success or have had limited success. These techniques may be classified as either direct or indirect. The direct methods involve exploration techniques dependent on measuring the actual presence of hydrocarbons in the near-surface soils derived from minute seepages of oil and/or gas, or measuring the physicochemical effects that seepage produces in the near-surface rocks and soils. The most important direct methods for geochemical analyses are:

1. Free hydrocarbon gases in soil
2. Adsorbed hydrocarbon gases in soil
3. Hydrocarbon gases dissolved in water
4. Bitumen (soil wax)

The indirect methods are based on the detection of any physical, chemical, or microbiological changes in the soils, waters, and surface rocks associated with the underlying petroleum accumulations or induced by the microseepage of hydrocarbons.

The most important indirect methods for detecting hydrocarbon reservoirs are:

1. Oxidation-reduction potential
2. Soil salt content (chloride, carbonate, sulfate, etc.)
3. Inorganic hydrochemicals (salts dissolved in water)
4. Microbiological (bacteria)
5. Geobotanical and biogeochemical

Although the mechanism involved in moving hydrocarbons from subsurface petroleum accumulations to the near-surface is not yet clearly understood, the evidence is available which substantiates the concept that this movement does occur. Some data and observations that represent some of this evidence are:

1. Hydrocarbon data from samples collected at depth have shown high concentrations of hydrocarbons.
2. Carbon isotope data from methane, obtained from near-surface samples located within a hydrocarbon anomaly over some fields, yield $^{13}\text{C}/^{12}\text{C}$ ratios which are almost identical to those of methane in the reservoir gas of the fields.
3. The composition of the light hydrocarbon fraction, in near-surface soil that is associated with an anomaly, is generally similar to that of the gas phase of the subsurface petroleum accumulation which the anomaly reflects (Jones and Drozd, 1983).
4. Light hydrocarbons desorbed from well cuttings from above the reservoir support the concept that hydrocarbons (HCS) leak from petroleum reservoirs.

Since vertical migration of light hydrocarbons is a required fundamental mechanism of all surface and near-surface exploration methods, it must be understood in order to utilize fully the strengths, and to realize the limitations of these methods.

Also, for the geochemical methods to be accepted in the petroleum industry, their basic principles and controlling parameters should be delineated. Such delineations have not occurred and the microseepage migration mechanism(s) are yet to be established. The understanding of the hydrocarbon microseepage mechanism(s) would allow better utilization of surface geochemical exploration methods and give them greater credibility.

Up to the present time, few reports dealt with the measurement of the vertical migration rate. This is because such measurement requires either the introduction of tracers into the reservoir and detection at the surface or artificial perturbation of the reservoir system and intensive monitoring at the near-surface over long periods of time.

It has been suggested that no simple explanation for vertical migration exists but it is a logical assumption that seeping gases migrate through the overlying sedimentary rocks by either one or a combination of seepage mechanisms.

The principal migration mechanisms proposed to explain light hydrocarbon microseepage are:

- I. Diffusion (Rosaire, 1940; Kartsev et al, 1959; Siegel, 1974; Donovan and Dalziel, 1977, Duchscherer, 1980, 1981a, b, 1983)
- II. Effusion (Rosaire, 1940; Kartsev et al, 1959; Donovan and Dalziel, 1977; and Duchscherer, 1981b, 1983)
- III. Vertical transport of light HCS dissolved in deep basinal water through capping rocks as a result of pressure (Pirson, 1960, 1963; Donovan and

Dalziel, 1977; Davidson, 1981; Duchscherer, 1981b, 1983; and Roberts, 1980)

Diffusion of gases, which is related to the tendency of petroleum accumulations to come to equilibrium, chemically and physically, with their surroundings, causes the flow of molecules from locations of high concentration in the reservoir to areas of low concentrations. The strongest arguments against diffusion are:

1. Diffusion is a spherically dispersive process, therefore, it cannot possibly account for the sharp surface outlines observed above hydrocarbon deposits.
2. Formation of "halo" anomalies is impossible.
3. Diffusion is far too slow to account for the rapid anomaly development and disappearance caused by changes in reservoir pressure (Hunt, 1984).
4. If diffusion were the migration mechanism responsible for hydrocarbon microseepage, surface anomalies would involve much greater concentration of C_6+ hydrocarbons than they do. However, slow diffusion of HCS through sediments and microfracture systems, over geologic time, is partly responsible for background surface hydrocarbon concentrations in petroleum-bearing sedimentary basins (Price, 1986).

Hunt (1979) has shown that appreciable vertical diffusion distances through shales can be achieved only over hundreds of millions of years, times far too long for relevance

to hydrocarbon microseepage. Smith et al. (1971) showed that it will take 140 million years for methane, 170 for ethane and 230 for propane to reach the surface by considering a reservoir depth of 1740 m and an average column porosity of 15.7%. Jones and Drozd (1983), on the basis of their studies, also suggest that diffusion is not a possible hydrocarbon microseepage mechanism.

Clearly, vertical diffusion from petroleum accumulations at depth is far too slow to account for the rapid anomaly development and/or disappearances caused by changes in reservoir pressure. However, diffusion of hydrocarbons through sediments and microfracture systems, slowly over geologic time is partly responsible for establishing background surface hydrocarbon concentration in the petroleum sedimentary basins.

Effusion of gases, taking place in accordance with Darcy's Law, depends on the difference between reservoir pressure and the pressure at the surface. The direction of effusive flow, therefore, is usually vertical because the vertical component is the shortest (Davidson, 1967). Such a mechanism would be useful if we consider the fact that fractures are small enough to transmit only the small molecules.

The vertical movement of low-molecular-weight hydrocarbons dissolved in water migrating through capping rocks has been proposed by many investigators as a possible mechanism for vertical migration of light hydrocarbons (Roberts, 1980).

2.0 RESEARCH OBJECTIVES

Two computer codes were designed to model light hydrocarbon migration from reservoirs to the near-surface soils. The codes model the flow of the hydrocarbons as a gas phase or in true solution. These are the most likely mechanisms, based on the previous discussion.

The codes are expected to produce data which will allow the determination of the most likely mechanism by which light hydrocarbons microseep from different reservoirs. They are also expected to determine the rates at which different light hydrocarbons can migrate from a reservoir of specified depth. The predicted concentration of the light hydrocarbons as a function of depth can also be obtained. The effect of overlying rock properties (permeability, porosity, etc.) on the rate of light hydrocarbons transport can be determined.

3.0 GROUNDWATER AND LIGHT HYDROCARBON MIGRATION

As discussed in the introduction, hydrocarbon gases may migrate primarily as a separate phase and/or may migrate in true solution. Upward movement of formation water in deep sedimentary basins has long been recognized as an important factor in geothermal heat flow and sedimentary mineral alteration (Jones, 1984). The most important function of a hydrocarbon trap is to leak water while retaining hydrocarbons (Roberts, 1980). The water can leak through the enclosing membrane and covering strata because of water saturation. It is evident that deep water discharge is an effective mechanism for the vertical migration of oil and gas (Jones, 1984).

Different investigators contend that hydrocarbon microseepage anomalies are due, at least in part, to vertical movement of deep-basin compaction waters, or driven by meteoric recharge water, moving through hydrocarbon reservoirs to the earth's surface (Pirson, 1960, 1963, 1964, 1969; Donovan and Dalziel, 1977; Roberts, 1980; and Davidson, 1982, 1984). Such waters are believed to carry hydrocarbons which result in the formation of hydrocarbon anomalies near the surface.

A marked decrease in solubility of normal alkanes with increasing molecular weight is shown in Fig. 1. The solubility of light hydrocarbon gases decreases with increasing temperature and salinity, and increases with increasing hydrocarbon pressure. It has also been documented that the solubility of gases in water is more dependent on pressure than temperature.

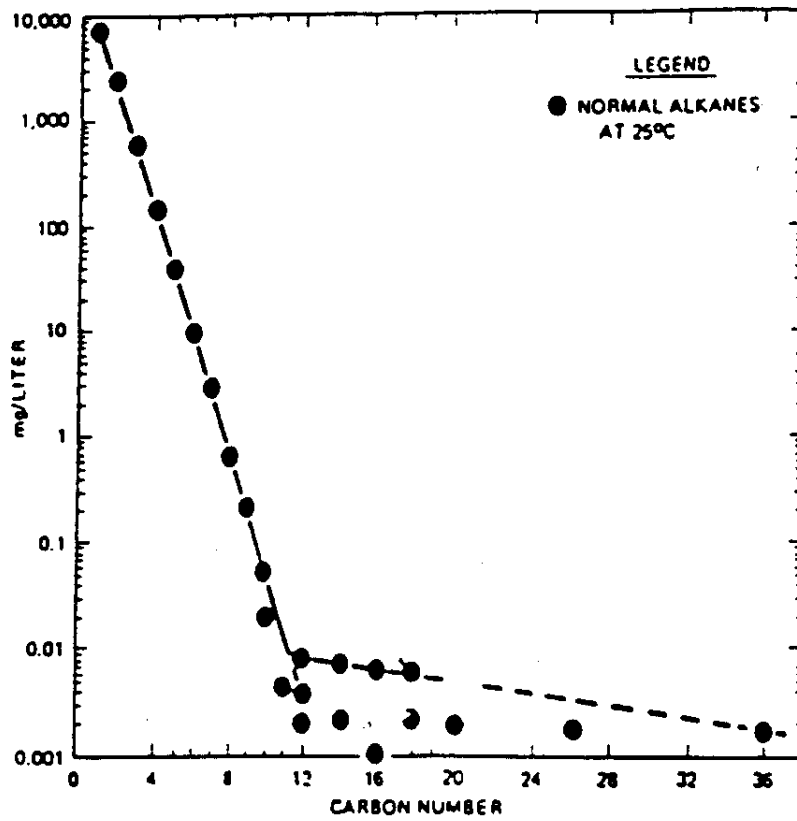


Fig. 1 Solubility of Normal Alkanes in Water
(from McAuliffe, 1978)

A relationship between depth and, in turn, pressure and gas solubility can be obtained from Henry's Law, which relates the pressure to gas solubility as follows:

$$C = K * P \quad (\text{Eq. 3.1})$$

$$C_o = K * P_o \quad (\text{Eq. 3.2})$$

Where:

K = Henry's constant, $\frac{\text{moles}/\ell}{\text{atm}}$

P = Pressure, atm

C = Concentration of gas in water, $\frac{\text{moles}}{\ell}$

P_o = Initial pressure, atm

C_o = Initial concentration of gas in water at P_o, $\frac{\text{moles}}{\ell}$

By combining the two equations we get:

$$C = \frac{C_o * P}{P_o} \quad (\text{Eq. 3.3})$$

Taking the initial pressure to be one atmosphere at a depth of 10 m at the surface of the water table and the pressure gradient of 1 atm/10 meters (≈ 0.5 psi/ft), the relationship between pressure and depth (ZL) in meters can be obtained as:

$$1 \text{ atm} \approx 10 \text{ m}$$

$$P \approx ZL$$

$$P = \frac{ZL}{10 \text{ m}}$$

$$P \approx \frac{ZL}{10} \text{ atm} \quad (\text{Eq. 3.4})$$

Substituting equation 3.4 into equation 3.3, we can get the following relationship between depth and gas solubility as a function of pressure:

$$C = \frac{C_o * ZL}{10} \quad (\text{Eq. 3.5})$$

The relationship in equation 3.5 is being used in the computer program which describes the migration of hydrocarbon gases in water.

The transport of hydrocarbon gas in water is influenced by both advection and hydrodynamic dispersion. Advection is a process by which gas is moving with the flowing water. Hydrodynamic dispersion is a process whereby gas molecules move in a direction different from that of the average ground water flow. Two mechanisms comprise the hydrodynamic dispersion phenomenon. These are mechanical dispersion, which is caused by variations in the water velocity as a result of the tortuous nature of the flow paths through porous media; and molecular diffusion, which results from variations in dissolved hydrocarbon gas concentrations. The dispersion coefficient (D_T) is then considered to be the sum of both the mechanical dispersion coefficient (D_1) and the molecular diffusion coefficient (D_2) (Bear, 1979).

$$D_T = D_1 + D_2 \quad (\text{Eq. 3.6})$$

The components of the two-dimensional hydrodynamic dispersion can be written as:

$$D_{T_{xx}} = \alpha_L \frac{V_x^2}{|V|} + \alpha_T \frac{V_z^2}{|V|} + D_2 \quad (\text{Eq. 3.7})$$

$$D_{T_{zz}} = \alpha_L \frac{V_z^2}{|V|} + \alpha_T \frac{V_x^2}{|V|} + D_2 \quad (\text{Eq. 3.8})$$

$$D_{T_{xz}} = D_{T_{zx}} = (\alpha_L - \alpha_T) V_x V_z / |V| \quad (\text{Eq. 3.9})$$

Where:

$D_{T_{xx}}, D_{T_{zz}}$ = total hydrodynamic dispersion in x, z direction, L^2/t

α_L = longitudinal dispersion (L)

α_T = transverse dispersion (T)

V_x, V_z = water velocity in both x and z directions, L/t

$|V|$ = the magnitude of the velocity, LT^{-1}

The assumption has been made that

$$D_{2_{xx}} = D_{2_{zz}} = D_2$$

and

$$D_{2xz} = D_{2zx} = 0$$

The flux of a single phase gas molecule due to advection and dispersion can be expressed as:

$$q_c = \epsilon (cV - D_T * \nabla c) \quad (\text{Eq. 3.10})$$

Where:

q_c = gas flux

V = Velocity of water, LT^{-1}

ϵ = Water content, L^3

D_T = Total dispersion coefficient, $L^2 t^{-1}$

c = The concentration of the dissolved gas, ML^{-3}

∇ = Del operator = $\frac{\partial}{\partial x} + \frac{\partial}{\partial z}$, L^{-1}

In the absence of chemical reaction and adsorption, the mass balance equation of the dissolved hydrocarbon gas will be reduced to:

$$\frac{\partial(\epsilon c)}{\partial t} = -\nabla * qc \quad (\text{Eq. 3.11})$$

Substituting 3.10 in Equation 3.11 yields the gas transport equation in water as shown in equation 3.12:

$$\frac{\partial \epsilon c}{\partial t} = \nabla \epsilon D_T * \nabla c - \nabla \epsilon \bar{V} c \quad (\text{Eq. 3.12})$$

This differential equation is solved by the computer program as described in later sections.

3.1 Numerical Solution

The solution of the two-dimensional differential equation 3.12 that describes hydrocarbon gas transport in water is obtained by using the finite difference numerical method. This method starts by a spatial discretization of the region of interest into a number of blocks by superimposing some type of a grid (Figure 2). Time is also discretized into a number of time steps during each of which the problem is solved to obtain new values of the unknown parameters. The partial differential equations are replaced by their finite difference equivalents. Central finite difference technique is used to approximate the unknown parameters at the center of the blocks. As a result of such approximations, the partial differential equation describing the hydrocarbon gas migration in water is replaced by a series of algebraic equations and then solved for the unknown parameters (Thomas, 1982).

3.1.1 The Implicit Method

Numerical methods for solving nonlinear partial differential equations consist of

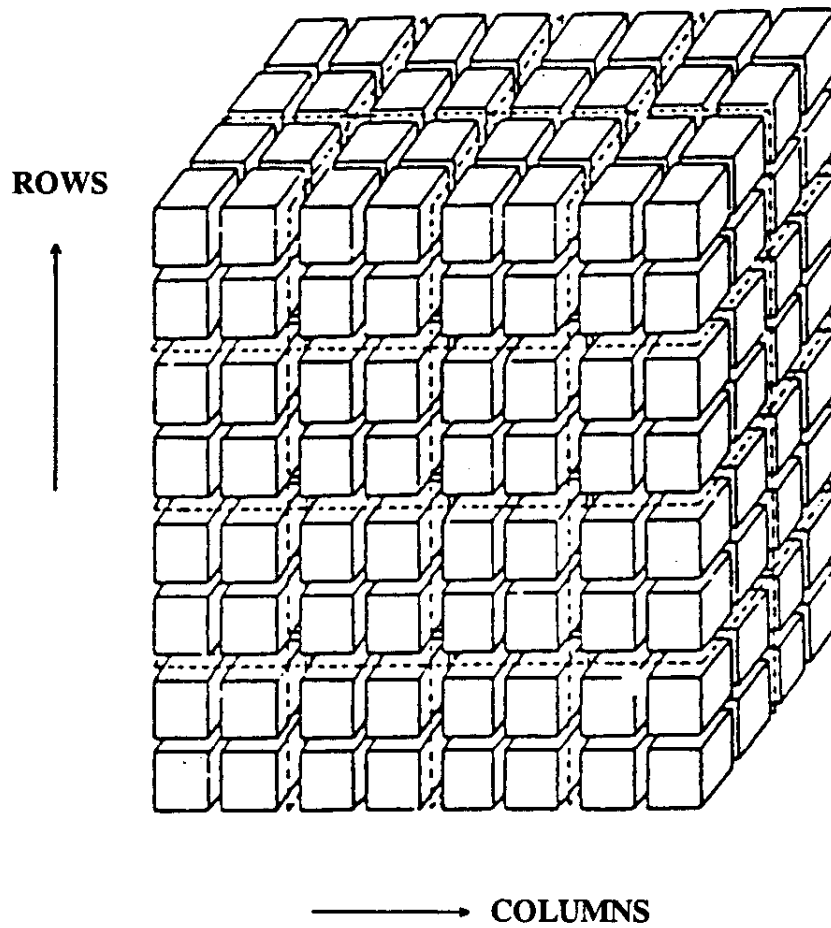


Fig. 2 Two-dimensional Centered-block, Finite-difference Block

various iterative schemes to estimate unknown values at advanced time levels. If the new values are calculated entirely on information from the previous time level, then the method is considered to be completely explicit. Time increments and block size restrictions are applied to this method. In a fully implicit scheme, the new unknown value is evaluated at the preceding time level (Carnahan, et al. 1969). The implicit method has an advantage over the explicit method in not having time increment and block size restrictions. The implicit method used to solve the transport equation in this computer program is the strongly implicit procedure (SIP).

3.1.2 Strongly Implicit Procedure (SIP)

The main purpose of the SIP method is to reduce a large number of simultaneous equations to more simply solved matrices by the elimination process working on a modified version of the original matrix system. The SIP has the advantage that iteration parameters can be more easily selected (Thomas, 1982).

Equation 3.12 can be written for each grid of volume v , within the solution domain as follows:

$$\int_v \frac{\partial(\epsilon c)}{\partial t} dv = \int_v \nabla * \epsilon D_T * \nabla c dv - \int_v \nabla * \epsilon \bar{V} c dv \quad (\text{Eq. 3.13})$$

By transforming the two volume integrals on the right-hand side to surface integrals using

Gauss divergence theorem (Thomas, 1982), we get:

$$\int_V \nabla * \epsilon D_T * \nabla c dv = \int_S \epsilon D_T * \nabla c * \bar{n} d\bar{s}$$

$$\int_V \nabla * \bar{V} \epsilon c dv = \int_S \bar{V} \epsilon c * \bar{n} d\bar{s}$$

where \bar{n} is the outward normal unit vector.

It is assumed that the volume, V , is small enough that within the block, its porosity, bulk density, and concentration can be considered constant, and then:

$$\int_V \partial \left(\frac{\epsilon c}{\partial t} \right) = v \frac{\partial \epsilon c}{\partial t}$$

we then have

$$v \frac{\partial(\epsilon c)}{\partial t} = \int_S \epsilon D_T * \nabla c * \bar{n} d\bar{s} - \int_S \bar{V} \epsilon c * \bar{n} d\bar{s} \quad (\text{Eq. 3.14})$$

The dispersive integral in equation 3.14 is approximated in two-dimensional flow by considering only four faces of the finite difference block (Fig. 3). We can write for the four faces:

$$\int_S \epsilon D_T * \nabla c * \bar{n} d\bar{s} = \sum_{t=1}^4 \int_{S_t} \epsilon D_T * \nabla c * \bar{n} * d\bar{S}_t$$

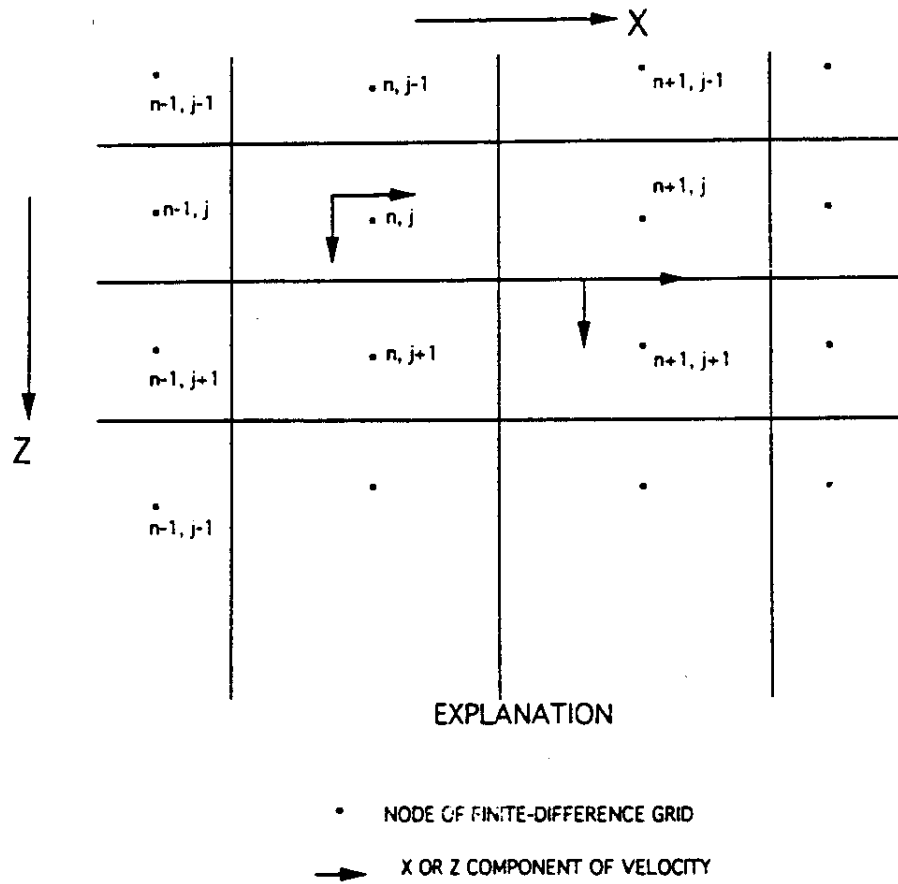


Fig. 3 Part of Finite-Difference Grid Showing Nodes in X and Z Directions and X and Z Component Velocity

$$\begin{aligned}
&= - \left[A\epsilon \left(D_{T_u} \frac{\partial c}{\partial x} + D_{T_u} \frac{\partial c}{\partial z} \right) \right]_{n - \frac{1}{2}, j} \\
&\quad + \left[A\epsilon \left(D_{T_u} \frac{\partial c}{\partial z} + D_{T_u} \frac{\partial c}{\partial x} \right) \right]_{n, j + \frac{1}{2}} \\
&\quad - \left[A\epsilon \left(D_{T_u} \frac{\partial c}{\partial z} + D_{T_u} \frac{\partial c}{\partial x} \right) \right]_{n, j - \frac{1}{2}} \\
&\quad + \left[A\epsilon \left(D_{T_u} \frac{\partial c}{\partial x} + D_{T_u} \frac{\partial c}{\partial z} \right) \right]_{n + \frac{1}{2}, j}
\end{aligned}$$

Where

ℓ = index to faces 4 block n,j

n = nodes in X direction

j = nodes in Z direction

$n \pm \frac{1}{2}, j \pm \frac{1}{2}$ = boundary facies of block n,j

A = surface area of cell face normal to flux direction

The following definitions should be considered in solving the gas transport equation in water:

$$\epsilon_{n-\frac{1}{2},j} = \frac{1}{2}(\epsilon_{n-1,j} + \epsilon_{n,j})$$

$$A_{n-\frac{1}{2},j} = A_{n+\frac{1}{2},j} = \Delta z_j$$

$$A_{n,j-\frac{1}{2}} = A_{n,j+\frac{1}{2}} = \Delta x_n$$

$$\frac{\partial c}{\partial x_{n-\frac{1}{2},j}} = \frac{c_{n,j} - c_{n-1,j}}{\frac{1}{2}(\Delta x_{n-1} + \Delta x_n)}$$

$$\frac{\partial c}{\partial z_{n-\frac{1}{2},j}} = \frac{1}{2} \left[\frac{c_{n,j+1} + c_{n-1,j+1} - c_{n,j-1} - c_{n-1,j-1}}{\Delta z_j + \frac{1}{2}(\Delta z_{j-1} + \Delta z_{j+1})} \right]$$

Spatial discretization of the advection component in Equation 3.14 is also accomplished by the central difference technique as follows:

$$\int_S \bar{V}_e c * \bar{n} * d\bar{s} = \sum_{\ell=1}^4 \int_{\ell} \bar{V}_e c * \bar{n} d\bar{s}$$

$$\approx -[A\epsilon V_x c]_{n-\frac{1}{2},j}$$

$$+[A\epsilon V_x c]_{n+\frac{1}{2},j}$$

$$-[A\epsilon V_z c]_{n,j-\frac{1}{2}}$$

$$+[A\epsilon V_z c]_{n,j+\frac{1}{2}} \quad \text{and}$$

$$V_{x_{n-1/2,j}} = \left[\frac{K}{\epsilon} \right]_{n-1/2,j} \frac{H_{n-1,j} - H_{n,j}}{\frac{1}{2}(\Delta x_n + \Delta x_{n-1})} \quad (\text{Eq. 3.15})$$

Where:

$V_{x_{n-1/2,j}}$ = velocity in X direction at $n - \frac{1}{2}$, +ve left to right

H = Total hydraulic head

K = Saturated hydraulic conductivity

The time derivative in Equation 3.14 is approximated by a fully implicit approximation written as:

$$\begin{aligned} \frac{\partial}{\partial t}(\epsilon c) &= c \frac{\partial \epsilon}{\partial t} + \epsilon \frac{\partial c}{\partial t} \\ &\approx c^{i+1/2} \frac{\epsilon^{i+1} - \epsilon^i}{\Delta t} + (\epsilon^{i+1/2}) \frac{c^{i+1/2} - c^i}{\Delta t} \end{aligned} \quad (\text{Eq. 3.16})$$

Where

- i = index for previous time step
- i+1 = index for current time step
- Δt = Length of the i+1 time step
- $c^{i+1/2}$ = c^{i+1}

$$\epsilon^{i+1/2} = \epsilon^{i+1}$$

The final finite-difference form for Equation 3.14 can now be written as:

$$A^{i+1}C_{n-1,j}^{i+1} + B^{i+1}C_{n,j-1}^{i+1} + C^{i+1}C_{n+1,j}^{i+1} + D^{i+1}C_{n,j+1}^{i+1} + D^{i+1}C_{n,j}^{i+1} = \text{RHS}$$

Where RHS is the right-hand side of the equation. The RHS approximations, definitions of above A, B, C & D symbols, as well as the remaining numerical equations are placed in the Appendix.

3.2 Initial and Boundary Conditions

In order to solve Equation 3.14, both initial and boundary conditions should be defined. The input boundary condition is described as a fixed concentration. A constant initial hydrocarbon gas concentration is entered as a constant value, C_o .

At the end of every time step, the mass flux into the system, as well as the change in mass stored in the system, is calculated. The total flux is the sum of both dispersion and advection fluxes.

3.3 Assumptions in the Model

Mathematical models are intended to replicate physical events with the laws of physics and applied mathematics. Unfortunately, our computational facilities and numerical analyses cannot solve many theoretical formulas without making simplifying

assumptions, which may compromise results. In addition, the theoretical equations that form the basis of a model often incorporate simplifications and assumptions because the actuality of the field situation is too complicated to describe with mathematical equations (Wang and Anderson, 1982).

Bacteria and other microorganisms can reduce the effective permeability of porous media (Singh, 1965). No allowance is made for any biological intervention. The flow is considered isothermal and independent of changes in ambient atmospheric pressure at the surface. Evaporation, as the fluid approaches the surface, is considered negligible. The model also assumes that hydrocarbon gases are non-reactive in the chemically reducing environment which exists in the sub-surface and that gradients of water density, viscosity and temperature do not affect the velocity distribution.

3.4 Computer Program

The computer program is written in Fortran and is operational on the VAX8600. The main routine of the program provides the instruction for reading the input data, select the printout requests and calls the subroutine that computes the new concentration at each successive new time step. The subroutine is a modified version of that documented by Healy (1990) which was used to describe solute flow in water. It was modified to account for vertical transport of the dissolved hydrocarbons in water by introducing some new input variables such as permeability and compressibility of the

overlying rocks. The solubility of light hydrocarbons in water at a specific depth (pressure) was also accounted for in the calculations. A complete program is listed in Appendix 1.

3.4.1 Input Parameters

A variety of input parameters were introduced to the computer model. These input parameters can be grouped into four categories. These are lithological data, water and hydrocarbon gas data, simulation data and numerical analysis parameters. The lithology data include rock permeabilities, rock compressibility and porosity. The selection of such values is based on values reported in the literature. Porosity is directly proportional to the rock grain size. Porosities of sandstone rock usually ranges from 5 to 30 per cent (Tissot, 1984). The porosity of carbonate rocks and shales is somewhat less than that of sandstone. The porosities of most hydrocarbon reservoirs are between 10 and 25 percent (Hagoort, 1988). Rock permeabilities to water are also selected on the basis of reported values from the literature. Permeability, k , is usually measured in cm^2 or in millidarcies (md) with the following relations:

$$1 \text{ cm/sec} = 1.02 \times 10^{-5} \text{cm}^2$$

$$1 \text{ md} = 9.8 \times 10^{-12} \text{cm}^2$$

Table 1 gives a summary of some values of rock permeability to water. The rock and water compressibility can be estimated by using Van der Knaap relation. This

relationship is shown in the subroutine called compressibility. The water and dissolved hydrocarbon gas data include water density, viscosity and diffusion coefficients. The simulation data include maximum simulation time, number of time increments and the number of columns and rows. The diffusion coefficients for the light hydrocarbons used in the computer program input data file were taken from Leythaeuser, et al., 1982, which are shown in Table 2. The solubilities of hydrocarbon in water at 25°C, which has been used as an input parameter, are shown in Table 3.

The upward water flux through the reservoir can be estimated by considering the permeability of the overlying rock directly above the reservoir. The estimated permeability is considered to be a very low value.

An example of an input data file with selected program variables definition is shown in Table 4. An output data file is shown in Table 5.

Table 1 Permeability of Porous Materials to Water*

Rock Type	Permeability (cm ²)
Soils, very fine sand	$8 \times 10^{-7} - 1 \times 10^{-12}$
Sandstone	$1 \times 10^{-10} - 1 \times 10^{-12}$
Shale	$1 \times 10^{-11} - 1 \times 10^{-14}$
Limestone and dolomite	$1 \times 10^{-12} - 1 \times 10^{-14}$
Breccia and granite	$1 \times 10^{-14} - 1 \times 10^{-16}$

* Modified from Bear and Veruijt (1987)

Table 2 Diffusion Coefficients In Water DIF(cm^2s^{-1}) at 25°C^*

CH_4	2.12×10^{-6}
C_2H_6	1.11×10^{-6}
C_3H_8	5.77×10^{-7}
n- C_4H_{10}	3.01×10^{-7}
iso- C_4H_{10}	3.75×10^{-7}
n- C_5H_{12}	1.57×10^{-7}
n- C_6H_{14}	8.20×10^{-8}
n- C_7H_{16}	4.31×10^{-8}
n- C_8H_{18}	1.00×10^{-8}
n- $\text{C}_{10}\text{H}_{22}$	6.08×10^{-9}

* (from Leythaeuser, 1982)

**Table 3 Solubility of Selected Hydrocarbon Compounds in Water
at 25°C in PPM (wt/wt)***

Methane	24.4 ± 1.0
Ethane	60.4 ± 1.3
Propane	62.4 ± 2.1
n-Butane	61.4 ± 2.6
Isobutane	48.9 ± 2.1
n-Pentane	38.5 ± 2.0
n-Hexane	9.5
n-Heptane	2.93 ± 0.2
n-Octane	0.66 ± 0.05

* (from McAuliffe, 1978)

Table 4 Input Data File for the Water Transport ModelOptions and Parameters

Maximum simulation time (Tmax in years)	1,000,000
Time increments (Delt in years)	100,000
Number of rows (Nrow)	100
Number of columns (Ncol)	3

Physical characteristics of overlying column and hydrocarbon gas

Column length (Depth in meters)	1000
Number of lithologies (Nlitho)	1
Lithology permeability (Perm. in cm ²)	1 X 10 ⁻⁸
Molecular diffusion (DIF in cm ² /sec)	1 X 10 ⁻⁶
Dispersion characteristic length (Alpha in cm)	10 ⁴
Overburden porosity (Poro)	0.2
Initial gas concentration (CI in g/cm ³)	0
Water flux rate (Wrate in cm/sec)	10 ⁻¹⁰

Table 5 Output Data File for the Water Transport Model

RESERVOIR DEPTH = 1000.00 METERS
 SIMULATION TIME = 1000000.0000 YEARS
 NUMBER OF ROWS = 100
 NUMBER OF COLUMNS = 3

LITHOLOGY # 1

PERMEABILITY= 1.0E-8 CM2

ETHANE CONCENTRATION (PPM)

Depth (m)	Time = 100,00 years	Time = 300,000 years	Time = 500,000 years
1000	5.94E+03	5.94E+03	5.94E+03
985	3.41E+03	4.77E+03	5.10E+03
975	1.96E+03	4.05E+03	4.40E+03
965	1.12E+03	3.25E+03	3.66E+03
955	6.46E+02	2.44E+03	2.97E+03
945	3.71E+02	1.73E+03	2.36E+03
935	2.13E+02	1.17E+03	1.84E+03
925	1.22E+02	7.72E+02	1.40E+03
915	7.02E+01	4.95E+02	1.04E+03
905	4.03E+01	3.11E+02	7.50E+02
895	2.31E+01	1.92E+02	5.29E+02
885	1.33E+01	1.17E+02	3.64E+02
875	7.63E+00	7.09E+01	2.45E+02
865	4.38E+00	4.24E+01	1.62E+02
855	2.52E+00	2.52E+01	1.06E+02
845	1.44E+00	1.49E+01	6.79E+01
835	8.30E-01	8.77E+00	4.30E+01
825	4.76E-01	5.14E+00	2.69E+01
815	2.74E-01	3.00E+00	1.67E+01
805	1.57E-01	1.75E+00	1.03E+01
795	9.02E-02	1.01E+00	6.26E+00
785	5.18E-02	5.88E-01	3.79E+00
775	2.98E-02	3.41E-01	2.28E+00
765	1.71E-02	1.97E-01	1.36E+00
755	9.82E-03	1.14E-01	8.11E-01
745	5.64E-03	6.56E-02	4.81E-01

Table 5 Output Data File (cont.)

Depth (m)	Time = 100,00 years	Time = 300,000 years	Time = 500,000 years
735	3.24E-03	3.78E-02	2.84E-01
725	1.86E-03	2.18E-02	1.67E-01
715	1.07E-03	1.25E-02	9.80E-02
705	6.14E-04	7.22E-03	5.74E-02
695	3.52E-04	4.16E-03	3.35E-02
685	2.02E-04	2.39E-03	1.95E-02
675	1.16E-04	1.37E-03	1.13E-02
665	6.68E-05	7.90E-04	6.59E-03
655	3.84E-05	4.54E-04	3.82E-03
645	2.20E-05	2.61E-04	2.21E-03
635	1.27E-05	1.50E-04	1.28E-03
625	7.27E-06	8.62E-05	7.39E-04
615	4.18E-06	4.95E-05	4.27E-04
605	2.40E-06	2.85E-05	2.46E-04
595	1.38E-06	1.64E-05	1.42E-04
585	7.92E-07	9.40E-06	8.18E-05
575	4.55E-07	5.40E-06	4.71E-05
565	2.61E-07	3.10E-06	2.71E-05
555	1.50E-07	1.78E-06	1.56E-05
545	8.63E-08	1.02E-06	8.99E-06
535	4.96E-08	5.88E-07	5.17E-06
525	2.85E-08	3.38E-07	2.97E-06
515	1.64E-08	1.94E-07	1.71E-06
505	9.40E-09	1.12E-07	9.83E-07
495	5.40E-09	6.41E-08	5.65E-07
485	3.10E-09	3.68E-08	3.25E-07
475	1.78E-09	2.12E-08	1.87E-07
465	1.02E-09	1.22E-08	1.07E-07
455	5.89E-10	6.98E-09	6.17E-08
445	3.38E-10	4.01E-09	3.55E-08
435	1.94E-10	2.31E-09	2.04E-08
425	1.12E-10	1.32E-09	1.17E-08
415	6.42E-11	7.61E-10	6.73E-09
405	3.69E-11	4.37E-10	3.87E-09
395	2.12E-11	2.51E-10	2.22E-09
385	1.22E-11	1.44E-10	1.28E-09
375	7.00E-12	8.30E-11	7.33E-10
365	4.02E-12	4.77E-11	4.21E-10
355	2.31E-12	2.74E-11	2.42E-10
345	1.33E-12	1.57E-11	1.39E-10
335	7.63E-13	9.05E-12	7.99E-11
325	4.39E-13	5.20E-12	4.59E-11
315	2.52E-13	2.99E-12	2.64E-11
305	1.45E-13	1.72E-12	1.52E-11

Table 5 Output Data File (cont.)

Depth (m)	Time = 100,00 years	Time = 300,000 years	Time = 500,000 years
295	8.33E-14	9.87E-13	8.71E-12
285	4.79E-14	5.67E-13	5.01E-12
275	2.75E-14	3.26E-13	2.88E-12
265	1.58E-14	1.87E-13	1.65E-12
255	9.09E-15	1.08E-13	9.50E-13
245	5.22E-15	6.19E-14	5.46E-13
235	3.00E-15	3.56E-14	3.14E-13
225	1.73E-15	2.04E-14	1.80E-13
215	9.92E-16	1.17E-14	1.04E-13
205	5.70E-16	6.75E-15	5.96E-14
195	3.28E-16	3.88E-15	3.42E-14
185	1.89E-16	2.23E-15	1.97E-14
175	1.09E-16	1.28E-15	1.13E-14
165	6.23E-17	7.37E-16	6.50E-15
155	3.58E-17	4.24E-16	3.73E-15
145	2.06E-17	2.43E-16	2.15E-15
135	1.18E-17	1.40E-16	1.23E-15
125	6.80E-18	8.05E-17	7.09E-16
115	3.91E-18	4.63E-17	4.07E-16
105	2.25E-18	2.66E-17	2.34E-16
95	1.29E-18	1.53E-17	1.35E-16
85	7.43E-19	8.79E-18	7.74E-17
75	4.28E-19	5.06E-18	4.46E-17
65	2.47E-19	2.92E-18	2.57E-17
55	1.44E-19	1.70E-18	1.50E-17
45	8.63E-20	1.02E-18	8.98E-18
35	5.55E-20	6.57E-19	5.78E-18
25	4.22E-20	5.00E-19	4.40E-18

Table 5 Output Data File for the Water Transport Model (cont.)

Depth (m)	Time = 600,00 years	Time = 700,000 years	Time = 800,000 years
1000	5.94E+03	5.94E+03	5.94E+03
	5.24E+03	5.24E+03	5.31E+03
985	4.47E+03	4.60E+03	4.66E+03
975	3.81E+03	3.95E+03	4.06E+03
965	3.18E+03	3.34E+03	3.48E+03
955	2.60E+03	2.78E+03	2.94E+03
945	2.08E+03	2.28E+03	2.46E+03
935	1.63E+03	1.84E+03	2.02E+03
925	1.26E+03	1.46E+03	1.63E+03
915	9.51E+02	1.13E+03	1.30E+03
905	7.03E+02	8.68E+02	1.02E+03
895	5.09E+02	6.53E+02	7.92E+02
885	3.61E+02	4.82E+02	6.03E+02
875	2.52E+02	3.50E+02	4.51E+02
865	1.72E+02	2.49E+02	3.33E+02
855	1.16E+02	1.75E+02	2.42E+02
845	7.66E+01	1.21E+02	1.73E+02
835	5.00E+01	8.21E+01	1.22E+02
825	3.23E+01	5.51E+01	8.50E+01
815	2.06E+01	3.65E+01	5.83E+01
805	1.30E+01	2.39E+01	3.95E+01
795	8.11E+00	1.54E+01	2.65E+01
785	5.02E+00	9.89E+00	1.75E+01
775	3.09E+00	6.27E+00	1.15E+01
765	1.89E+00	3.94E+00	7.44E+00
755	1.14E+00	2.46E+00	4.78E+00
745	6.91E-01	1.52E+00	3.04E+00
735	4.15E-01	9.37E-01	1.92E+00
725	2.48E-01	5.73E-01	1.21E+00
715	1.47E-01	3.48E-01	7.51E-01
705	8.73E-02	2.10E-01	4.65E-01
695	5.16E-02	1.27E-01	2.86E-01
685	3.04E-02	7.58E-02	1.75E-01
675	1.78E-02	4.53E-02	1.06E-01
665	1.04E-02	2.69E-02	6.44E-02
655	6.11E-03	1.59E-02	3.88E-02
645	3.56E-03	9.41E-03	2.33E-02
635	2.07E-03	5.54E-03	1.39E-02
625	1.21E-03	3.26E-03	8.30E-03
615	7.00E-04	1.91E-03	4.93E-03
605	4.06E-04	1.12E-03	2.92E-03
595	2.35E-04	6.52E-04	1.72E-03
585	1.36E-04	3.80E-04	1.01E-03
575	7.86E-05	2.21E-04	5.96E-04
565		1.29E-04	3.50E-04

Table 5 Output Data File (cont.)

Depth (m)	Time = 600,00 years	Time = 700,000 years	Time = 800,000 years
555	4.54E-05	1.29E-04	3.30E-04
545	2.62E-05	7.46E-05	2.05E-04
535	1.51E-05	4.32E-05	1.20E-04
525	8.71E-06	2.50E-05	6.97E-05
515	5.02E-06	1.45E-05	4.06E-05
505	2.89E-06	8.37E-06	2.36E-05
495	1.67E-06	4.84E-06	1.37E-05
485	9.59E-07	2.79E-06	7.96E-06
475	5.52E-07	1.61E-06	4.61E-06
465	3.17E-07	9.29E-07	2.67E-06
455	1.83E-07	5.35E-07	1.54E-06
445	1.05E-07	3.08E-07	8.93E-07
435	6.04E-08	1.78E-07	5.16E-07
425	3.47E-08	1.02E-07	2.98E-07
415	2.00E-08	5.89E-08	1.72E-07
405	1.15E-08	3.39E-08	9.91E-08
395	6.59E-09	1.95E-08	5.71E-08
385	3.79E-09	1.12E-08	3.29E-08
375	2.18E-09	6.45E-09	1.90E-08
365	1.25E-09	3.71E-09	1.09E-08
355	7.19E-10	2.13E-09	6.28E-09
345	4.13E-10	1.23E-09	3.62E-09
335	2.38E-10	7.04E-10	2.08E-09
325	1.36E-10	4.05E-10	1.20E-09
315	7.84E-11	2.33E-10	6.89E-10
305	4.51E-11	1.34E-10	3.96E-10
295	2.59E-11	7.69E-11	2.28E-10
285	1.49E-11	4.42E-11	1.31E-10
275	8.55E-12	2.54E-11	7.53E-11
265	4.91E-12	1.46E-11	4.33E-11
255	2.82E-12	8.39E-12	2.49E-11
245	1.62E-12	4.82E-12	1.43E-11
235	9.32E-13	2.77E-12	8.22E-12
225	5.36E-13	1.59E-12	4.72E-12
215	3.08E-13	9.14E-13	2.71E-12
205	1.77E-13	5.26E-13	1.56E-12
195	1.02E-13	3.02E-13	8.97E-13
185	5.84E-14	1.74E-13	5.15E-13
175	3.36E-14	9.97E-14	2.96E-13
165	1.93E-14	5.73E-14	1.70E-13
155	1.11E-14	3.29E-14	9.78E-14
145	6.37E-15	1.89E-14	5.62E-14
135	3.66E-15	1.09E-14	3.23E-14
125	2.10E-15	6.25E-15	1.86E-14
115	1.21E-15	3.59E-15	1.07E-14

Table 5 Output Data File (cont.)

Depth (m)	Time = 600,00 years	Time = 700,000 years	Time = 800,000 years
105	6.95E-16	2.06E-15	6.13E-15
95	4.00E-16	1.19E-15	3.52E-15
85	2.30E-16	6.82E-16	2.03E-15
75	1.32E-16	3.93E-16	1.17E-15
65	7.64E-17	2.27E-16	6.73E-16
55	4.45E-17	1.32E-16	3.92E-16
45	2.66E-17	7.91E-17	2.35E-16
35	1.71E-17	5.09E-17	1.51E-16
25	1.30E-17	3.87E-17	1.15E-16

Table 5 Output Data File for the Water Transport Model (cont.)

Depth (m)	Time = 900,000 years	Time = 1,000,000 years
1000	5.94E+03	5.94E+03
985	5.33E+03	5.37E+03
975	4.74E+03	4.79E+03
965	4.15E+03	4.24E+03
955	3.60E+03	3.71E+03
945	3.08E+03	3.21E+03
935	2.61E+03	2.74E+03
925	2.18E+03	2.32E+03
915	1.79E+03	1.94E+03
905	1.46E+03	1.60E+03
895	1.17E+03	1.30E+03
885	9.24E+02	1.05E+03
875	7.21E+02	8.35E+02
865	5.54E+02	6.56E+02
855	4.20E+02	5.09E+02
845	3.14E+02	3.89E+02
835	2.32E+02	2.94E+02
825	1.69E+02	2.20E+02
815	1.21E+02	1.62E+02
805	8.57E+01	1.18E+02
795	6.00E+01	8.49E+01
785	4.14E+01	6.03E+01
775	2.83E+01	4.24E+01
765	1.91E+01	2.95E+01
755	1.28E+01	2.03E+01
745	8.46E+00	1.38E+01
735	5.54E+00	9.29E+00
725	3.60E+00	6.20E+00
715	2.32E+00	4.10E+00
705	1.48E+00	2.69E+00
695	9.40E-01	1.75E+00
685	5.92E-01	1.13E+00
675	3.70E-01	7.24E-01
665	2.30E-01	4.60E-01
655	1.42E-01	2.91E-01
645	8.75E-02	1.83E-01
635	5.35E-02	1.14E-01
625	3.26E-02	7.08E-02
615	1.97E-02	4.38E-02
605	1.19E-02	2.69E-02
595	7.17E-03	1.64E-02
585	4.29E-03	1.00E-02
575	2.56E-03	6.08E-03
565	1.53E-03	3.67E-03
555	9.05E-04	2.21E-03

Table 5 Output Data File (cont.)

Depth (m)	Time = 900,000 years	Time = 1,000,000 years
545	5.36E-04	1.33E-03
535	3.16E-04	7.93E-04
525	1.86E-04	4.73E-04
515	1.09E-04	2.81E-04
505	6.42E-05	1.67E-04
495	3.76E-05	9.85E-05
485	2.20E-05	5.81E-05
475	1.28E-05	3.42E-05
465	7.46E-06	2.01E-05
455	4.34E-06	1.18E-05
445	2.52E-06	6.91E-06
435	1.47E-06	4.04E-06
425	8.50E-07	2.36E-06
415	4.92E-07	1.37E-06
405	2.85E-07	8.00E-07
395	1.65E-07	4.65E-07
385	9.53E-08	2.70E-07
375	5.50E-08	1.57E-07
365	3.18E-08	9.08E-08
355	1.83E-08	5.26E-08
345	1.06E-08	3.04E-08
335	6.10E-09	1.76E-08
325	3.51E-09	1.02E-08
315	2.02E-09	5.88E-09
305	1.17E-09	3.39E-09
295	6.71E-10	1.96E-09
285	3.86E-10	1.13E-09
275	2.22E-10	6.51E-10
265	1.28E-10	3.75E-10
255	7.36E-11	2.16E-10
245	4.23E-11	1.24E-10
235	2.43E-11	7.17E-11
225	1.40E-11	4.13E-11
215	8.05E-12	2.37E-11
205	4.63E-12	1.37E-11
195	2.66E-12	7.86E-12
185	1.53E-12	4.52E-12
175	8.79E-13	2.60E-12
165	5.05E-13	1.50E-12
155	2.90E-13	8.60E-13
145	1.67E-13	4.94E-13
135	9.59E-14	2.84E-13
125	5.51E-14	1.63E-13
115	3.17E-14	9.39E-14
105	1.82E-14	5.40E-14
95	1.05E-14	3.10E-14
85	6.02E-15	1.79E-14
75	3.46E-15	1.03E-14
65	2.00E-15	5.93E-15
55	1.16E-15	3.46E-15
45	6.97E-16	2.07E-15
35	4.48E-16	1.33E-15
25	3.41E-16	1.01E-15

4.0 RESULTS AND DISCUSSION FOR THE WATER TRANSPORT MODEL

A great variety of techniques have been developed to extract and subsequently analyze light hydrocarbons from rock samples. Basically, all of them use gas chromatography (Tissot, 1984). Over the past years, the gas chromatography (for separating HC compounds) coupled with the hydrogen-flame ionization detector (for measuring concentration of hydrocarbon) has been developed. The concentration of light hydrocarbons can be measured to a detection limit of parts per billion (ppb). The detection limit is of relevance in the discussion of subsequent figures.

Figure 4 shows the relationship between time and ethane concentration as a function of vertical water velocity. It is clear the vertical water velocity plays an important role in moving the hydrocarbon gas to a shallower depth. A relationship between depth and ethane concentration as a function of reservoir depth is shown in Figure 5. In 10,000 years, ethane is able to reach the surface from a 500 m deep reservoir while that from a 1000 m reservoir reaches only a depth of 500 m in that same time. Figure 6 shows the relationship between methane, ethane and butane concentrations and depth. It shows that the concentration of heavier hydrocarbons increases with depth. Ethane concentration vs. depth at different porosities is shown in Figure 7. Not much difference has been noticed between the results at porosity 0.5 and 0.05.

A relationship between depth and ethane concentration at different rock

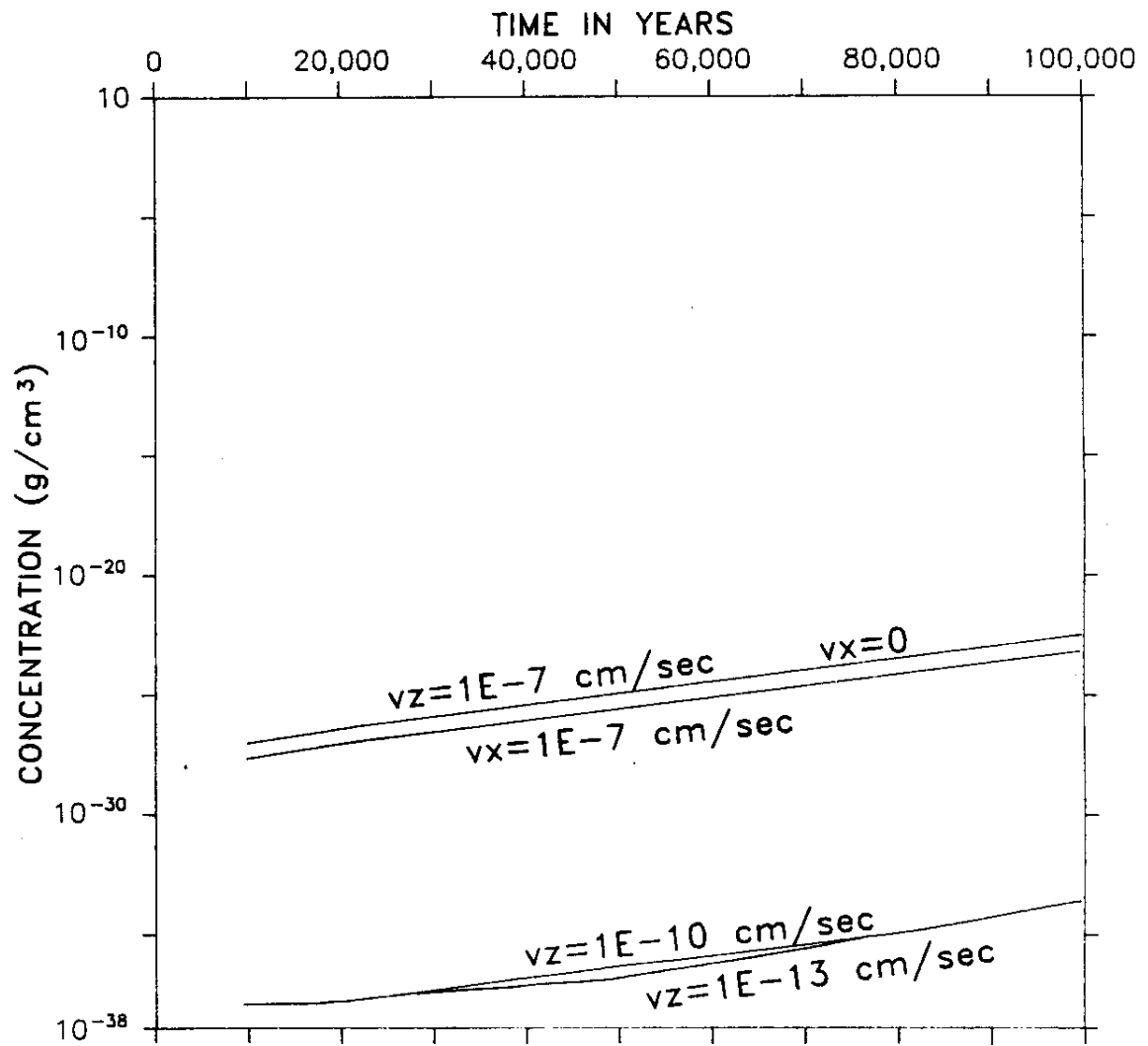


Fig. 4 Ethane Concentration vs. Time at Different Water Velocities

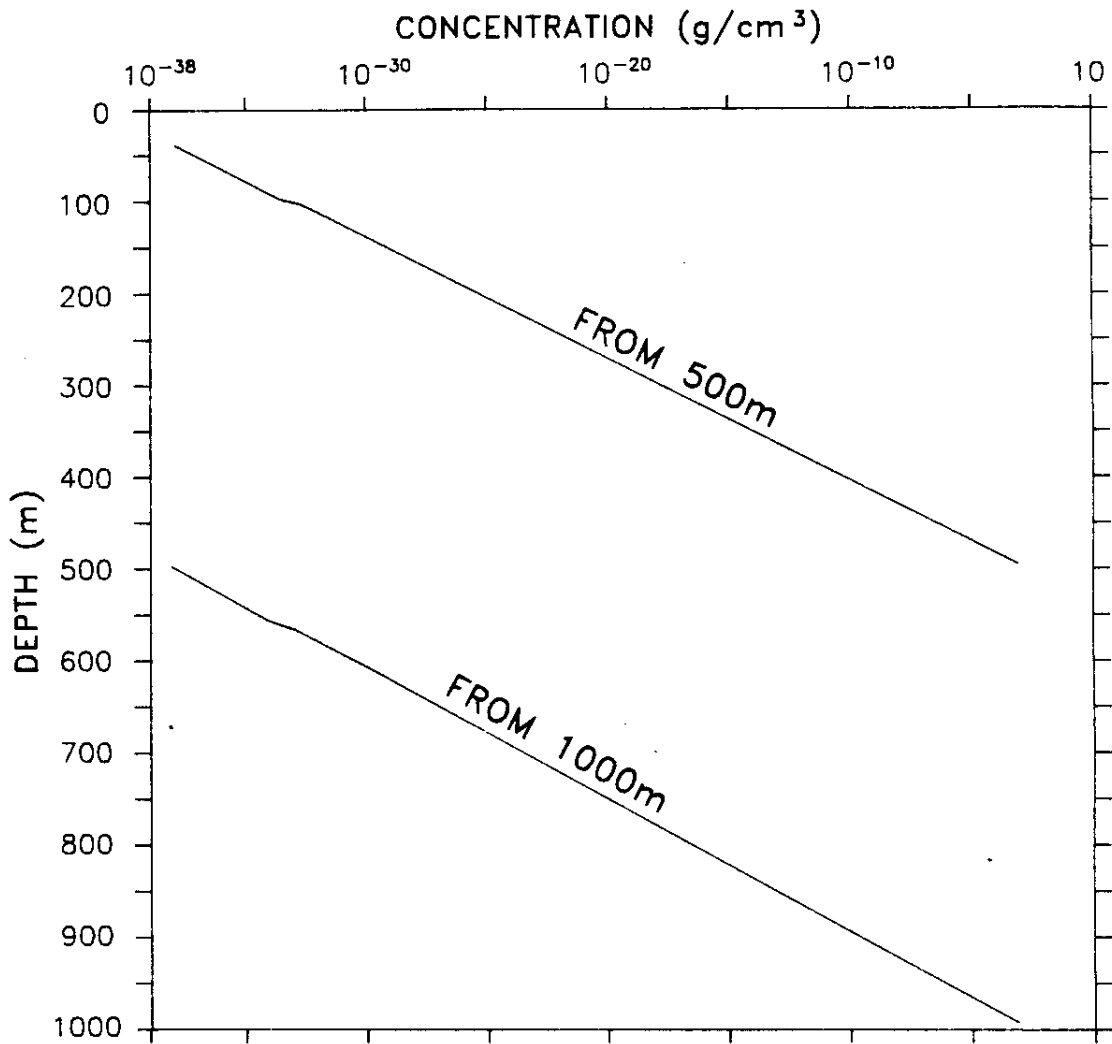


Fig. 5 Ethane Concentration vs. Depth (10,000 years)

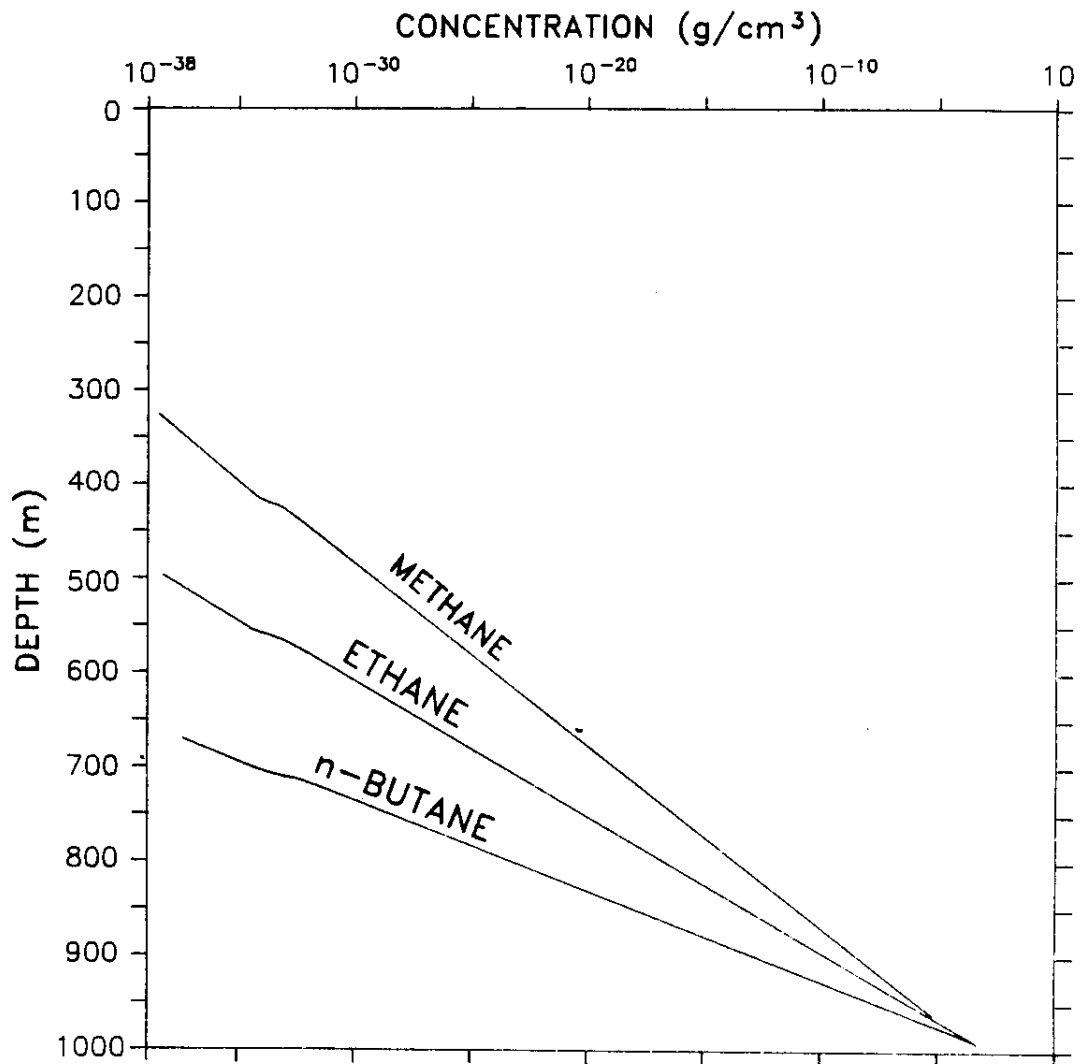
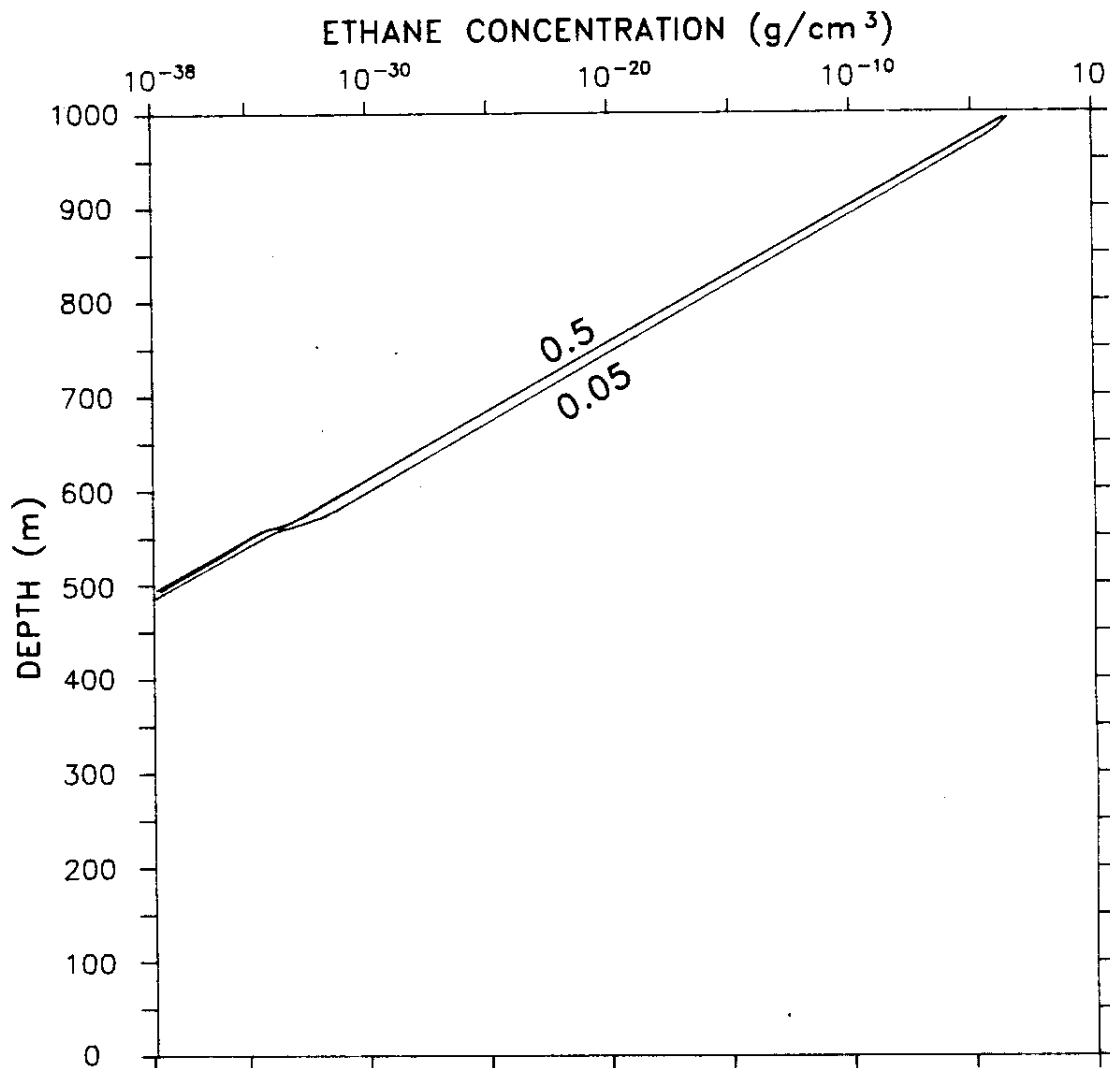


Fig. 6 Concentration of Ethane, Methane, Butane vs. Depth at 10,000 Years



**Fig. 7 Ethane Concentration vs. Depth
as a Function of Porosity at 10,000 Years**

permeabilities are also shown in Figure 8. It is evident that higher permeability is required for a hydrocarbon gas to reach the near-surface in a measurable amount in a short time.

Table 6 shows the concentration of the methane, n-butane, n-hexane and n-decane as a function of depth after 10,000 years of simulated migration. It can be seen from the table that lighter hydrocarbons travel faster than heavier ones (Fig. 9). It can also be seen that with depth, the concentration of the different hydrocarbons increases. At a specific depth, the concentration of hydrocarbons decreases with increasing molecular weight. As an example, at a depth of 945 m the methane concentration is about 5,000 times n-butane after 10,000 years.

Figure 10 shows the relationship between depth and hydrocarbon concentrations at 500,000 years, assuming 3 lithologies of different permeabilities and thicknesses. These are 200 m with a permeability of $1 \times 10^{12} \text{ cm}^2$, 400 m with a permeability of $1 \times 10^8 \text{ cm}^2$, and 400 m with a permeability of $1 \times 10^6 \text{ cm}^2$. It is clear that lighter hydrocarbons (methane and ethane) reach a shallower depth in detectable amounts while heavier hydrocarbons (n-decane) reach only deeper depths.

The mass of a gas reaching the surface can also be calculated. Ethane mass is also plotted against time in Figure 11. Ethane mass, which is brought to the surface, is increasing with increasing time starting with small changes and then increasing with time in a non-linear relationship.

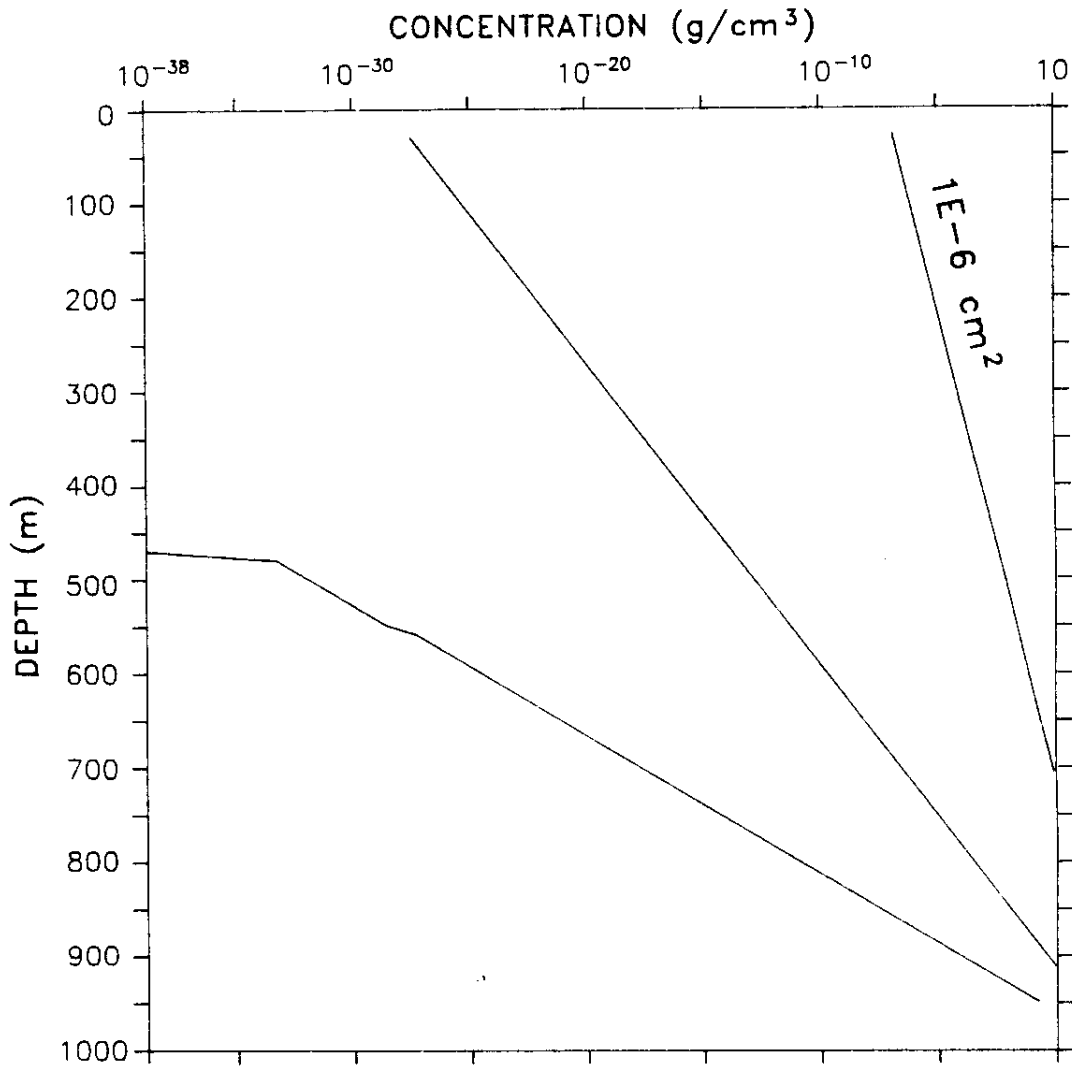


Fig. 8 Ethane Concentration vs. Depth at Constant Water Rate and Different Permeabilities
Permeability = $1E-6$, $1E-8$, $1E-10 \text{ cm}^2$, Water Rate = $1E-10 \text{ cm/sec}$

Table 6 Methane, n-Butane, n-Hexane and n-Decane Concentration vs. Depth

Depth (m)	Methane (ppm)	n-Butane (ppm)	n-Hexane (ppm)	n-Decane (ppm)
1000	1.00E+06	1.00E+06	1.00E+06	1.00E+06
985	3.87E+05	9.03E+04	2.59E+04	2.07E+03
975	1.01E+05	4.35E+03	3.42E+02	2.15E+00
965	1.97E+04	1.43E+02	3.05E+00	1.52E-03
955	3.05E+03	3.60E+00	2.08E-02	8.28E-07
945	3.91E+02	7.44E-02	1.16E-04	3.75E-10
935	4.34E+01	1.32E-03	5.54E-07	1.49E-13
925	4.27E+00	2.06E-05	2.35E-09	5.40E-17
915	3.82E-01	2.93E-07	9.03E-12	1.85E-20
905	3.14E-02	3.84E-09	3.21E-14	6.21E-24
895	2.42E-03	4.72E-11	1.07E-16	2.09E-27
885	1.76E-04	5.50E-13	3.41E-19	3.97E-32
875	1.23E-05	6.13E-15	1.04E-21	0.00E+00
865	8.24E-07	6.59E-17	3.09E-24	0.00E+00
855	5.36E-08	6.90E-19	8.91E-27	0.00E+00
845	3.40E-09	7.05E-21	2.44E-29	0.00E+00
835	2.11E-10	7.08E-23	4.39E-33	0.00E+00
825	1.29E-11	7.01E-25	0.00E+00	0.00E+00
815	7.80E-13	6.87E-27	0.00E+00	0.00E+00
805	4.67E-14	6.58E-29	0.00E+00	0.00E+00
795	2.77E-15	2.42E-31	0.00E+00	0.00E+00
785	1.64E-16	0.00E+00	0.00E+00	0.00E+00
775	9.69E-18	0.00E+00	0.00E+00	0.00E+00
765	5.71E-19	0.00E+00	0.00E+00	0.00E+00
755	3.36E-20	0.00E+00	0.00E+00	0.00E+00
745	1.98E-21	0.00E+00	0.00E+00	0.00E+00
735	1.17E-22	0.00E+00	0.00E+00	0.00E+00
725	6.93E-24	0.00E+00	0.00E+00	0.00E+00
715	4.11E-25	0.00E+00	0.00E+00	0.00E+00
705	2.44E-26	0.00E+00	0.00E+00	0.00E+00
695	1.45E-27	0.00E+00	0.00E+00	0.00E+00
685	8.65E-29	0.00E+00	0.00E+00	0.00E+00
675	4.97E-30	0.00E+00	0.00E+00	0.00E+00
665	1.04E-31	0.00E+00	0.00E+00	0.00E+00
655	0.00E+00	0.00E+00	0.00E+00	0.00E+00
645	0.00E+00	0.00E+00	0.00E+00	0.00E+00

of Lithology = 1, Permeability = $1 \times 10^{-10} \text{ cm}^2$,
 Water Rate = $1 \times 10^{-10} \text{ cm/sec}$, Time = 10,000 years

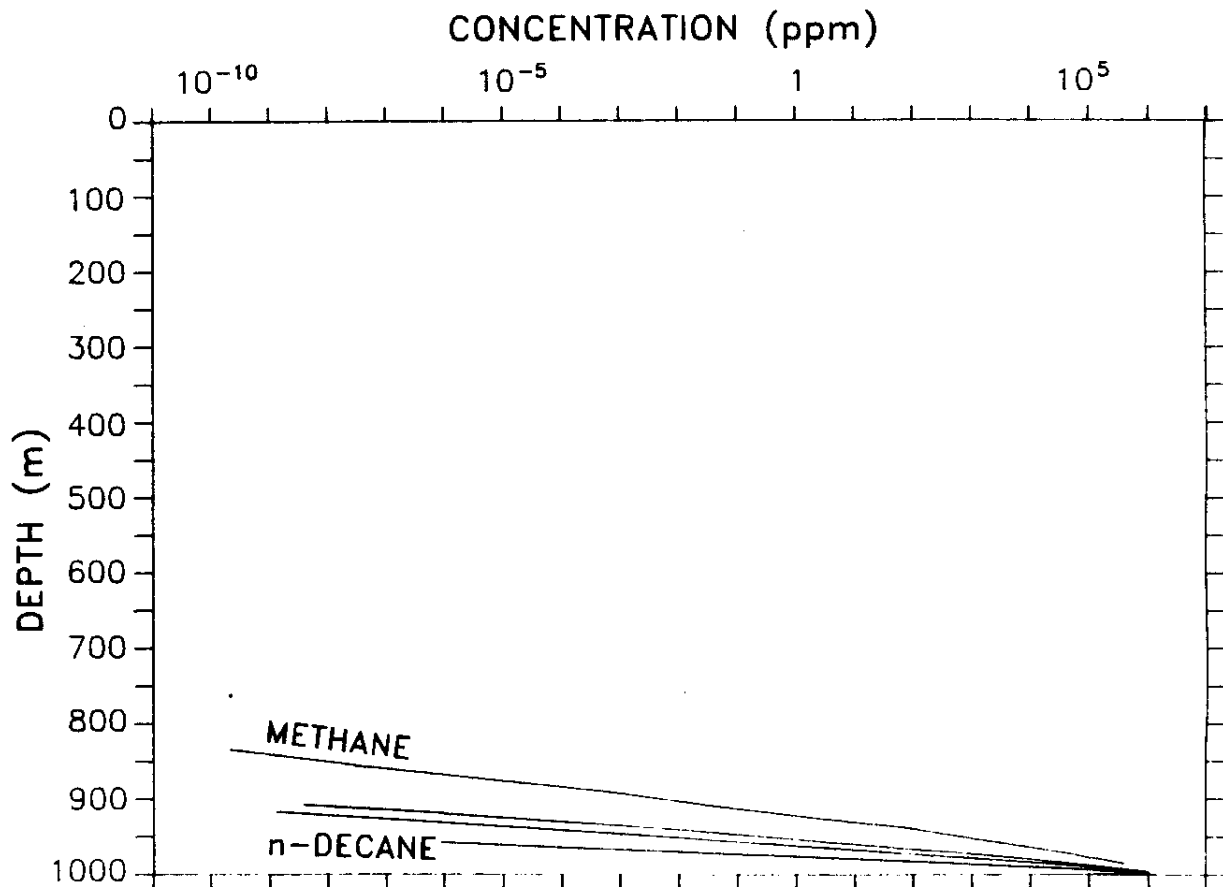


Fig. 9 Methane, Butane, n-Heptane and n-Decane Concentration vs. Depth
#Lithology=1, Permeability= 1×10^{-12} cm², Water Rate= 1×10^{-10} cm/sec,
Time=10,000 years

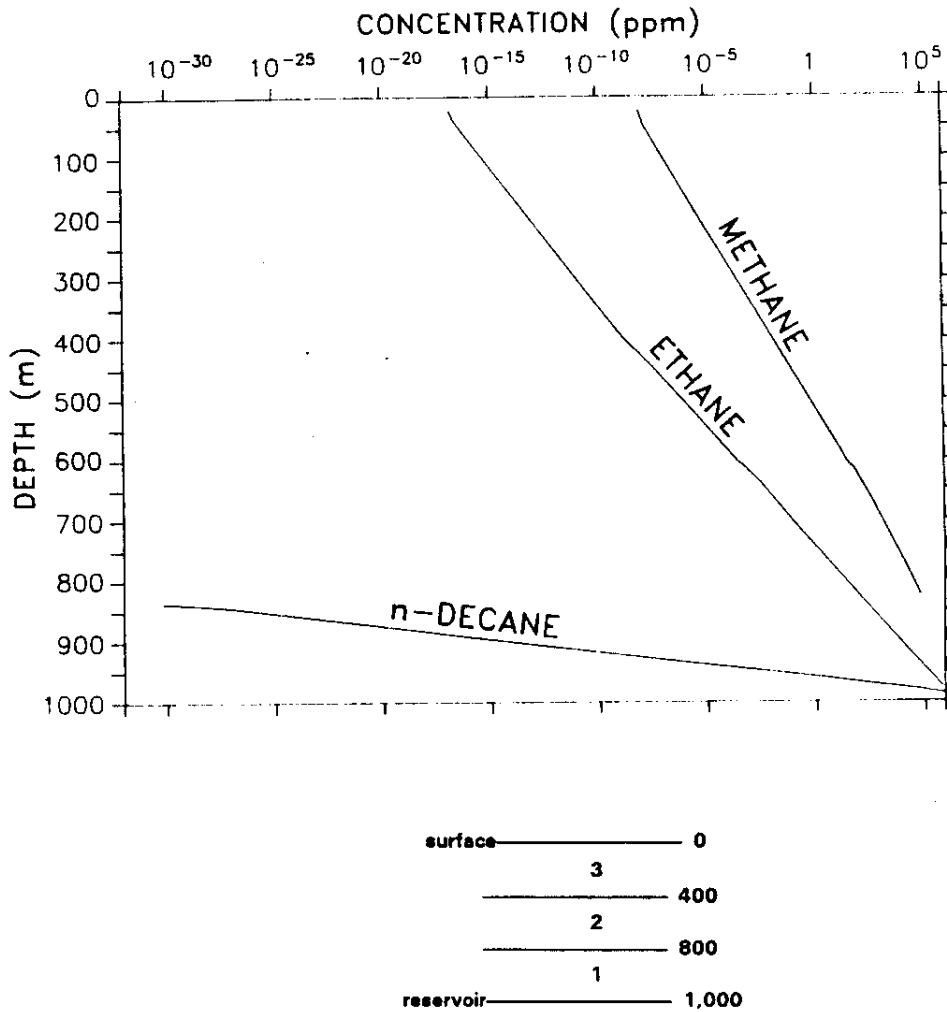


Fig. 10 Methane, Ethane and n-Decane Concentration vs. Depth at 500,000 Years

#Lithology=3, Permeabilities=(1 X 10⁻¹² cm², thickness=200 m), (1 X 10⁻⁸ cm², thickness=400 m), (1 X 10⁻⁶ cm², thickness=400 m), Water Rate=1 X 10⁷ cm/sec

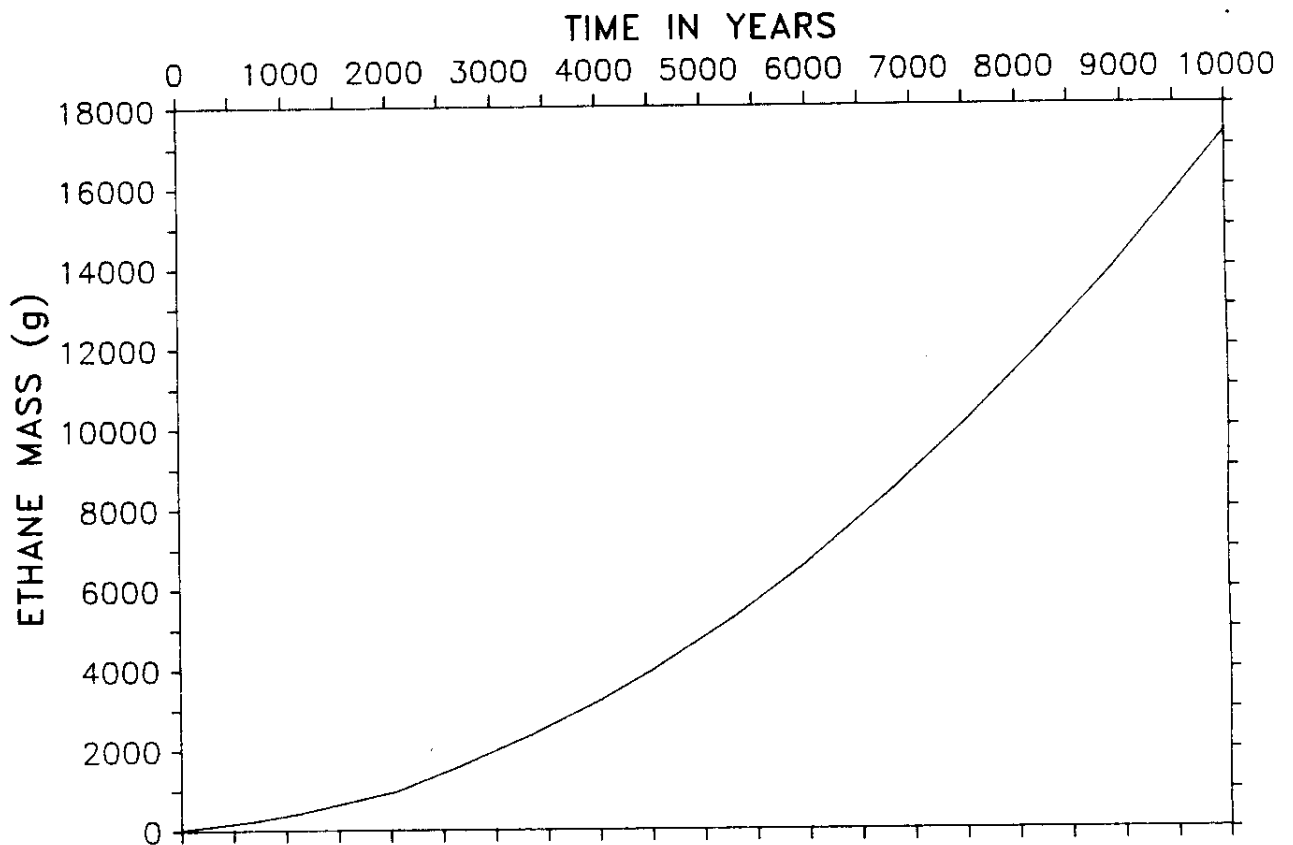


Fig. 11 Ethane Mass vs. Time, Water rate = 1×10^{-8} cm/sec
from an area of 100^2 m²

5.0 CONCLUSIONS FROM PREVIOUS DATA

From the previous discussion the conclusions that can be drawn are as follows:

1. Permeability is the most important factor in determining the rate of migration of hydrocarbon gas dissolved in water.
2. Reservoir depth is also another important factor to be considered if the microseepage mechanism is as a hydrocarbon gas dissolved in water. Shallower reservoir depths and/or higher permeability are required for the hydrocarbon gas to reach the surface in detectable amounts in a short time.
3. An average permeability in the range of 10^{-8} - 10^{-6} cm² are necessary for getting the hydrocarbon gas to the near-surface at detectable amounts from a relatively shallow reservoir.
4. Hydrocarbon concentrations increase with depth when approaching a reservoir.
5. At a specific depth, the concentration of hydrocarbons decreases with increasing molecular weight.
6. Lighter hydrocarbons move vertically faster than heavier ones.

6.0 HYDROCARBON GASES - WATER FLOW IN POROUS MEDIA

The rocks located above the oil and/or gas reservoirs are considered to be of great importance for the retention of hydrocarbons within the structural boundaries of the reservoir. If overpressure conditions are sustained in the reservoir, the possibility of gas leaking through the overlying rocks exists (Tek et al, 1966).

The hydrocarbon gas leakage through the overlying rocks may be attributed to either one of the following:

1. Exceeding the threshold pressure of the overlying rocks.
2. Mechanically fracturing the overlying rocks due to excessive overpressure.
3. By fractures extending through and across the overlying rocks as a result of the drilling processes.

The threshold pressure is the pressure required for gas to start moving water or displacing water out of the water saturated rocks. The presence of water prevents gas flow since surface forces prevent gas from displacing the water. The ability of a rock to contain gas is expressed in terms of its threshold pressure (Thomas, 1967). If the capillary pressure (i.e., pressure difference between gas and water) becomes equal to or greater than displacement pressure (threshold pressure) the hydrocarbons can enter the pore spaces of the cap rock and flow through it. A negative relationship is found between the rock's displacement pressure and their water permeability, as shown in Figure 12.

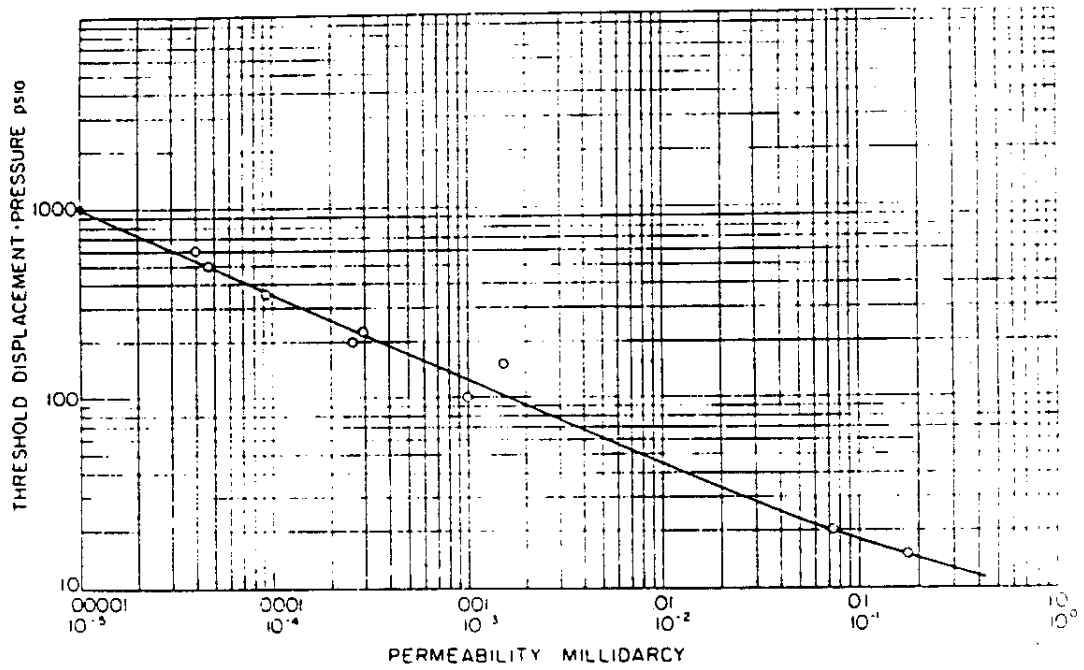


**Fig. 12 Threshold Displacement Pressure vs. Water Permeability
(from Katz and Coats, 1968)**

6.1 Derivation of the Gas-water Flow in Porous Media

As described in the previous section, a certain displacement pressure, dictated by capillary forces within the overlying rock must be attained before the gas starts to displace water. At the displacement pressure, gas will start displacing water from permeable channels within the overlying rock and thus establish communication with the more porous and permeable formations above. Some questions need to be answered, which include:

- a) Will the hydrocarbon gas displace water from the overlying rock?
- b) How far vertically will the hydrocarbon gas reach?
- c) How much hydrocarbon gas will be accumulated at a specific depth or distance above the reservoir?

The basic equations describing hydrocarbon gas and water flow in porous media are the continuity equations for each phase. For both gas and water, Darcy's law is proportional to the potential gradient of each phase (Tek et al, 1966).

$$\vec{V}_w = -K \frac{K_w}{\mu_w} \nabla * \phi_w \quad (\text{Eq. 6.1})$$

$$\vec{V}_g = -K \frac{K_g}{\mu_g} \nabla * \phi_g \quad (\text{Eq. 6.2})$$

where:

\vec{V}_g = velocity of gas

\vec{V}_w = velocity of water

K = rock permeability

K_g, K_w = relative permeability of gas and water

μ_g = gas viscosity

μ_w = water viscosity

ϕ_g = gas potential, $\phi_g = P + \rho gh$

ϕ_w = water potential, $\phi_w = P + \rho gh$

∇ = $\text{del} \left(\frac{\partial}{\partial x}, \frac{\partial}{\partial y}, \frac{\partial}{\partial z} \right)$

The relative permeabilities of both gas (K_g), and water (K_w) will depend on the water saturation (Figure 13). The relative permeability of gas increases with decreasing water saturation.

6.1.1 Mass Conservation

The rate of accumulation per unit volume of a medium equals the net rate of influx into that volume:

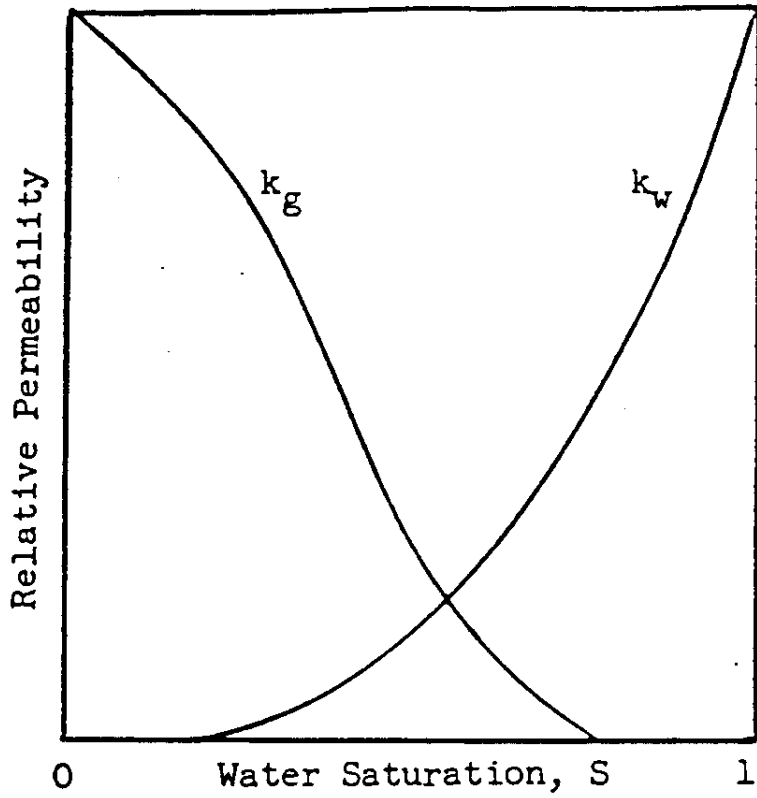


Fig. 13 Relative Permeability Curves for Water and Hydrocarbon Gas

$$\epsilon \frac{\partial S_w}{\partial t} = \nabla K \frac{K_w}{\mu_w} \nabla \phi_w \quad (\text{Eq. 6.3})$$

$$\epsilon \frac{\partial S_g}{\partial t} = -\nabla V_g + q_g = \nabla K \frac{k_g}{\mu_g} \nabla \phi_g + q_g \quad (\text{Eq. 6.4})$$

where

- ϵ = average porosity of the overlying rocks (dimensionless)
- μ_g = viscosity (cp)
- μ_w = water viscosity (cp)
- q_w = the rate of flow of water
- q_g = the rate of flow of gas

6.2 Relative Permeability and Capillary Pressure

When more than one fluid phase is present, the transport properties of porous media are modified both because the effective permeability for each phase depends on the saturation of that phase and because there is a saturation-dependent difference in the effective pressures for each phase.

The hydrocarbon gas saturation (S_g) is related to the water saturation by the following:

$$S_g = 1 - S_w$$

The relative permeabilities of both water K_w and gas K_g , can be obtained from Corey (1954) relationships as follows:

$$K_w = S_w^4$$

$$K_g = (1 - S_w)^2$$

The pressure in the gas phase exceeds that in the water by the capillary pressure (P_c).

$$P_c = P_g - P_w = \phi_g - \phi_w + (\rho_w - \rho_g)gh \quad (\text{Eq. 6.5})$$

where:

g = acceleration gravity, ML^{-2}

h = elevation, L

The relationship between capillary pressure and water saturation as well as the capillary pressure changes with time can be obtained by using the chain rule as follows:

$$\frac{\partial s}{\partial t} = \frac{\partial s}{\partial P_c} * \frac{\partial P_c}{\partial t} \quad (\text{Eq. 6.6})$$

$$P_c = P_g - P_w = \phi_g - \phi_w + (\rho_w - \rho_g)gh,$$

$$\frac{\partial P_c}{\partial t} = \frac{\partial(\phi_g - \phi_w)}{\partial t} \quad (\text{Eq. 6.7})$$

From the previous discussion, the following simultaneous non-linear partial differential equations of both gas and water potentials as dependent variable can be

obtained:

$$\nabla K \frac{K_g}{\mu_g} \nabla \phi_g + q_g = -\epsilon \frac{\partial s}{\partial P_c} \left[\frac{\partial \phi_g}{\partial t} - \frac{\partial \phi_w}{\partial t} \right] \quad (\text{Eq. 6.8})$$

$$\nabla K \frac{k_w}{\mu_w} \nabla \phi_w + q_w = \epsilon \frac{\partial s}{\partial P_c} \left[\frac{\partial \phi_g}{\partial t} - \frac{\partial \phi_w}{\partial t} \right] \quad (\text{Eq. 6.9})$$

To solve these transport equations, both initial and boundary conditions need to be specified. Both initial water and gas potentials are considered to be constant and uniform throughout the overlying rocks. From those initial potentials and also from the displacement pressure, the initial water and gas saturations as well as the relative permeability of each phase will be determined.

The gas potential on the lower surface and both gas and water potentials on the upper surface should be specified at

$$\begin{aligned} X=0 \quad \phi_g &= \phi_{gt} & \phi_{wt} &= \text{Initial water potential} \\ X=L \quad \phi_g &= \phi_{gt} & \phi_{gt} &= \text{Initial gas potential} \\ X=L \quad \phi_w &= \phi_{wt} & & \text{where } L = \text{reservoir depth} \end{aligned}$$

In this model, flow of water across the lower boundary of the overlying rocks is considered to be negligible.

To satisfy the mass balance condition, the total rate of flow of both gas and water should be zero as:

$$q_{g0} + q_{gl} + q_{wl} = 0 \quad (6.10)$$

The transport equations 6.8 and 6.9, can be written in terms of dimensionless quantities using the following definitions:

$$t = \frac{tK\phi_w l}{l^2 \epsilon \mu_w}$$

$$X = \frac{X}{L}$$

$$Q_w = \frac{q_w L^2 \mu_w}{K\phi_{wt}} \quad (\text{Eq. 6.11})$$

$$Q_s = \frac{q_s L^2 \mu_w}{K\phi_{wt}}$$

$$\Phi_w = \frac{\phi_w}{\phi_{wt}}$$

$$\Phi_s = \frac{\phi_s}{\phi_{wt}}$$

$$PC = \frac{PC}{\phi_{wt}} \quad (\text{Eq. 6.12})$$

where:

- t = dimensionless time
 x = dimensionless distance
 Q_w = water potential
 Q_g = dimensionless gas potential
 P_c = dimensionless capillary pressure

In terms of the dimensionless quantities equation 6.8 and 6.9 may be written in the following dimensionless forms as:

$$\frac{\partial}{\partial X} K_w \frac{\partial \phi_w}{\partial X} = \frac{\partial S}{\partial P_c} \left[\frac{\partial \phi_g}{\partial t} - \frac{\partial \phi_w}{\partial t} \right] \quad (\text{Eq. 6.13})$$

$$\frac{\partial}{\partial X} K_g \frac{\partial \phi_g}{\partial X} = - \frac{\partial S}{\partial P_c} \frac{\mu_g}{\mu_w} \left[\frac{\partial \phi_g}{\partial t} - \frac{\partial \phi_w}{\partial t} \right] \quad (\text{Eq. 6.14})$$

Some new terms are introduced which are required by the numerical technique method, which are:

$$P = [\Phi_s + \Phi_w]/2$$

$$R = [\Phi_s - \Phi_w]/2$$

$$E = \frac{\mu_w K_s}{\mu_g} + K_w \quad (\text{Eq. 6.15})$$

$$F = \frac{\mu_w K_s}{\mu_g} - K_w$$

By substituting in equations 6.8 and 6.9 equation 6.16 and 6.17 which will be solved by the computer code can be obtained:

$$\frac{\partial}{\partial X} F \frac{\partial P}{\partial X} + \frac{\partial}{\partial X} E \frac{\partial R}{\partial X} + Q_s - Q_w = -4S \frac{\partial R}{\partial t} \quad (\text{Eq. 6.16})$$

$$\frac{\partial}{\partial X} E \frac{\partial P}{\partial X} + \frac{\partial}{\partial X} F \frac{\partial R}{\partial X} + Q_s + Q_w = 0 \quad (\text{Eq. 6.17})$$

6.3 Numerical Analysis

The solution to the differential equations 6.16 and 6.17 requires that both initial and boundary conditions be specified. To solve those non-linear partial differential equations, either analytical or numerical methods can be used. These transport equations

are too complex to be solved analytically. Numerical methods are more adaptable to solving such equations (Crichlow, 1977).

In this model, the numerical method used is the finite difference method. It is used because of its successful applications in reservoir engineering and also because it can be solved more easily by a computer compared to other numerical techniques, such as, the finite element method. The partial differential equations are approximated by their finite-difference equivalent using the "leap-frog" approach. The advantage of using the "leap-frog" technique is that substantially less time is required to arrive at a solution. The basis of the technique is to eliminate one of the two unknowns and thus reducing the computing time by introducing two new independent variables and two functions. These are the P, R, E & F shown in previous equations.

The finite difference approximations of equations 6.16 and 6.17 are

$$\Delta E^m \Delta R^{m+1} + \Delta F^m \Delta P^{m+1} + Q_g^m - Q_w^m = -\frac{4\Phi S}{\Delta t} [R_{ijk}^{m+1} - R_{ijk}^m] \quad (\text{Eq. 6.18})$$

$$\Delta E^m \Delta P^{m+1} + \Delta F^m \Delta R^m + Q_w^m + Q_g^m = 0 \quad (\text{Eq. 6.19})$$

where $m, m+1 =$ time levels. Equation 6.17 is used to determine P at the $(m+1)$ time level using known values of R, E, and F from the previous level. Then P^{m+1} is used in equation 6.16 to solve for the remaining unknown R^{m+1} .

7.0 RESULTS AND DISCUSSION FOR THE TWO-PHASE FLOW MODEL

The computer program used to describe the movement of the hydrocarbons in the gas phase through the overlying rocks is written in Fortran and is operational on the VAX8600. The original code which solves the finite difference equations for both water and hydrocarbon gas transport is obtained from Tek, et al. (1966). A number of modifications were made to account for vertical transport of hydrocarbon gas mixture. A complete listing of the modified code is attached in Appendix 2. An example of an input data file, with selected program variable definitions, is shown in Table 7.

The input parameters are composed of overlying rock properties (porosity and permeability), which are taken to be the weighted average of all the overlying rocks by considering the rock type percentage and their respective porosity and permeability. The hydrocarbon gas properties are determined in this program by first calculating the gas mixture (C_1 - C_6) mass and then applying different known relations in calculating hydrocarbon gas viscosity at specified temperature and pressure. The other parameters including reservoir depth, grid block size, time steps, maximum simulation times as well as initial and boundary condition data are also used as input parameters.

The expected results from the displacement program are that the water saturation of the overlying rocks decreases with time since the water is displaced by hydrocarbon gas. The water saturation decrease should be high near the hydrocarbon gas reservoir and decrease with increasing distance above the reservoir. At the same time, the gas

Table 7 Input Parameters for Gas Migration Model

Reservoir depth (meters)	1,000
Simulation time (years)	27
No. of overburden layers	1
Reservoir gas potential (psi)	3,000
Layer permeability (md)	0.001
Porosity	0.1

saturation should increase with time and such increase should be high near the hydrocarbon gas reservoir.

Table 8 shows an output data file using the input data parameters in Table 7. It shows that gas potential at a specific depth increases with time. A plot of such data is shown in Figure 14. It can also be seen from the graph that the change in gas potential is small at short times and the change increases with increasing time. The importance of overlying rock permeability in determining the extent to which the gas migrates to the near surface is illustrated in Figures 14 and 15. By comparing Figures 14 and 15, which were obtained with the same input parameters but with different permeabilities, we can observe that at a specific depth the change in gas potential decreases with decreasing permeability. Figure 16 shows the relationship between permeability and gas potential at a depth of 100 m from the reservoir at different times. It can be seen that gas potential at specific depths increases with increasing permeability. The increase in gas potential becomes significant as time increases.

A relationship between the hydrocarbon gas saturation of the overlying rocks is shown in Figure 17. At a specific depth, the hydrocarbon gas saturation is found to be increasing with time.

At 100 meters above the reservoir, the relationship between hydrocarbon gas and depth as a function of time is shown in Fig. 18.

Table 8 Output Data File for the Two-phase Transport Model

DEPTH(m)	GAS POTENTIAL(PST) TIME=0 YEARS	GAS POTENTIAL(PST) TIME=2 YEARS	GAS POTENTIAL(PST) TIME=5 YEARS	GAS POTENTIAL TIME=10 YEARS	GAS POTENTIAL TIME=27 YEARS
10	1000.1	1028.6	1030.7	1034.9	1045.5
119	1000.1	1058.3	1062.5	1071.1	1092.7
228	1000.1	1089.4	1095.9	1109.1	1142.1
337	1000.1	1122.5	1131.3	1149.3	1194.6
446	1000.1	1158.2	1169.6	1192.9	1251.4
555	1000.1	1198.0	1212.3	1241.4	1314.7
664	1000.1	1244.7	1262.3	1298.3	1388.9
773	1000.1	1305.1	1327.1	1372.0	1484.9
882	1000.1	1405.5	1434.8	1494.4	1644.6
1000	1000.1	1967.2	2040.7	2190.3	2563.4

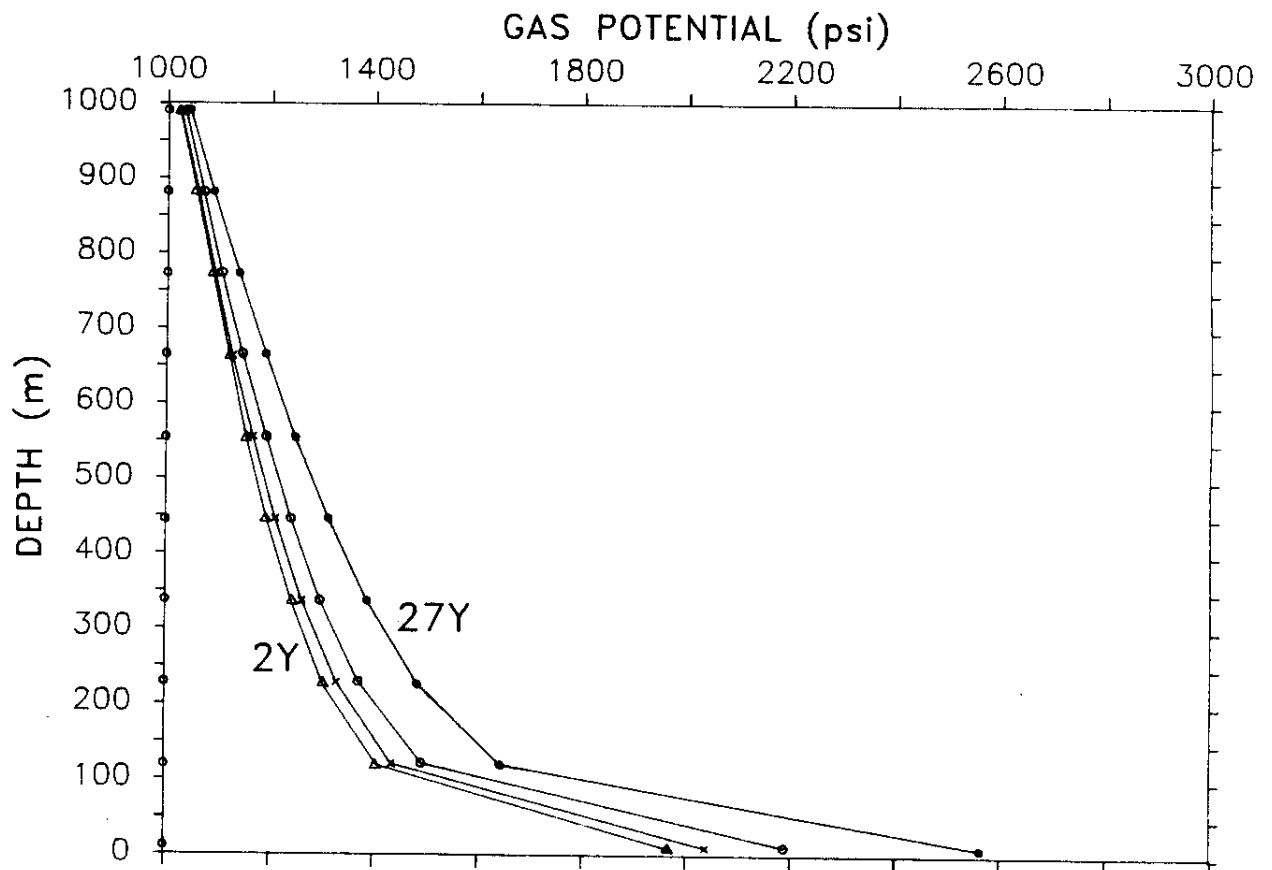


**Fig. 14 Hydrocarbon Gas Potential vs. Depth
at 2, 5, 10 and 27 Years
Permeability = 0.001 md Porosity = 0.1 Reservoir pressure = 3,000 psi**

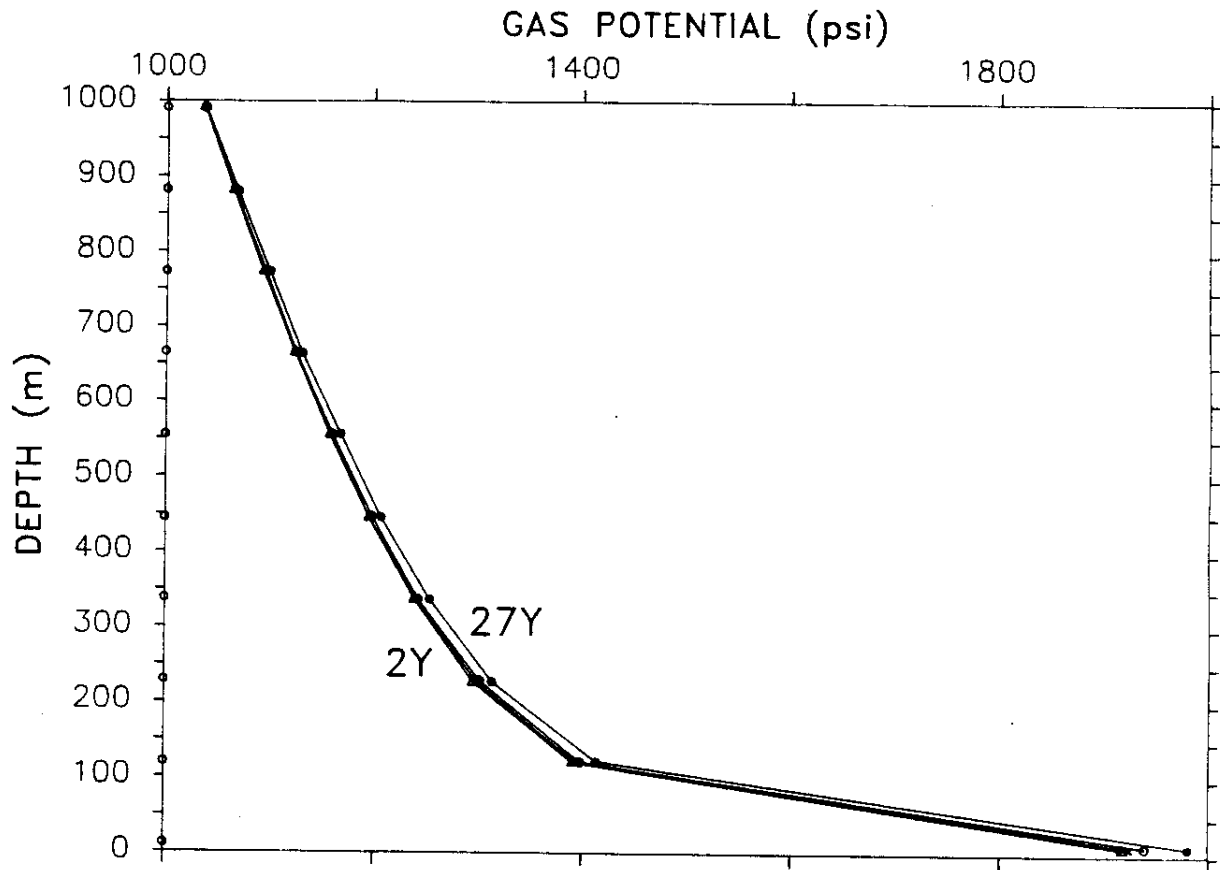
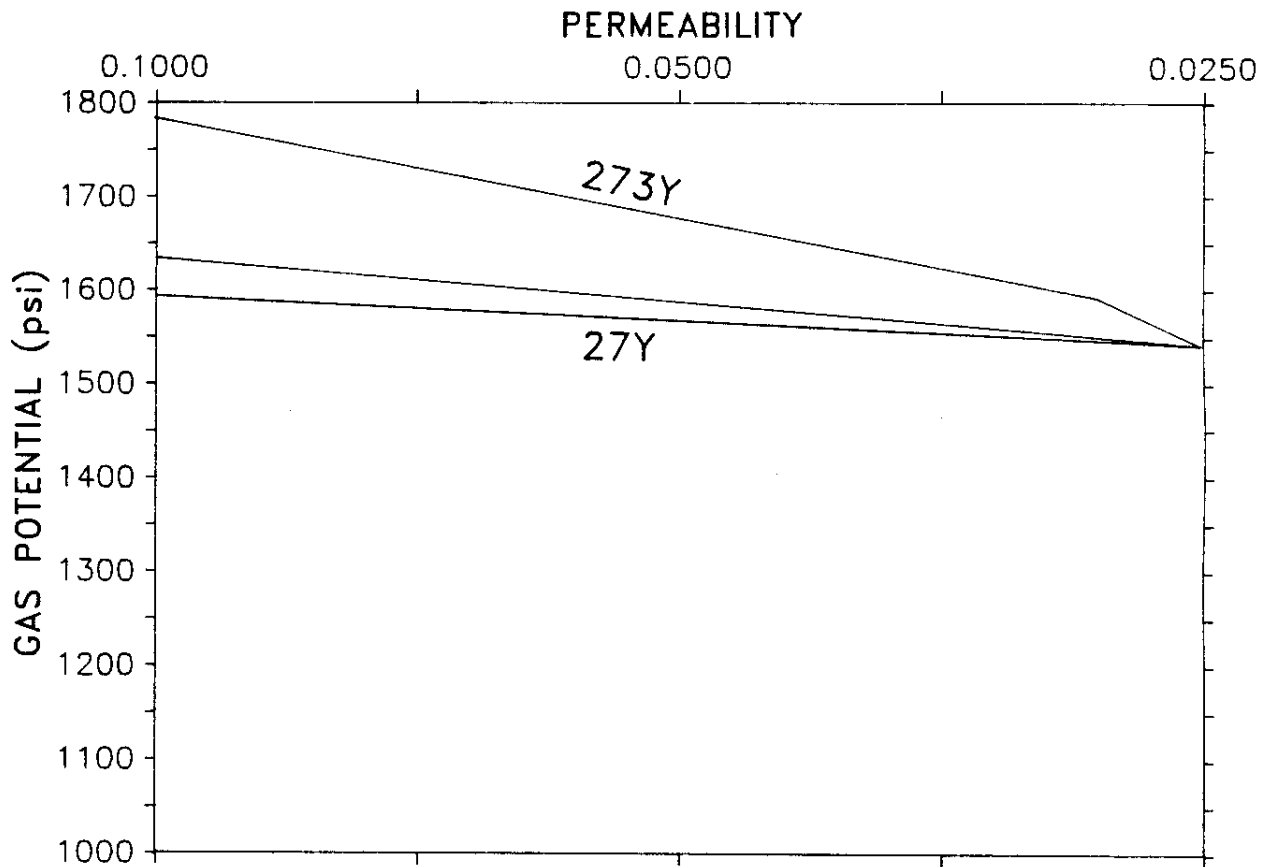
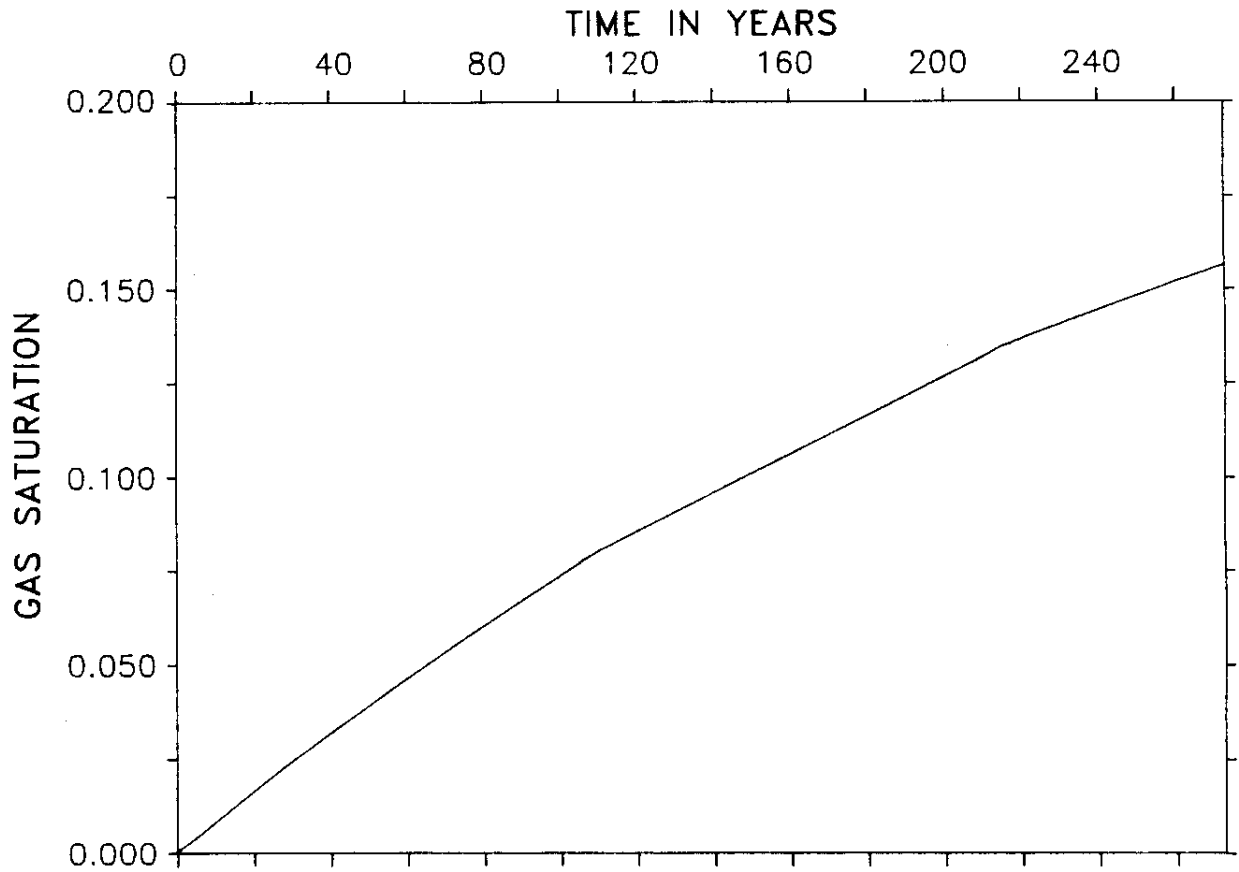


Fig. 15 Hydrocarbon Gas Potential vs. Depth
at 2, 5, 10 and 27 Years
Permeability = 0.0001 md Porosity = 0.1 Reservoir pressure = 3,000 psi



**Fig. 16 Gas Potential vs. Permeability at 27, 54 and 273 Years
at 100 Meters Above the Reservoir
Porosity = 0.1 Reservoir = 2,000 psi**



**Fig. 17 Hydrocarbon Gas Saturation vs. Time
at 100 m Above the Reservoir
Permeability = 0.1 md Porosity = 0.1
Reservoir Pressure = 2,000 psi Reservoir depth = 1,000 m**

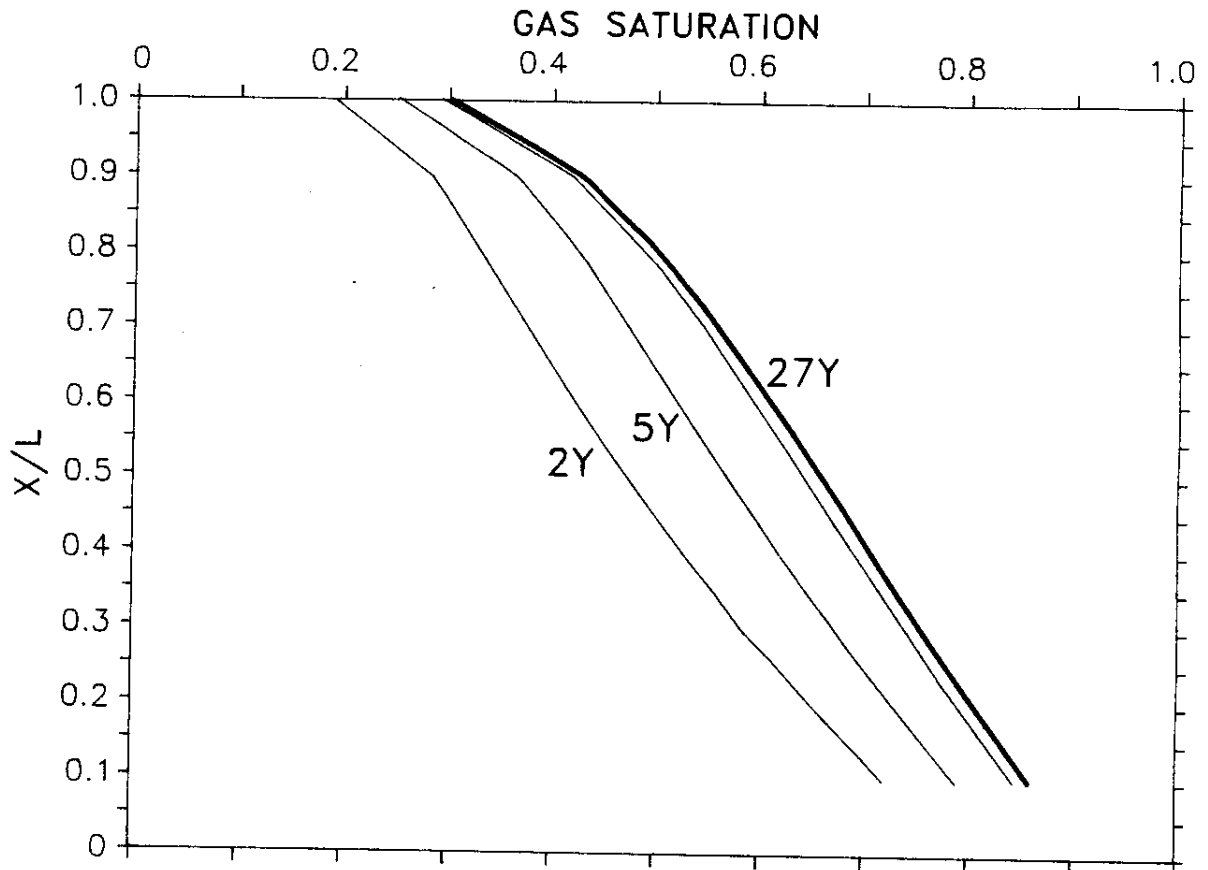


Fig. 18 Hydrocarbon Gas Saturation vs. Depth Within the 100 m Interval Above the Reservoir, at 2, 5, 10 and 27 Years
Permeability = 0.1 md Porosity = 0.1
Reservoir Pressure = 3,000 psi Reservoir Depth = 1,000 m

It can be seen that hydrocarbon gas saturation at different times increases throughout the overlying column, and such increase is sharp near the reservoir.

An important relationship between hydrocarbon gas potential and time (2, 5, 10 and 27 years) as a function of reservoir potential at two depths of 10 meters from the surface (A, B and C) and at 10 meters from the reservoir (D, E and F) is shown in Figure 19. The reservoir pressure values were chosen to be in a range between a minimum, which represents the hydrostatic gradient of approximately 0.5 psi/ft and a maximum, which represents the lithostatic gradients of approximately 1.0 psi/ft. Three important conclusions can be drawn from the graph. The hydrocarbon gas potential increases with time at a specific depth. The hydrocarbon gas potential change at the near surface does not change significantly (A, B and C) but there is some change even at the near surface, while 10 meters above the reservoir, the hydrocarbon gas potential is considered to be significant with increasing reservoir potential (D, E and F). It can also be seen that with decreasing or increasing the reservoir pressure, the gas potential at a specific depth will be decreasing or increasing, causing the disappearance or appearance of the hydrocarbon gas anomalies even at 10 meters from the surface. This explains the change in hydrocarbon anomalies in soil gas after short periods of time.

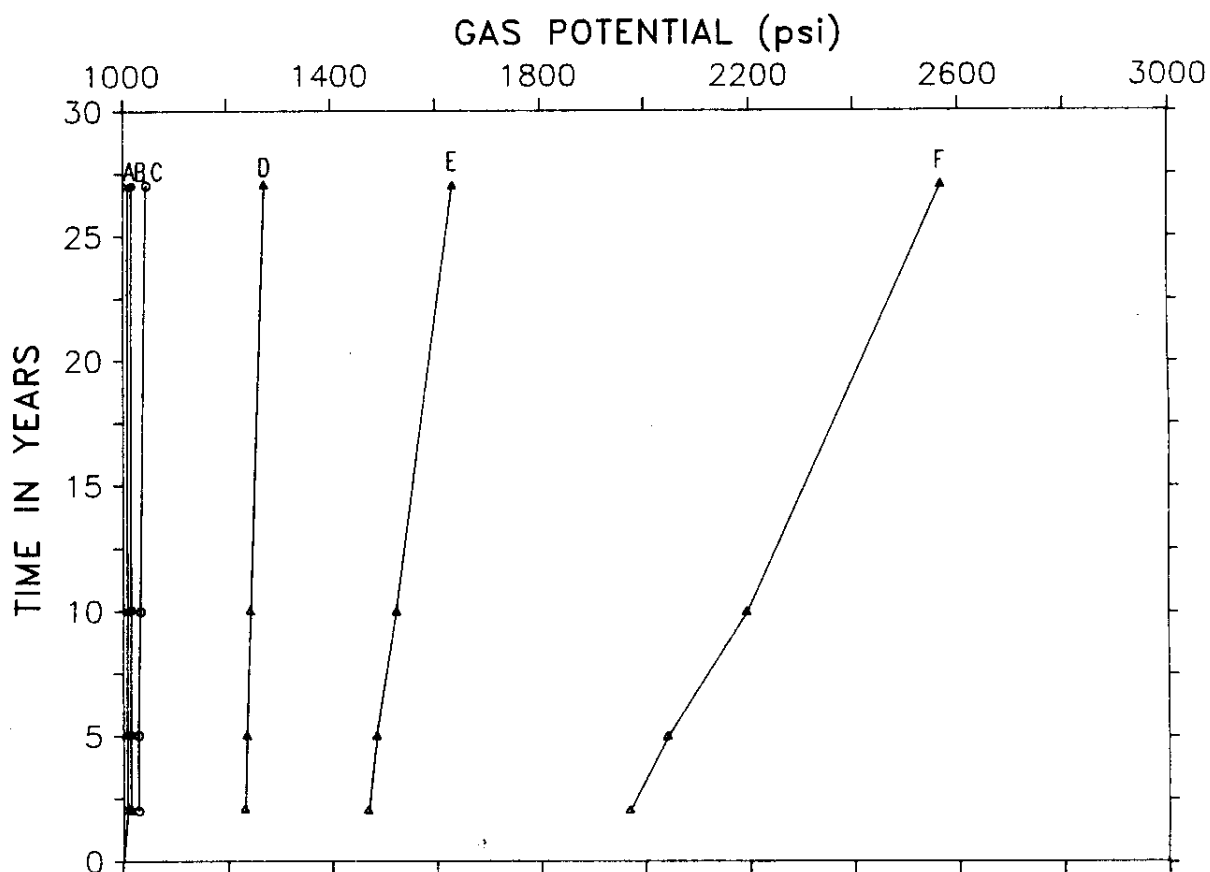
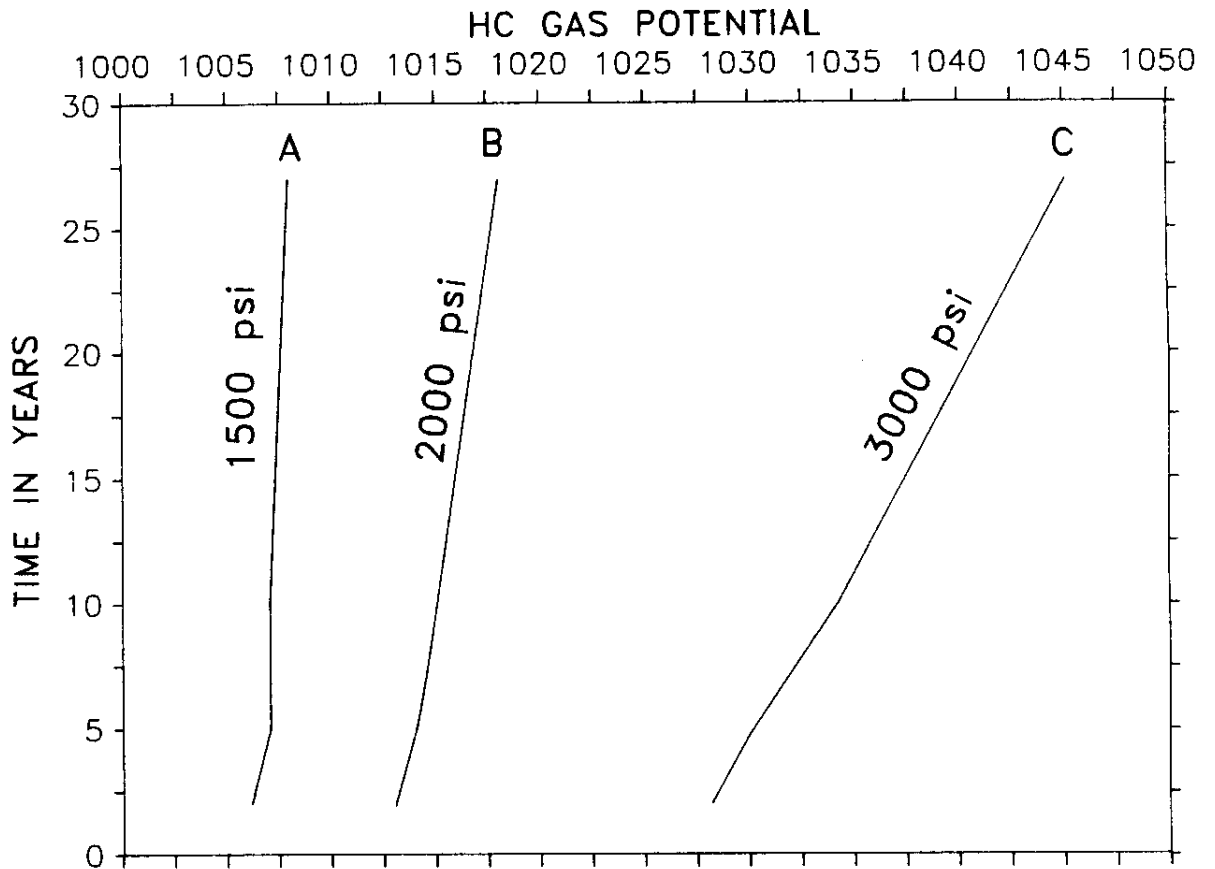


Fig. 19 Hydrocarbon Gas Potential vs. Time as a Function of Reservoir Potential
 Permeability = 0.001 md Porosity = 0.1
 Reservoir Pressures = 1500, 2000, 3000 psi Reservoir Depth = 1,000 m
 A, B and C at 10 m from Surface D, E and F at 10 m from Reservoir

An expanded view of the hydrocarbon gas potential distribution at the near surface (A, B, C from previous figure) as a function of reservoir pressure is illustrated in Figure 20. It can be seen that hydrocarbon gas pressure potential at the surface, increases with time at a specific reservoir pressure but the increase is greater if the reservoir pressure is large. This can be seen from the slope of the lines A, B and C. The figure shows that at approximately 30 years, a total of 20-psi pressure change can be produced from a 3000-psi reservoir pressure potential, while a change of only 4 psi can be obtained if the reservoir pressure is equal to 2000 psi.

Figure 21 also shows a relationship between time and pressure change at the surface as a function of reservoir pressure. It can be seen that the hydrocarbon gas pressure increases with time and that such an increase is sharp at first and then approaches a maximum amount. The figure also shows that a total of 55 psi can be observed at the surface in 100 years from a reservoir of 3000 psi pressure potential, while a total of less than 10 psi can be observed from a reservoir of 1500 psi.



**Fig. 20 Hydrocarbon Gas Potential vs. Time Near Surface
as a Function of Reservoir Potential
Permeability = 0.001 md Porosity = 0.1
Reservoir Pressure = 1500, 2000, 3000 psi Reservoir depth = 1,000 m**

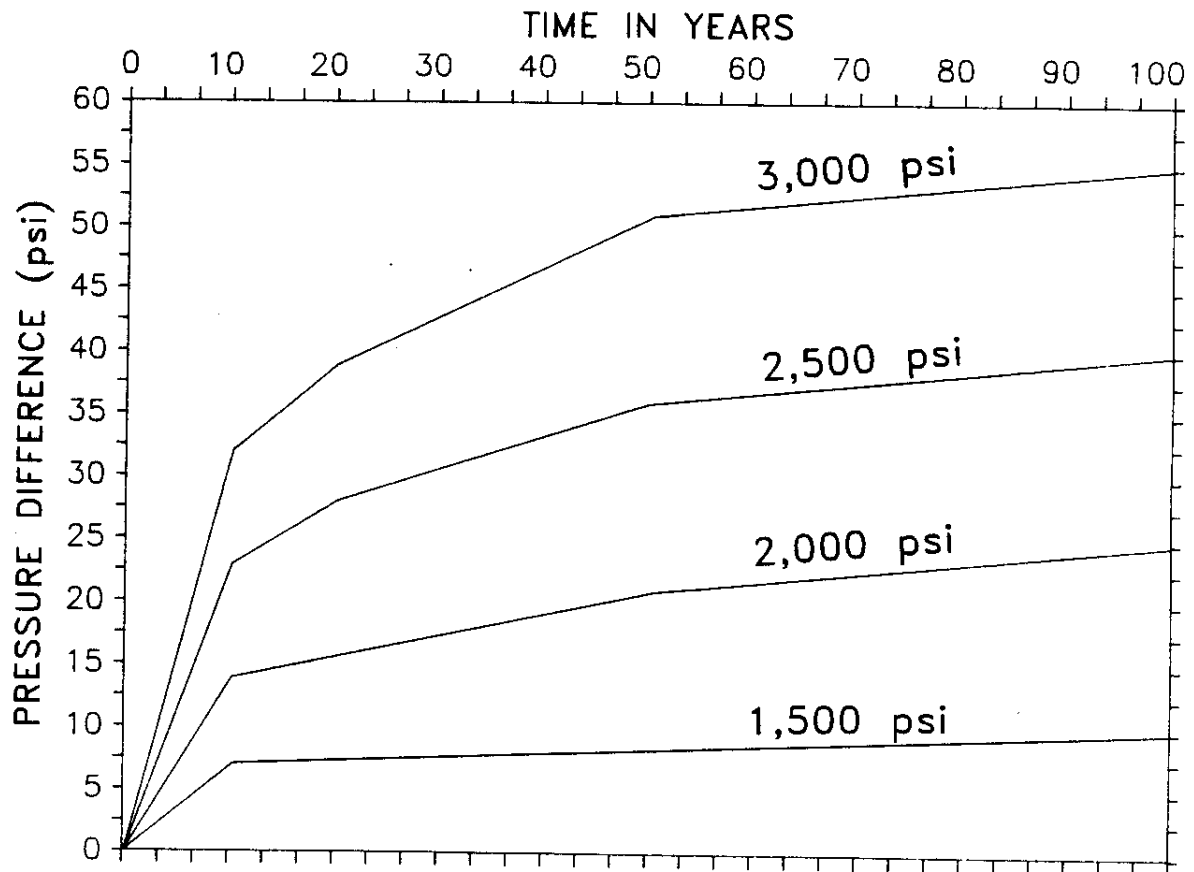


**Fig. 21 Pressure Change at Surface vs. Time
as a Function of Reservoir Pressure
Permeability = 0.001 md Porosity = 0.1**

8.0 CONCLUSIONS FOR THE TWO-PHASE TRANSPORT MODEL

The conclusions that can be drawn from the previous discussion are the following:

1. Hydrocarbon gas potential change within the overlying column as a function of time is found to be pronounced near the reservoir and such change becomes small toward the surface. This conclusion can be related to the observation that the hydrocarbon anomaly appears and/or disappears in short time.
2. The hydrocarbon gas potential at a specific depth increases with time.
3. Overlying rock permeability is a very important parameter in determining the extent to which the hydrocarbon gas can migrate. The hydrocarbon gas potential at a specific depth increases with permeability.
4. The hydrocarbon gas saturation increases with time and depth throughout the overlying rocks, and such increase is pronounced near the reservoir.
5. The hydrocarbon gas potential changes with time near the reservoir and is largest near the reservoir, while near the surface such change is smaller but detectable.
6. With increasing the reservoir pressure, the hydrocarbon gas potential at a specific depth increases and the increase is pronounced with depth. This computed result can be compared to observed data of the hydrocarbon gas anomalies at the surface with increasing reservoir pressure.
7. Decreasing the reservoir pressure causes the decrease of the hydrocarbon gas

potential. This can be compared to observed data that the hydrocarbon anomaly disappears as the reservoir pressure decreases.

9.0 COMPARISON OF THE MODELS' RESULTS WITH DATA FROM NATURE

For the hydrocarbon microseepage mechanism model to be acceptable, such a mechanism should provide results which are in accordance with data that have been observed in nature. Four most important groups of data and observations should be compared to the model results for any model to be accepted. These groups of data include:

1. Surface hydrocarbon anomalies have been observed to appear or disappear in a relatively short time as a result of changes in reservoir pressure. This observation suggests that the vertical movement of hydrocarbon gases is rapid. Horvitz (1968) surveyed the Hastings Field, Texas (which was discovered in 1939), over which he found a hydrocarbon anomaly in 1946 (Fig. 22). Twenty-two years later, when more than 75% of the ultimate reserve has been produced, the 1946 anomaly had disappeared (Fig. 23). Hunt (1979) cited a study which showed that a few months after initiation of underground storage of natural gas, the gas content of sand located 300 m above the reservoir was increased ten times. Heroy (1980) showed that repressurization during secondary recovery caused a surface anomaly to increase in intensity at Hilbig Field, Texas.
2. The actual hydrocarbon microseepage flux rates must be low compared to

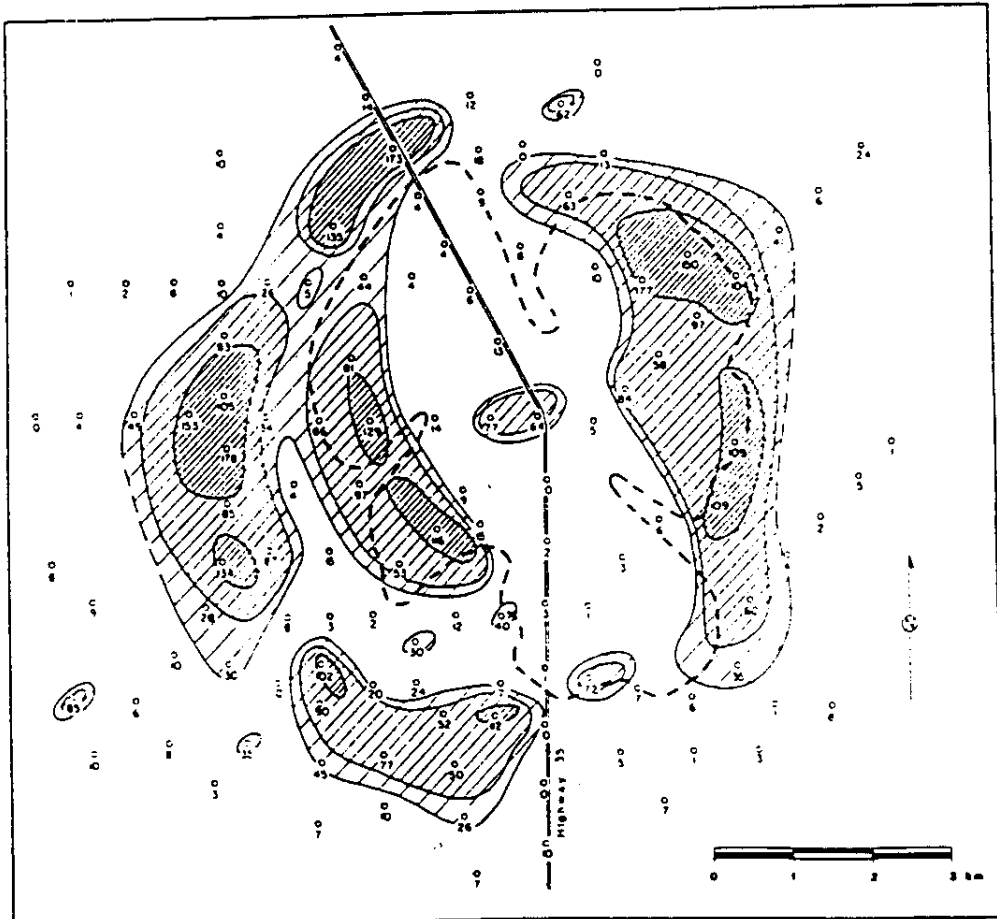


Fig. 22 Ethane Plus Heavier Hydrocarbon Concentration at Hastings Field, Texas, 1946 (ppb, from Davidson, 1982)

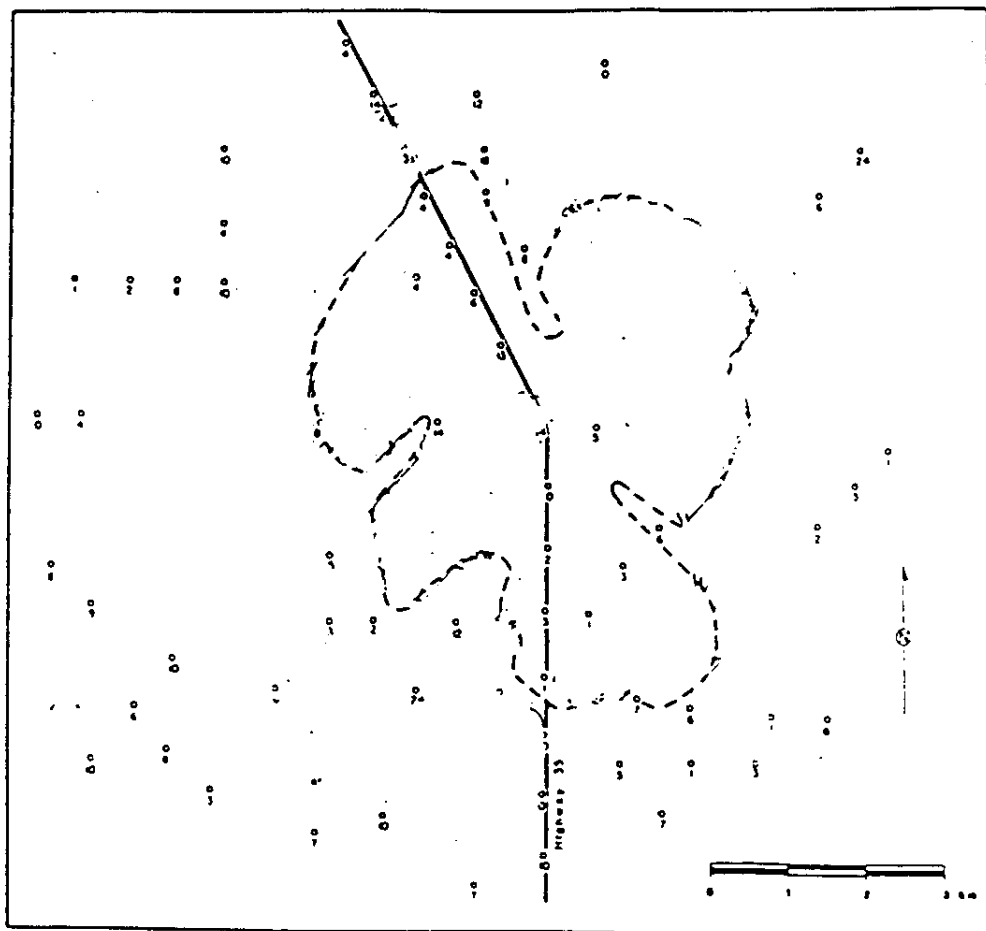


Fig. 23 Ethane Plus Heavier Hydrocarbon Concentration at Hastings Field, Texas, 1968 (ppb, from Davidson, 1982)

those already published, which seem unrealistically high. Rosaire (1938) estimated the microseepage flux rate at Hastings Field, Texas, to be about 10,000 barrels of oil per day (bopd). Pirson (1941) estimated the maximum microseepage flux rate for ethane at the Music Mountain gas field, Pennsylvania, to be approximately $23 \text{ mm}^3/24 \text{ hrs/ft}^2$. Duschsher (1981) has estimated the total hydrocarbon gas loss to be about 300 cu ft/year/yd² by considering reasonable reservoir parameters. If such rates are believed to be correct, a tremendous amount of hydrocarbons should have been lost, which in turn will be just a small percentage of the original reservoir. This will lead to a huge reservoir compared to the amount lost during microseepage process.

These published microseepage rates are not practical. Millions, or even hundreds of millions times smaller rates could be practical (Price 1981).

3. The third group of data which can be used to compare the model data is based on the fact that the concentration of hydrocarbons increases with depth (i.e. the light hydrocarbons were found throughout the sedimentary column at parts per billion concentrations in shallow sediments and at parts per million in deep sediments (Hunt 1984)). Sokolov and others (1971) noted that in the deeper coring programs, a chromatographic effect is noticed over oil deposits, with a progressive increase in the appearance and concentration of

higher molecular weight hydrocarbons with increasing depth (Fig. 24). Horvitz (1939) noted that the concentration of the hydrocarbons tends to increase with depth at Jefferson Davis Parish, Louisiana (Fig. 25). The hydrocarbon concentration as a function of depth at Rosenberg, Fort Bend County, Texas (producing), and at Harris County, Texas (dry) is shown in Fig. 26 (Price, 1986). It is clear that hydrocarbon concentrations are higher at the producing well and also that their concentrations increase with depth as the reservoir is approached. Variation of gas hydrocarbon concentration in shale as a function of depth in a hole drilled near Walvis Ridge (off the west coast of Africa) is shown in Fig. 27 (Hunt, 1984). It shows that hydrocarbon concentrations increase with depth. Rocks from the near-surface intervals of three shallow core holes drilled in shale from west Greenland shows a pronounced depletion in concentration of light hydrocarbons towards the surface (Fig. 28) (Leythaeuser, 1980).

4. The fact that hydrocarbon microseeps are composed dominantly of C_1 to C_4 hydrocarbons, is another piece of data that should be considered in interpreting the results obtained by any proposed microseepage mechanism(s). The hydrocarbon anomaly usually does not involve detectable C_{6+} hydrocarbons.

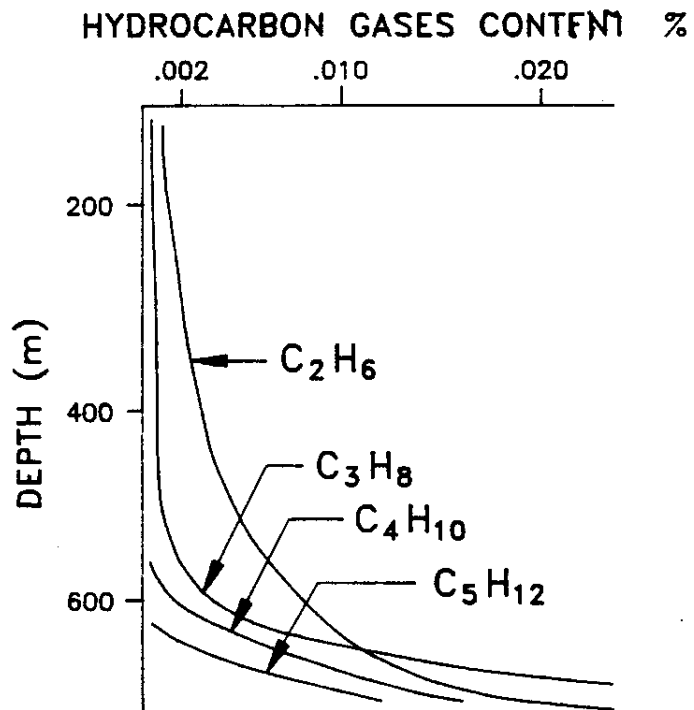
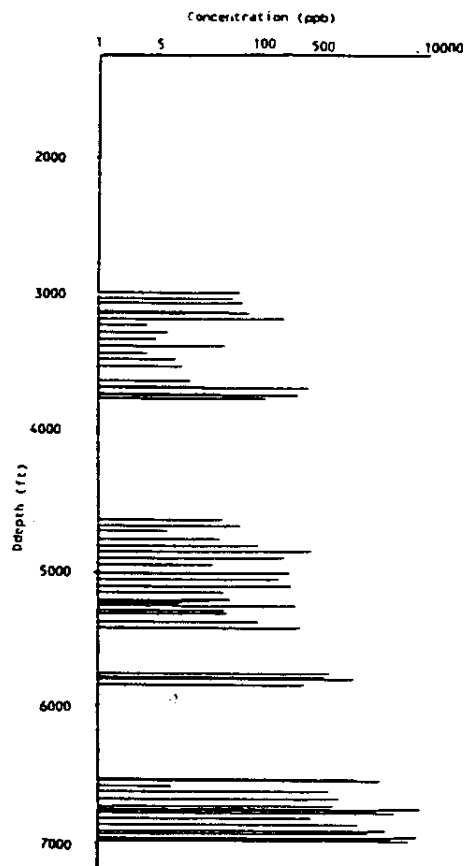


Fig. 24 Chromatographic Distribution of C₂ - C₅ Hydrocarbons Through the Stratigraphic Section of the Kumdag Field (from Sokolov, 1971)



**Fig. 25 C₂+ Hydrocarbons vs. Depth
(from Horvitz, 1939)**

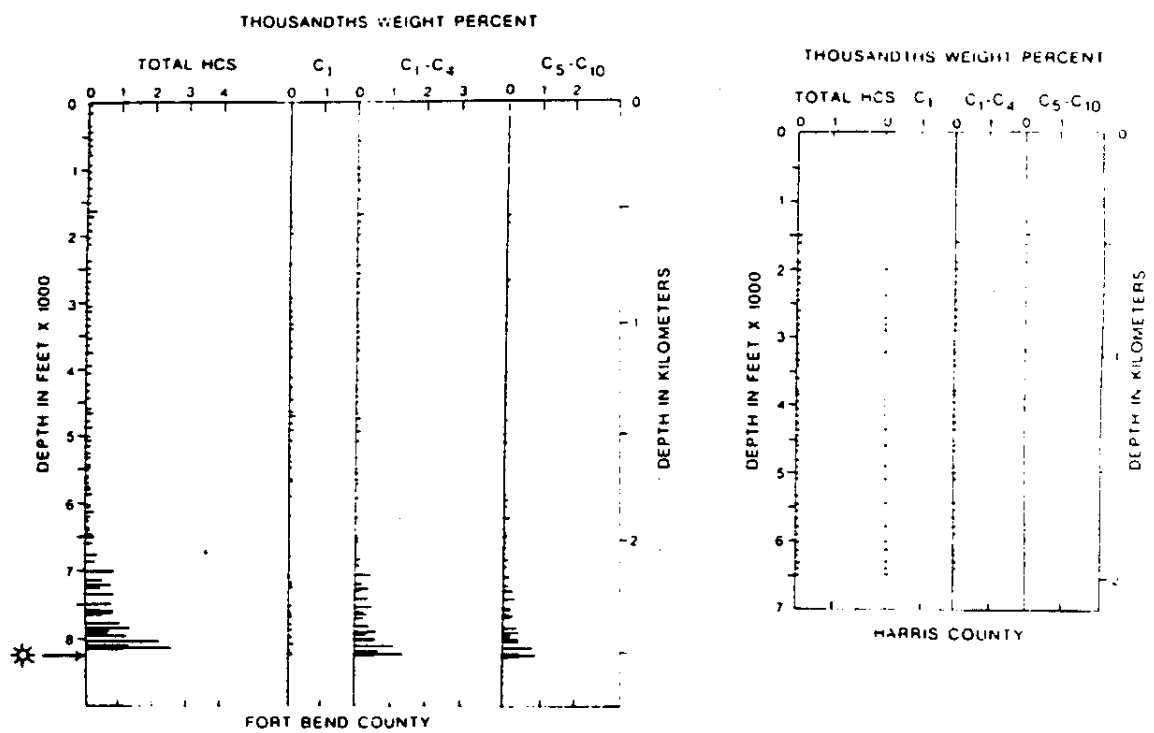


Fig. 26 Hydrocarbon Concentration vs. Depth at Rosenberg, Fort Bend Co., Texas (producing) and at Harris Co., Texas (dry) (from Price, 1986)

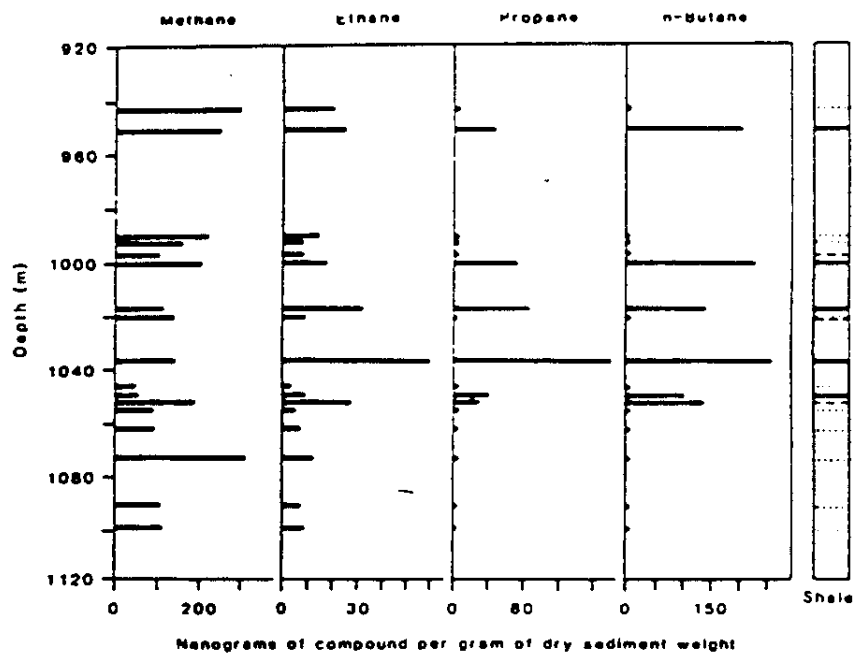


Fig. 27 Gaseous Hydrocarbon Concentrations vs. Depth near Walvis Ridge (off west coast of Africa) (from Hunt, 1984)

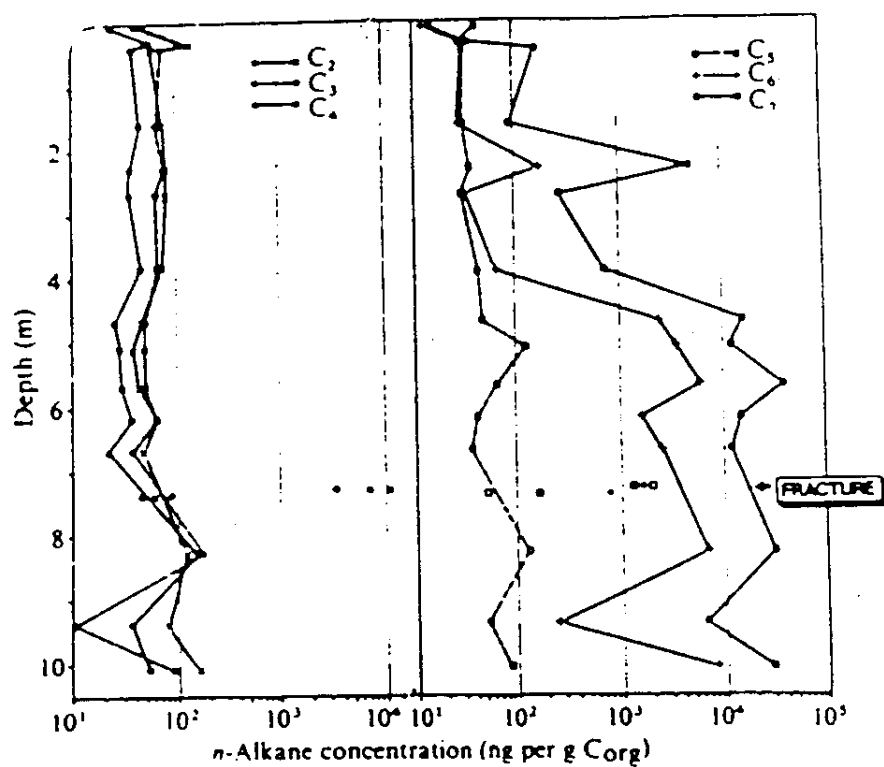


Fig. 28 Hydrocarbon (C₂ - C₂₅) Concentration in the Near-surface Interval of Plienbachian Shale (from Leythaeuser, 1980)

10.0 COMPARISON OF THE TWO MODELS

Both models show that permeability of overlying rocks and reservoir depth are the most important parameters in determining the rate of migration of the light hydrocarbons. They also show that light hydrocarbon concentration increases with depth. The models demonstrate that at a specific depth the concentration of light hydrocarbons decreases with increasing molecular weight, and increases with time. The time required for a light hydrocarbon to reach the near surface dissolved in water, considering reasonable properties of both the overlying rocks and fluid, is far more than that required to reach the surface by considering the two-phase flow model. The hydrocarbon gas-water transport model explains that hydrocarbon amount at the near surface is not so significant, but it is significant at deeper depth. This can be compared to the observed data that only a small concentration of light hydrocarbons are observed on the near surface sediment even when considering geologic time. The hydrocarbon gas-water model explains that with increasing or decreasing reservoir pressure, the light hydrocarbon anomaly at the near surface could appear or disappear respectively. This piece of data supports the observation that with the increase or decrease of reservoir pressure, the anomaly may appear or disappear in a relatively short time.

From the above discussion, it can be stated that shallow reservoir depth and/or high permeability of the overlying rocks are required for light hydrocarbons to reach the surface dissolved in water in detectable amounts in a relatively short time. Also, it can

be stated the most plausible light hydrocarbon microseepage mechanism can be attributed to the hydrocarbon gas-water transport model because it shows the best agreement with the existing observed data.

11.0 REFERENCES

- Bear, J., 1972, *Dynamics of Fluids in Porous Media*, New York, American Elsevier Publishing Co., 764 p.
- Bear, J., 1979, *Hydraulics of ground water*, New York: McGraw-Hill, 567 p.
- Carnahan, B. H., and J. Wilkes, 1969, *Applied Numerical Methods*, New York: John Wiley and Sons, 604 p.
- Crichlow, M.B., 1977, *Modern Reservoir Engineering—A Simulation Approach*, New Jersey, Prentice Hall, Inc., 345 p.
- Davidson, M., 1967, Petroleum geochemical exploration from space: A radical new technology: National Aero space administration (NASA) manuscript.
- , 1982, Toward a general theory of vertical migration. *Oil and Gas Journal*. June 21, p. 288-300.
- , 1984, State of the art and direction of unconventional oil and gas exploration, in Davidson, M.J., and Gottlieb, B. M., eds., *Unconventional methods in exploration for petroleum and natural gas III*: Dallas, Southern Methodist University Press, p. 4-8.
- Denison, D., 1983, Geochemistry exploration techniques being used to help pin down hydrocarbon prospects in Michigan. *Michigan's Oil and Gas News*, December 23, p. 161-164.
- Donovan, T.J. and Dalziel, M.C., 1977, Late diagenetic indicators of buried oil and gas, *U.S. Geological Survey Open-File Report 77-817*, 44 p.
- Duchscherer, W., 1980, Geochemical methods of prospecting. *Oil and Gas Journal*, December 1, p. 194-208.
- , 1981a, Carbonates and isotope ratios from surface rocks—A geochemical guide to underlying petroleum accumulations, in Gottlieb, B.M., ed., *Unconventional methods in exploration for petroleum and natural gas II*: Dallas, Southern Methodist University Press, p. 201-218.

- , 1981b, Non gasometric geochemical prospecting for hydrocarbons with case histories, *Oil and Gas Journal*, October 19, p. 312-327.
- Hagoort, J., 1988, *Fundamentals of gas reservoir engineering* New York, Elsevier Publishing Co., 327 p.
- Healy, R.W., 1990, Simulation of solute transport in variably saturated porous media with supplemental information on modification to the U.S. Geological survey computer program VS2D, *Water Resources Investigation Report 90-4025*, 125 p.
- Horvitz, L., 1939, On geochemical prospecting, *Geophysics*, v.4, p. 210-228.
- , 1969, Hydrocarbon geochemical prospecting after thirty years, in Heroy, W.B., ed, *Unconventional methods in exploration for petroleum and natural gas*, Dallas: Southern Methodist University Press, p. 205-218.
- Hunt, J.M., 1979, *Petroleum geochemistry and geology*, San Francisco: Freeman and Company, 617 p.
- , 1984, Generation and migration of light hydrocarbons, *Science*, v. 226, p. 1265-1270.
- Jones, V.I., and R.J. Drozd, 1983, Predictions of oil or gas potential by near-surface geochemistry, *American Association of Petroleum Geologists Bulletin*, v. 67, p. 932-952.
- Jones, P.H., 1984, Deep water discharge: A mechanism for the vertical migration of oil and gas, in Davidson, M.J., and Gottlieb, B.M. eds., *Unconventional methods in exploration for petroleum and natural gas III*, Dallas: Southern Methodist University Press, p. 254-271.
- Kartsev, A.A., Z.A. Tabasaranskii, M.I. Subbota, and G. Mogilevskii, 1959, *Geochemical methods of prospecting and exploration for petroleum natural gas*, Los Angeles: University of California Press, 349 p. (Eng. translation edited by P.A. Witherspoon, and W.D. Romey).
- Katz, D., and K. Coats, 1968, *Underground Storage of Fluids*, Ann Arbor: Ulrich's Books, Inc., Michigan, 575 p.

- Laubmeyer, G., 1933, A new geophysical prospecting method, especially for deposits of hydrocarbons, *Petroleum* (London), v. 29, p. 1-4.
- Leythaeuser, D., R.G. Shaefer and A. Yukler, 1980, Diffusion of light hydrocarbons through near-surface rocks, *Nature*, v. 284, p. 522-525.
- Leythaeuser, D., R.G. Schaefer and A. Yukler, 1982, Role of diffusion in primary migration of hydrocarbons, *AAPG Bull.*, v. 66, p. 408-429.
- McAuliffe, C.D., 1978, Role of solubility in migration of petroleum from source, *in* Roberts, W.H., and Cordell, R.J., eds., *Physical and chemical constraints on petroleum migration*, Tulsa, Oklahoma: American Association of Petroleum Geologists, p. C-1 — C-39.
- Pirson, S.J., 1941, Measure of gas leakage applied to oil search, *Oil and Gas Journal*, February 20, p. 21 and 32.
- , 1960, How to make geochemical exploration succeed, *World Oil*, April, p. 93-96.
- , 1963, Projective well log interpretation, *World Oil*, October, p. 116-120.
- , 1964, Projective well log interpretation, *World Oil*, October, p. 180-182.
- , 1969, Geological, geophysical and chemical modifications of sediments in the environment of oil fields, *in* Heroy, W.B., ed, *Unconventional methods in exploration for petroleum and natural gas*, Dallas: Southern Methodist University Press, p. 159-186.
- Price, L.C., 1985, A critical overview of and proposed working model for hydrocarbon microseepage, *USGS open-file report 85-271*, 83 p.
- Roberts, W.H., 1980, Design and function of oil and gas traps, *in* Roberts, W.H., and Cordell, R.J., eds., *Problems of petroleum migration: American Association of Petroleum Geologists Studies in Geology*, v. 10, p. 217-240.
- Rosaire, E.E., 1938, Shallow stratigraphic variations over Gulf Coast structures: *Geophysics*, v. 3, p. 96-121.
- , 1940, Geochemical prospecting for petroleum, *in* *Symposium on Geochemical Exploration: AAPG Bulletin*, v. 24, p. 1400-1433.

- Siegel, F.R., 1974, Applied geochemistry, in Geochemical prospecting for hydrocarbons, New York: John Wiley and Sons, p. 228-255.
- Singh, R., 1965, Unsteady and unsaturated flow in soils in two dimensions, Department of Civil Engineering, Stanford University, Technical Report No. 54, 130 p.
- Smith, J.E., J.G. Erdman, and D.A. Morris. 1971. Migration, accumulation and retention of petroleum in the earth. In 8th World Petroleum Congress, Proc. Moscow, 1971. London: Applied Science Publishers, pp. 13-26.
- Sokolov, V.A., 1971, The theoretical foundations of geochemical prospecting for petroleum and natural gas and the tendencies of its development, Canadian Institute of Mining, special volume 11, p. 544-549.
- Sokolov, V.A., F.A. Alexeyev, E.A. Bars, A.A. Geodekyan, Y.M. Yurovsky and B.P. Yasenev, 1959, Investigations into direct oil detection methods, in Proceedings of the Fifth World Petroleum Congress, Section I: Geology and Geophysics, p. 667-687.
- Tek, M., J.O. Wilkes, and D. Katz, 1966, New Concepts in Underground Storage of Natural Gas, New York: The American Gas Association, 342 p.
- Thomas, C.W., 1982, Principles of Hydrocarbon Reservoir Simulation, Boston: International Human Resources Development Corporation, 207 p.
- Tissot, B.P., and D.H. Welte, 1984, Petroleum formation and occurrence, New York: Springer-Verlag, 699 p.
- Wang, H.F., and Mary P. Anderson, 1982, Introduction to ground water modelling: Finite difference and finite element methods, San Francisco: W.H. Freeman and Co., p.

12.0 APPENDIX 1 - Water Transport Computer Code

```

C *****
C
C   COMPUTER PROGRAM TO SOLVE TWO DIMENSIONAL VERTICAL MIGRATION
C   OF HYDROCARBON GASES DISSOLVED IN WATER IN A POROUS MEDIA,
C   USING FINITE DIFFERENCE NUMERICAL TECHNIQUE.
C *****

C-----VARIABLES-----

C   TMAX:  MAXIMUM SIMULATION TIME
C   TIMIN:  INITIAL TIME
C   DELT:  TIME INCREMENT
C   NCOL:  NUMBER OF COLUMNS
C   NROW:  NUMBER OF ROWS
C   XGRID:  GRID DISTANCE IN X-DIRECTION
C   ZGRID:  GRID DISTANCE IN Z-DIRECTION
C   RELAX:  RELAXATION PARAMETER
C   ERROR1:  CLOSURE CRITERIA FOR TRANSPORT EQUATION
C   MAXIT:  MAXIMUM ITERATIONS
C   WDENSI:  WATER DENSITY
C   NLITHO:  NUMBER OF DIFFERENT ROCK TYPES IN COLUMN
C   PERM:  ROCK PERMEABILITY TO WATER
C   WVISCO:  WATER VISCOSITY
C   WCOMPR:  WATER COMPRESSIBILITY
C   RCOMPR:  ROCK COMPRESSIBILITY
C   PORO:  ROCK POROSITY
C   LCO:  LEFT COLUMN
C   RCOL:  RIGHT COLUMN
C   TPROW:  TOP ROW
C   WRATE:  WATER FLUX RATE

C-----
C   INCLUDE 'ARRAY.DAT'
C-----
C   READ AND WRITE SIMULATION DATA
C-----

CHARACTER*30 MICROSEEPAGE
WRITE(*,*) 'ENTER NAME OF INPUT DATA FILE'
READ(*, '(a)') MICROSEEPAGE
OPEN(2, FILE=MICROSEEPAGE, STATUS='OLD')

WRITE(*,*) 'WHAT IS THE RESESRVOIR DEPTH IN METERS'
READ(*,*) DEPTH
READ (2,*) TMAX,TIMIN,DELT
READ (2,*) NCOL,NROW,XGRID,ZGRID
NXRR=NROW-1
NLYY=NCOL-1
NODES=NROW*NCOL

C-----
C   INITIALIZING ARRAYS & CONSTANTS
C-----

```

```

ICONVG=0
NTIM=0
NITT=0
NITT1=0
JFLAG=1
KP=0

DO I=1,NODES

    P(I)= 0.0
    PP(I)=0.0
    HSPERM(I)=0.0
    WATCON1(I)=0.0
    WATCON2(I)=0.0
    HPERM(I)=0.0
    VPERM(I)=0.0
    FLUX(I)=0.0
    A(I)=0.0
    B(I)=0.0
    C(I)=0.0
    D(I)=0.0
    E(I)=0.0
    RHS(I)=0.0
    XI(I)=0.0
    DX1(I)=0.0
    DX2(I)=0.0
    DZ1(I)=0.0
    DZ2(I)=0.0
    VX(I)=0.0
    VZ(I)=0.0
    CC(I)=0.0
    COLD(I)=0.0
    CS(I)=0.0
    NCTYP(I)=0

END DO
C   ASSIGN HORIZONTAL AND VERTICAL COORDINATES

DO I=1,NCOL
XXGRID(I)=XGRID
END DO
DO I=1,NROW
ZZGRID(I)=ZGRID
END DO
CONTINUE
DO N=2,NCOL
NDIS(N)=NDIS(N-1)+0.5*(XXGRID(N-1)+XXGRID(N))
END DO
DO J=2,NROW
VDIS(J)=VDIS(J-1)+0.5*(ZZGRID(J-1)+ZZGRID(J))
END DO
CONTINUE

C
C   CALL SUBROUTINES TO READ, WRITE AND CALCULATE VARIABLES
C   -----

CALL INPUT
CALL SOLUTION
CALL OUTPUT
60  CALL SEQUENCE

IF(.NOT.SSTATE) CALL SETUP

CALL COEF
NITT=NITT+NIT

IF (.NOT.SSTATE) CALL TVELO
IF(.NOT.SSTATE) CALL TCOEF

```

```

IF (.NOT.SSTATE) CALL TSETUP
NITT1=NITT1+NITT

C COMPUTE MASS BALANCE COMPONENTS

CALL OUTPUT
CALL MASS
IF(JSTOP.NE.1) GO TO 60
END

-----
C SUBROUTINE INPUT:
C TO READ INPUT DATA
C -----
C SUBROUTINE INPUT
C -----
C INCLUDE 'ARRAY.DAT'
C -----
C READ AND WRITE INITIAL DATA
C -----

READ (2,*) ERROR,RELAX,ERROR1
READ (2,*) NINIT,MAXIT
READ (2,*) WSENSI
READ (2,*) NLITHO

IF(MAXIT.GT.200) GO TO 150

C READ AND WRITE ROCK PROPERTIES FOR EACH LITHOLOGY

DO 20 J22=1,10
DO 10 J23=1,100
10 HK(J22,J23)=0.
DO 20 J23=1,100
20 HT(J22,J23)=0.
DO 30 J22=1,NLITHO

READ (2,*) J
g=980.0

C CALL WVISCOSITY (WVISCO,WSENSI)

READ (2,*) PERM
HK(J,11)=PERM*WSENSI*g/WVISCO

C UNITS IN CM/DAY

HK(J,1)=HK(J,11)*60*60*24

CALL COMPRESSIBILITY (WCOMPR,RCOMPR,DISTANCE,NLITHO)

READ (2,*) PORO

C TO CONVERT FROM 1/PSI UNITS TO CM SEC2/g

WCOMPR1=((WCOMPR*2.54*2.54)/(453*980))
RCOMPR1=((RCOMPR*2.54*2.54)/(453*980))
HK2=(WSENSI*g*((PORO*WCOMPR1)+RCOMPR1))
HK(J,2)=HK2
HK(J,3)=PORO
READ (2,*) HT(J,1),HT(J,2),HT(J,8)
HT(J,3)=HT(J,8)*60*60*24

30 WRITE(10,2000) (HT(J,I),I=1,3)
CONTINUE
WRITE (10,3000)

```

```

C   READ LITHOLOGY TYPE
      JTP=1
40   READ (2,*) TPROW,ICCODE
      DO 50 N=1,NCOL
          IDUM(N)=ICCODE
50   CONTINUE
      DO 60 J=JTP,TPROW
          DO 60 N=1,NCOL
              IN=NROW*(N-1)+J
              J22=IDUM(N)
              HSPERM(IN)=HK(J22,1)
              JTEX(IN)=J22
60   CONTINUE
          IF(TPROW.EQ.NROW) GO TO 70
          JTP=TPROW+1
          GO TO 40
70   CONTINUE

C   BORDERS OF DOMAIN ARE ALL SET TO NO FLOW BOUNDARIES
      DO 80 I=1,NROW
          I1=NODES-I+1
          HSPERM(I)=0
          HSPERM(I1)=0
80   DO 90 I=2,NCOL
          I1=(I-1)*NROW
          HSPERM(I1)=0
          HSPERM(I1+1)=0
90   CONTINUE

      DO 120 J=1,NROW
          DO 100 N=1,NCOL
              DUM(N)=0
100  DO 110 N=1,NCOL
              IN=NROW*(N-1)+J
              Z1=VDIS(J)
              P(IN)=-Z1
              PP(IN)=P(IN)
110  CONTINUE
120  CONTINUE

C   COMPUTE INITIAL NONLINEAR COEFFICIENT VALUES
      CALL COEF
      CONTINUE

      DO 130 IN=1,NODES
          NCTYP(IN)=0
          IF(HSPERM(IN).EQ.0) GO TO 130
          WATCONZ(IN)=WATCON1(IN)
130  CONTINUE

      CC(N)=0.0
      COLD(N)=0.0
140  CONTINUE

C   COMPUTE INTERCELL PERMEABILITIES
      CALL PERMEABILITY
      RETURN
150  WRITE(*,*) MAXIT
      STOP
2000 FORMAT(9X,10(1PD12.3))
3000 FORMAT(1H,5X,14,2X,100I1)
      END

```

```

C-----
C  SUBROUTINE SEQUENCE:
C  TO CONTROL THE TIME SEQUENCE OF SIMULATION
C-----
C  SUBROUTINE SEQUENCE
C-----
C  INCLUDE 'ARRAY.DAT'
C-----

C  ADVANCE TO NEXT TIME STEP

      NTIM=NTIM+1
      IF (NTIM.NE.1.AND.JSTOP.EQ.1) RETURN
      JSTOP=0
      JPLT=0
      NIT=0
      NIT1=0
      IF(NTIM.EQ.1) KPLT=1
      IF(JFLAG.EQ.1) GO TO 10
      GO TO 70
10     CONTINUE
      KP=KP+1
      SSTATE=.FALSE.
      READ (2,*) MAXPC,ERROR
      MAXPC=ABS(MAXPC)

      CALL SOLUBILITY(CONC,DEPTH)
      WRITE(*,*) CONC,DEPTH

C-----
C  READ IN BOUNDARY CONDITIONS FOR SIMULATION
C-----

20     READ (2,*) JJJ,JJR,WRATE
      WRATED=WRATE*60*60*24

      IF(JJJ.GE.9999) GO TO 40
      CONTINUE
      DO 30 JJ=JJJ,JJR
      DO 30 NN=1,NCOL
      IN=NROW*(NN-1)+JJ
      CS(IN)=CONC
      CC(IN)=CONC
      NCTYP(IN)=1
      Z1=VDIS(JJ)
      CONTINUE
C     SET FLUX TO WATER FLUX RATE

      AREA=XXGRID(NN)
      FLUX(IN)=WRATED*AREA
30     CONTINUE
      GO TO 20
40     CONTINUE

      TMPX=TIMIN+TMAX
      IF(TMPX+.5*DELT.GT.TMAX) TMPX=TMAX

C  CALCULATE NEW COEFFICIENTS

70     IF(NTIM.NE.1)CALL COEF
      CONTINUE

C  INITIALIZE REQUIRED ARRAYS FOR BOUNDARY CONDITION, UPDATE
C  PP,WATCONZ. COMPUTE MAXIMUM PRESS. CHANGE DURING LAST TIME STEP

      PDIF=0.
      IF(NTIM.NE.1.AND..NOT.SSTATE) THEN

```

```

DO 80 J=2,NXRR
DO 80 N=2,NLYY
IN=NROW*(N-1)+J
IF(HSPERM(IN).EQ.0.) GO TO 80
P12=P(IN)-PP(IN)
PTMP=ABS(P12)
IF(PTMP.GT.PDIF)PDIF=PTMP
PP(IN)=P(IN)
WATCON2(IN)=WATCON1(IN)
80 CONTINUE

C CHECK FOR STEADY STATE
IF(PDIF.LE.ERROR) THEN
SSSTATE=.TRUE.
END IF
END IF
JFLAG=0

C INITIALIZE DHMX
DO I=1,201
DHMX(I)=0.
END DO
KPLT=KPLT+1
JPLT=1
TIMIN=TIMIN+DELT
IF(TMAX-TIMIN.LT.0.5*DELT) THEN

JSTOP=1
JPLT=1
END IF
RETURN
END

C-----
C SUBROUTINE SETUP:
C TO SET UP COEFFICIENT MATRICES AND CALL ALGORITHM.
C-----
SUBROUTINE SETUP
C-----
INCLUDE 'ARRAY.DAT'
C-----

C UPDATE COEFFICIENTS

10 I13=0
20 GO TO 30
30 CONTINUE
30 IF (NIT.NE.0) CALL COEF

C-----
C LOOP TO CALCULATE COEFFICIENT MATRIX
C-----

DO 40J=2,NXRR
DO 40I=2,NLYY
N=NROW*(I-1)+J
IF(HSPERM(N).GT.0.) THEN
JM1=N-1
JP1=N+1
IM1=N-NROW
IP1=N+NROW
VOL=XXGRID(I)*ZZGRID(J)
JJ=JTEX(N)

C CALCULATE STORAGE TERMS
Z1=VDIS(J)
PTMP=P(N)+Z1
SS=HK(JJ,2)/HK(JJ,3)
GSS=VOL*WATCON1(N)*SS
G1=0

```

```

C   APPLY NEWTON-RAPHSON LINEARIZATION TO STORAGE TERM.
      IF(NIT.GT.0.AND.XI(N).NE.0)G1=(P(N)-PP(N))*(GSF+GSS-PITT(N))/
&   XI(N)
      PITT(N)=GSS
      G1=-G1/DELT
      GSS=-GSS/DELT

C   SET THE PENTA-DIAGNOL COEFFICIENT MATRIX (E IS MAIN DIAGNOL)
C   AND RIGHT HAND SIDE
      A(N)=HPERM(N)
      B(N)=VPERM(N)
      C(N)=HPERM(IP1)
      D(N)=VPERM(JP1)
      E(N)=-A(N)-B(N)-C(N)-D(N)
      RHS(N)=VOL*(WATCON1(N)-WATCON2(N))/DELT-(FLUX(N))-A(N)
&   *P(IM1)+B(N)*P(JM1)+C(N)*P(IP1)+D(N)*P(JP1)+(E(N)+GSS)*P(N)
&   +GSS*PP(N)
      E(N)=E(N)+GSS+G1
      END IF
40   CONTINUE

C   CALL SOLUTION ALGORITHM
      NIT=NIT+1
      CALL SLVSIP
      IF(NIT.LT.MINIT) GO TO 30

C   IF SOLUTION HAS BEEN FOUND THEN RETURN
      IF(ICONVG.EQ.0) RETURN
      IF(NIT.LE.MAXIT) GO TO 30

C   RESET HEADS TO VALUES AT END OF PREVIOUS TIME STEP
      DO 50 I1=1,NODES
        IF(HSPERM(I1).GT.0) P(I1)=PP(I1)
50   CONTINUE
      NIT=1
      GO TO 10
      END

-----
C   SUBROUTINE COEF:
C   TO COMPUTE ALL VALUES OF NONLINEAR COEFFICIENT USING RECENT VALUES
C   SUBROUTINE COEF
-----
C   INCLUDE 'ARRAY.DAT'
-----
      DO 10 J=2,NXRR
        DO 10 N=2,NLYY
          IN=NROW*(N-1)+J
          IF(HSPERM(IN).GT.0.) THEN
            J1=JTEX(IN)

C   COMPUTE PRESSURE TO USE IN FUNCTIONS
            Z1=VDIS(J)
            PTHP=P(IN)+Z1
            HK(1,3)=PORO
            WATCON1(IN)=HK(1,3)
          END IF
10   CONTINUE
      RETURN
      END

```

```

-----
C
C   SUBROUTINE PERMEABILITY:
C           TO COMPUTE INTERCELL PERMEABILITIES
C-----
C   SUBROUTINE PERMEABILITY
C-----
C   INCLUDE 'ARRAY.DAT'
C-----

C   COMPUTE HARMONIC MEANS OF HSPERM

      DO 10 J=2,NROW
      DO 10 N=2,NCOL
      IN=NROW*(N-1)+J
      JM1=IN-1
      NM1=IN-NROW
      IF(HSPERM(IN).EQ.0.) GO TO 10
      AREA=XXGRID(N)

C   VERTICAL PERMEABILITY THROUGH BOTTOM

      VPERM(IN)=2.0*AREA*HSPERM(IN)*HSPERM(JM1)/(HSPERM(JM1)
& *ZZGRID(J)+HSPERM(IN)*ZZGRID(J-1))
      AREA=ZZGRID(J)

C   HORIZONTAL PERMEABILITY THROUGH LEFT-HAND SIDE

      HPERM(IN)=2.0*AREA*HSPERM(IN)*HSPERM(NM1)/(HSPERM(NM1)*XXGRID(N)
& +HSPERM(IN)*XXGRID(N-1))
10   CONTINUE
      RETURN
      END

-----
C   SUBROUTINE SOLUTION:
C           TO SOLVE THE MATRIX EQUATIONS USING THE STRONGLY IMPLICIT METHOD.
C-----
C   SUBROUTINE SOLUTION
C-----
C   INCLUDE 'ARRAY.DAT'
C-----

      DATA IORDER/1,2,3,4,5,1,2,3,4,5,11*/

C   COMPUTE ITERATION PARAMETERS

      J2=NCOL-2
      I2=NROW-2
      L2=5
      PL2=L2-1
      W=0.
      PIE=0.
      W9=100.

C   COMPUTE MAXIMUM PARAMETER

      DO 10 I=2,NXRR
      DO 10 J=2,NLYY
      N=NROW*(J-1)+I
      IF(HSPERM(N).EQ.0.) GO TO 10
      IM1=JTEX(N)
      PIE=PIE+1.
      DX=XXGRID(J)/NDIS(MCOL)
      DY=ZZGRID(I)/VDIS(NROW)
      DX3=DX*DX
      DY2=DY*DY
      W=W+1.-DMIN1((DX3+DX3)/(1.+DX3/DY2),(DY2+DY2)/
& (1.+DY2/DX3))
10   CONTINUE
      W=W/PIE

```

```

C COMPUTE PARAMETERS IN GEOMETRIC SEQUENCE
      PJ=-1.
      DO 20 I=1,L2
      PJ=PJ*1.
20    TEMP(I)=1.-(.1.-W)**(PJ/PL2)

C ORDER SEQUENCE OF PARAMETERS
      DO 30 J=1,L2
30    HM(J)=TEMP(IORDER(J))
      RETURN

C STRONGLY IMPLICIT ALGORITHM
      ENTRY SLVSIP
      I2=NROW-2
      J2=NCOL-2

C SELECT ITERATION PARAMETER. INITIALIZE ARRAYS
      NT=NIT1
      IF(MOD(NT,L2).EQ.0.OR.NT.EQ.1)NTH=0

      NTH=NTH+1
      W=HM(NTH)
      ICONVG=0
      DO 40 I=1,NODES
      SIP1(I)=0.
      SIP2(I)=0.
      SIP3(I)=0.
40    XI(I)=0.
      BIGI=0.
      BIGI1=0.

C CHOOSE SIP NORMAL OR REVERSE ALGORITHM
      IF(MOD(NT,2)) 50,80,50
C -----
C ORDER EQUATIONS WITH ROW 1 FIRST - EXAMPLE:
C 1 2 3
C 4 5 6
C 7 8 9
C -----
50    DO 60 I=2,NXRR
      DO 60 J=2,NLYY
      N=I+NROW*(J-1)

C ----- SKIP COMPUTATIONS OF NODE IS OUTSIDE OF SOLUTION DOMAIN
      IF(NSPERM(N).EQ.0.) GO TO 60

      IF(NCTYP(N).EQ.1) GO TO 60

      NL=N-NROW
      NA=N-1
      NB=N+1

C ----- SIP "NORMAL" ALGORITHM -----
C ----- FORWARD SUBSTITUTE, COMPUTING INTERMEDIATE VECTOR V -----
      CH=SIP1(NA)*B(N)/(1.+W*SIP1(NA))
      GH=SIP2(NL)*A(N)/(1.+W*SIP2(NL))
      BH=B(N)-W*CH
      DH=A(N)-W*GH
      EH=E(N)+W*CH+W*GH
      FH=C(N)-W*CH
      HH=D(N)-W*GH

```

```

ALFA=8H
BETA=0H
GAMA=EH-ALFA*SIP2(NA)-BETA*SIP1(NL)
SIP1(N)=FH/GAMA
SIP2(N)=HH/GAMA
RES=RHS(N)
SIP3(N)=(RELAX*RES-ALFA*SIP3(NA)-BETA*SIP3(NL))/GAMA
60 CONTINUE

C ----- BACK SUBSTITUTE FOR VECTOR XI -----

DO 70 I=1,I2
I3=NROW-I
DO 70 J=1,J2
J3=NCOL-J
N=I3+NROW*(J3-1)
IF(HSPERM(N).EQ.0.)GO TO 70

IF(NCTYP(N).EQ.1) GO TO 70

XI(N)=SIP3(N)-SIP1(N)*XI(N+NROW)-SIP2(N)*XI(N+1)

C FIND MAXIMUM PRESSURE CHANGE

TCHK=ABS(XI(N))
IF(TCHK.GE.BIG1) THEN
BIG1=TCHK
BIG11=XI(N)
END IF
70 CONTINUE
GO TO 110

C -----
C ORDER EQUATIONS WITH THE LAST ROW FIRST - 3X3 EXAMPLE
C       7 8 9
C       4 5 6
C       1 2 3
C -----

80 DO 90 II=1,I2
I=NROW-II
DO 90 J=2,NLII
N=I+NROW*(J-1)
NL=N-NROW
NA=N-1
NB=N+1

C ----- SKIP COMPUTATIONS IF NODE IS OUTSIDE OF SOLUTION DOMAIN

IF(HSPERM(N).EQ.0.) GO TO 90
IF(NCTYP(N).EQ.1) GO TO 90

C ----- SIP "REVERSE" ALGORITHM -----
C ----- FORWARD SUBSTITUTE, COMPUTING INTERMEDIATE VECTOR V

CH=SIP1(NB)*D(N)/(1.+W*SIP1(NB))
GH=SIP2(NL)*A(N)/(1.+W*SIP2(NL))
BH=D(N)-W*CH
DH=A(N)-W*GH
EH=E(N)+W*CH+W*GH
FH=C(N)-W*CH
HH=B(N)-W*GH
ALFA=BH
BETA=DH
GAMA=EH-ALFA*SIP2(NB)-BETA*SIP1(NL)
SIP1(N)=FH/GAMA
SIP2(N)=HH/GAMA
RES=RHS(N)
SIP3(N)=(RELAX*RES-ALFA*SIP3(NB)-BETA*SIP3(NL))/GAMA
90 CONTINUE

```

```

C -- BACK SUBSTITUTE FOR VECTOR XI
      DO 100 I3=2,NXRR
      DO 100 J=1,J2
      J3=NCOL-J
      N=I3+NROW*(J3-1)
      IF(HSPERM(N).EQ.0.) GO TO 100
      IF(NCTYP(N).EQ.1) GO TO 100

      XI(N)=SIP3(N)-SIP1(N)*XI(N+NROW)-SIP2(N)*XI(N-1)

C   FIND MAXIMUM PRESSURE CHANGE
      TCHK=ABS(XI(N))
      IF(TCHK.GE.BIGI) THEN
      BIGI=TCHK
      BIGI1=XI(N)
      END IF
100   CONTINUE

C   COMPUTE RELAXATION PARAMETER W FOR PRESSURE CHANGES. ALGORITHM
C   IS FROM COOLEY (1983)
110   S=1.
      IF(NT.GT.1.AND.W1.NE.0.0) S=BIGI1/W1
      S1=ABS(S)
      IF(S.LT.-1.) THEN

      W=1./(S1+S1)
      ELSE

      W=(3+S)/(3+S1)
      END IF

      IF(W.EQ.W9) W=.9*W
      W1=W*BIGI
      IF(W1.GT.MAXPC) W=MAXPC/BIGI
      IF(BIGI1.LT.0) W1=-W1

C   ADD CHANGES TO PRESSURE MATRIX
      W9=W
      IF(TRANSP) THEN
      DO 140 N=NROW+1,NODES
      IF(HSPERM(N).GT.0.) CC(N)=CC(N)+W*XI(N)
140   CONTINUE
      IF(BIGI.GT.ERROR1) ICONVG=1
      ELSE
      DO 145 N=NROW+1,NODES
      IF(HSPERM(N).GT.0) P(N)=P(N)+W*XI(N)
145   CONTINUE

C   COMPARE MAXIMUM PRESSURE CHANGE TO CLOSURE CRITERION.
      IF(BIGI.GT.ERROR) ICONVG=1
      DHMX(NIT)=BIGI
      END IF
      RETURN
4000  FORMAT(1X,15,25HSP ITERATION PARAMETERS: ,6D15.7/(28X,6D15.7//)
      END

C-----
C SUBROUTINE MASS:
C           TO COMPUTE FLUXES AND MASS BALANCE
C-----
      SUBROUTINE MASS
C-----
      INCLUDE 'ARRAY.DAT'
C-----

C   INITIALIZE BALANCE VARIABLES USED FOR ENTIRE SIMULATION
      IF(NTIM.EQ.1) THEN

```

```

DO 10 I=1,72
  BL(I)=0.
10 CONTINUE
END IF

C INITIALIZE MASS BALANCE VARIABLES USED FOR CURRENT
C TIME STEP

  BLTEMP=0
  BL(9)=0.
  BL(12)=0.
  BL(68)=0.
  DO 20 J=2,NXRR
  DO 20 N=2,NLYY
  IN=NROW*(N-1)+J
  IF(HSPERM(IN).EQ.0.) GO TO 20
  JM1=IN-1
  JP1=IN+1
  NM1=IN-NROW
  NP1=IN+NROW
  VOL=XXGRID(N)*ZZGRID(J)

C SUM CHANGE IN STORAGE

  GSF=VOL*(WATCON1(IN)-WATCON2(IN))
  JJ=JTEX(IN)
  SS=HK(JJ,2)/HK(JJ,3)
  GSS=VOL*WATCON1(IN)*SS

  BL(68)=BL(68)+VOL*(
& CC(IN)*WATCON1(IN)*(1+SS*P(IN))-COLD(IN)*WATCON2(IN)*
& (1+SS*P(IN)))

  SS=-HT(JJ,4)*(WATCON1(IN)+WATCON1(IN)*P(IN)*SS)*DELT

  BL(62)=BL(62)+ VOL*SS*CC(IN)
  BLTEMP=BLTEMP

  IP2=NP1-1
  IM2=NM1+1
  IM3=NM1-1
  IP3=NP1+1
  TS=(DX1(NP1)*(CC(IN)-CC(NP1))-DX2(NP1)*(.5)*(
& CC(JP1)-CC(JM1)+CC(IP3)-CC(IP2)))
& +(DX1(IN)*(CC(IN)-CC(NM1))+DX2(IN)*(.5)*(
& CC(JP1)-CC(JM1)+CC(IM2)-CC(IM3)))
& +(DZ1(JP1)*(CC(IN)-CC(JP1))-DZ2(JP1)*(.5)*(
& CC(NP1)-CC(NM1)+CC(IP3)-CC(IM2)))
& +(DZ1(IN)*(CC(IN)-CC(JM1))+DZ2(IN)*(.5)*(
& CC(NP1)-CC(NM1)+CC(IP2)-CC(IM3)))

C CALCULATE FLUX RATES ACROSS DOMAIN BOUNDARIES
C FLUX FOR NEUMAN CELLS

  IF(FLUX(IN).LE.0) THEN
  BL(12)=BL(12)+FLUX(IN)
  BL(45)=BL(45)+FLUX(IN)*CC(IN)
  ELSE
  BL(9)=BL(9)+FLUX(IN)
  BL(42)=BL(42)+FLUX(IN)*CS(IN)
  END IF
20 CONTINUE

C TRANSPORT MASS BALANCE COMPONENTS

  BL(67)=BL(67)+BL(68)
  BL(65)=BLTEMP-BL(64)
  BL(64)=BLTEMP
  BL(54)=BL(36)+BL(42)+BL(48)

```

```

DO 40 I=35,59,3
  BL(I)=DELT*BL(I+1)
40  CONTINUE
  BL(52)=BL(52)+BL(53)

  WRITE (15,1000) (BL(M),M=52,53)
  WRITE (15,2000) (BL(M),M=67,68)

1000  FORMAT(2X,'TOTAL FLUX INTO DOMAIN ',
& 15X,2(1PE15.5,5X)/)

2000  FORMAT(2X,' CHANGE IN SOLUTE STORED IN DOMAIN -- ',
& 2(1PE15.5,5X)/)

  RETURN
  END

C-----
C  SUBROUTINE OUTPUT:
C  TO DISPLAY OUTPUT RESULTS
C-----
  SUBROUTINE OUTPUT
C-----
  INCLUDE 'ARRAY.DAT'
C-----

  IF(NTIM.EQ.0) GO TO 10
  IF(JSTOP.EQ.1.OR.JPLT.EQ.1.) GO TO 10
  IF(JFLAG.EQ.0.)RETURN
10  WRITE(10,4000) TIMIN/365.0,NTIM

C  PRINT CONCENTRATION

  WRITE(10,5000)
  CALL PRINT2D(1,CC)
130  CONTINUE
  RETURN

4000  FORMAT(10X,/5X,20HTOTAL ELAPSED TIME =,1PE12.3/10X,
& 10HTIME STEP ,15,/)

5000  FORMAT(51X,' CONCENTRATION')
  END

C-----
C  SUBROUTINE PRINT2D:
C  TO PRINT TWO DIMENSIONAL ARRAYS
C-----
  SUBROUTINE PRINT2D(IV,VPRNT)
C-----
  INCLUDE 'ARRAY.DAT'
C-----

  WRITE (10,1000)
  WRITE (10,2000) (HDIS(I)/100,I=2,NLYY)
  DO 30 J=2,NXRR
  DO 10 N=2,NLYY
  IN=NROW*(N-1)+J
  DUM1(N)=VPRNT(IN)
  IF(HSPERM(IN).EQ.0.) DUM1(N)=0.
10  CONTINUE
  WRITE(10,3000) ((DEPTH)-(VDIS(J))/100),(DUM1(N)*1E6,N=2,NLYY)
30  CONTINUE
  RETURN

```

```

1000  FORMAT(1H,1X,9HDEPTH (m)/2X,10X,19HHORZ DISTANCE (m) )
2000  FORMAT(1H,18X,13(F12.3)/(19X,13(F12.3)))
3000  FORMAT(1X,F10.3,10X,13(1PE9.2)/(19X,13(1PE9.2)))
4000  FORMAT(1X,F8.2,10X,13F9.3/(9X,13F9.3))
      END

```

```

-----
C  SUBROUTINE SOLUBILITY (CONC,DEPTH):
C      TO CALCULATE THE INITIAL LIGHT HC CONCENTRATION IN WATER
C-----
      SUBROUTINE SOLUBILITY (CONC,DEPTH)
C-----
      WRITE(*,*) 'ENTER TYPE OF LIGHT HC METHANE-? 1-? '
      READ(*,*) TYPE

```

```

      IF(TYPE.EQ.1) GO TO 10
      IF(TYPE.EQ.2) GO TO 20
      IF(TYPE.EQ.3) GO TO 30
      IF(TYPE.EQ.4) GO TO 40
      IF(TYPE.EQ.5) GO TO 50
      IF(TYPE.EQ.6) GO TO 60
      IF(TYPE.EQ.7) GO TO 70
      IF(TYPE.EQ.8) GO TO 80

```

```

C      CO*1E-6 TO CONVERT TO g/cm3

```

```

10      CO=24.1*1E-6
      CONC=CO*DEPTH/10.16
      RETURN

```

```

20      CO=60.4*1E-6
      CONC=CO*DEPTH/10.16
      RETURN

```

```

30      CO=1.
      CONC=CO*1/1.
      RETURN

```

```

40      CO=48.9*1E-6
      CONC=CO*DEPTH/10.16
      RETURN

```

```

50      CO=38.5*1E-6
      CONC=CO*DEPTH/10.16
      RETURN

```

```

60      CO=9.5*1E-6
      CONC=CO*DEPTH/10.16
      RETURN

```

```

70      CO=2.9*1E-6
      CONC=CO*DEPTH/10.16
      RETURN

```

```

80      CO=.66*1E-6
      CONC=CO*DEPTH/10.16
      RETURN

```

```

      END

```

```

-----
C  SUBROUTINE TVELO:
C      TO CALCULATE WATER VELOCITY
C-----
      SUBROUTINE TVELO
C-----
      INCLUDE 'ARRAY.DAT'
C-----

```

```

DO 10 I=2,NLYY
N1=NROW*(I-1)
DO 10 J=2,NXRR
N=N1+J
VX(N)=0
VZ(N)=0
IF(HSPERM(N).NE.0) THEN
JM1=N-1
IM1=N-NROW
IF(HSPERM(JM1).NE.0) THEN

```

C CALC. VERTICAL VELOCITY

```

AREA=XXGRID(I)
GRAD=P(JM1)-P(N)
THETA1=.5*(WATCON1(N)+WATCON1(JM1))*AREA

VZ(N)=VPERM(N)*GRAD/THETA1
END IF
END IF
IF(HSPERM(IM1).NE.0) THEN

```

C CALC. HORIZONTAL VELOCITY

```

GRAD=P(IM1)-P(N)
AREA=ZZGRID(J)
THETA1=.5*(WATCON1(N)+WATCON1(IM1))*AREA

VX(N)=HPERM(N)*GRAD/THETA1
END IF

```

```

10 CONTINUE
RETURN
END

```

```

C-----
C SUBROUTINE TCOEF:
C TO CALCULATE DISPERSION COEFFICIENTS AS A FUNCTION OF
C DISPERSIVITIES AND VELOCITIES
C-----

```

SUBROUTINE TCOEF

```

C-----
INCLUDE 'ARRAY.DAT'
C-----

```

```

DO 10 I=2,NLYY
N1=NROW*(I-1)
DO 10 J=2,NXRR
N=N1+J
DX1(N)=0
DX2(N)=0
DZ1(N)=0
DZ2(N)=0
PEX=0.
PEZ=0.
IMX=0
JMX=0
IMZ=0
JMZ=0
IF(HSPERM(N).NE.0) THEN
N2=JTEX(N)
ALPHAL=HT(N2,1)
ALPHAT=HT(N2,2)
DIFF=HT(N2,3)
V1=VX(N)
V2=VZ(N)
JM1=N-1

```

```

IM1=N-NROW
JP1=N+1
IP1=N+NROW
IP2=IP1-1
IM2=IM1+1
IF(HSPERM(JM1).NE.0) THEN
V3=.25*(V1+VX(IP1)+VX(IP2)+VX(JM1))
V32=V3*V3
V22=V2*V2
VV2=V32+V22

```

C CALC. DZ1 AND DZ2

```

N2=JTEX(JM1)
ALPHAL1=DSQRT(AL*HT(N2,1))
ALPHAT1=DSQRT(AT*HT(N2,2))
DIFF1=DSQRT(DIFF*HT(N2,3))
AREA=XXGRID(I)
T1=.5*(WATCON1(JM1)+WATCON1(N))
DD1=(VDIS(J)-VDIS(J-1))/AREA
T2=T1/DD1
IF(VV2.EQ.0.) THEN
DZ1(N)=DIFF1
ELSE
VAVE=DSQRT(VV2)
DL=ALPHAL1*VAVE
DT=ALPHAT1*VAVE
DZ1(N)=(DL*V22+DT*V32)/VV2+DIFF1
DD1=(HDIS(I+1)-HDIS(I-1))/AREA
DZ2(N)=T1*(DL-DT)*V2*V3/(DD1*VV2)
END IF
END IF

```

C CALC. DX1 AND DX2

```

N2=JTEX(IM1)
ALPHAL1=DSQRT(ALPHAL*HT(N2,1))
ALPHAT1=DSQRT(ALPHAT*HT(N2,2))
DIFF1=DSQRT(DIFF*HT(N2,3))
AREA=ZZGRID(J)
DD1=(HDIS(I)-HDIS(I-1))/AREA
T1=.5*(WATCON1(IM1)+WATCON1(N))

T2=T1/DD1
IF(VV2.EQ.0.) THEN
DX1(N)=DIFF1
ELSE
VAVE=DSQRT(VV2)
DL=ALPHAL1*VAVE
DT=ALPHAT1*VAVE
DX1(N)=(DL*V12+DT*V32)/VV2+DIFF1
DD1=(VDIS(J+1)-VDIS(J-1))/AREA
DX2(N)=T1*(DL-DT)*V1*V3/(DD1*VV2)
END IF
END IF
10 CONTINUE

RETURN
END

```

```

C-----
C  SUBROUTINE TSETUP:
C      TO SOLVE MATRIX EQUATION FOR ADVECTION-DISPERSION EQUATION
C      AND CALL MATRIX SOLVER
C-----
      SUBROUTINE TSETUP
C-----
      INCLUDE 'ARRAY.DAT'
C-----

      IF(NTIM.EQ.1) THEN
        JFLAG1=1
        DO 10 N=1,NODES
          AO(N)=0
          BO(N)=0
          CO(N)=0
          DO(N)=0
          EO(N)=0
10      CONTINUE
        END IF

C  INITIALIZE VARIABLES

        DO 20 I=2,NLYY
          N1=NROW*(I-1)
          DO 20 J=2,NXRR
            N=N1+J

            A(N)=0
            B(N)=0
            C(N)=0
            D(N)=0
            E(N)=0
            RHS(N)=0
            COLD(N)=CC(N)
            IF(HSPERM(N).NE.0) THEN
              N2=JTEX(N)
              IM1=N-NROW
              JM1=N-1
              JP1=N+1
              IP1=N+NROW
              IP2=IP1-1
              IM2=IM1+1
              IM3=IM1-1
              IP3=IP1+1
              AREAX=ZZGRID(J)
              AREAX1=AREAX
              AREAZ=XXGRID(I)
              VOL=AREAZ*ZZGRID(J)
              AREAX=AREAX*.5*(WATCON1(IM1)+WATCON1(N))
              AREAX1=AREAX1*.5*(WATCON1(IP1)+WATCON1(N))
              AREAZ1=AREAZ*.5*(WATCON1(JP1)+WATCON1(N))
              AREAZ=AREAZ*.5*(WATCON1(JM1)+WATCON1(N))
            END IF

C  CALC. LHS OF MATRIX EQUATION

            SS=WATCON1(N)*P(N)*HK(N2,2)/HK(N2,3)
            E(N)=-DX1(N)-DZ1(N)-DX1(IP1)-DZ1(JP1)
            & -VOL*(HT(N2,4)*(WATCON1(N)+SS))

            SS=WATCON1(N)+SS+SS-WATCON2(N)*(1+PP(N)*HK(N2,2)/HK(N2,3))
            IF(HSPERM(IM1).NE.0) THEN
              A(N)=OX1(N)+.5*(+OZ2(N)-OZ2(JP1))
              VV=AREAX*.5*VX(N)
              A(N)=A(N)+VV
              E(N)=E(N)+VV
            END IF

```

```

      IF(HSPERM(JM1).NE.0) THEN
      B(N)=DZ1(N)+.5*(+DX2(N)-DX2(IP1))

      VV=AREA2*.5*VZ(N)
      B(N)=B(N)+VV
      E(N)=E(N)+VV
      END IF

      IF(HSPERM(IP1).NE.0) THEN
      C(N)=DX1(IP1)+.5*(-DZ2(N)+DZ2(JP1))
      VV=.5*AREAX1*VX(IP1)
      C(N)=C(N)-VV
      E(N)=E(N)-VV
      END IF

      IF(HSPERM(JP1).NE.0) THEN
      D(N)=DZ1(JP1)+.5*(-DX2(N)+DX2(IP1))

      VV=.5*AREA21*VZ(JP1)
      D(N)=D(N)-VV
      E(N)=E(N)-VV
      END IF

      E(N)=E(N)

      IF(FLUX(N).LT.0.) E(N)=E(N)+FLUX(N)
20    CONTINUE

C    BEGIN LOOP TO CALCULATE RHS AND CALL MATRIX SOLVER

      DO 50 IT=1,MAXIT
      DO 30 I=2,NLYY
      N1=NROW*(I-1)
      DO 30 J=2,NXRR
      N=N1+J
      IM1=N-NROW
      JM1=N-1
      JP1=N+1
      IP1=N+NROW
      IP2=IP1-1
      IM2=IM1+1
      IM3=IM1-1
      IP3=IP1+1
      VOL=ZZGRID(J)*XXGRID(I)
      N2=JTEX(N)

      IF(IT.GT.1) THEN
      IF(JFLAG.NE.1) THEN
      T1=.5
      ELSE
      T1=1.
      END IF
      E(N)=E(N)
      END IF

C    CALC.  RHS OF MATRIX EQUATIONS

      RHS(N)=-VOL*(WATCON1(N)*(1+P(N)*HK(N2,2)/HK(N2,3))*COLD(N)/
& DELT+.5*(DX2(N)*(CC(IM2)-CC(IM3))+
& DX2(IP1)*(CC(IP2)-CC(IP3))+DZ2(N)*(CC(IP2)-CC(IM3))
& +DZ2(JP1)*(CC(IM2)-CC(IP3)))-A(N)*CC(IM1)-B(N)*CC(JM1)
& -C(N)*CC(IP1)-D(N)*CC(JP1) E(N)*CC(N)

30    IF(FLUX(N).GT.0.) RHS(N)=RHS(N)-FLUX(N)*CS(N)
      CONTINUE
      NIT1=NIT1+1

```

```

C      CALL MATRIX SOLVER

      CALL SLVSIP
      IF(ICONVG.EQ.0) THEN
      DO 40 I=2,NLYY
      N1=NROW*(I-1)
      DO 40 J=2,NXRR
      N=N1+J
      IF(HSPERM(N).EQ.0) GO TO 40
      AD(N)=A(N)
      BD(N)=B(N)
      CD(N)=C(N)
      DD(N)=D(N)

      AREAZ=XXGRID(1)
      VOL=AREAZ*ZZGRID(J)
      N2=JTEX(N)
      SS=HK(N2,2)/HK(N2,3)
      SS=WATCON1(N)*(1+(SS+SS)*P(N))-WATCON2(N)*(1+SS*PP(N))

      EO(N)=E(N)+VOL*(WATCON1(N)+SS)/DELT
40    CONTINUE
      JFLAG1=JFLAG
      RETURN
      END IF
50    CONTINUE
      JFLAG1=JFLAG
      WRITE(10,4000)

      JSTOP=1
      JFLAG=1
      RETURN
4000  FORMAT(' MAXIMUM NO. OF ITERATIONS EXCEEDED FOR TRANSPORT'
& ' EQUATION')
      END

```

```

-----
C
C      SUBROUTINE COMPRESSIBILITY:
C              TO CALCULATE THE WATER COMPRESIBILITY AND ASSIGN ROCK
C              COMPRESSIBILITY USING VAN DER KNAAP EQUATION
C
-----

```

```

      SUBROUTINE COMPRESSIBILITY ( DISTANCE,NLITHO,WCOMPR,RCOMPR)
-----

```

```

C      CHOOSE C VALUES C=3.0E-13 FOR SS, SHALE
C              C=4.5E-3  LS
C
      WRITE (*,*) 'ENTER C VALUES EITHER 3.0E-13 OR 4.5E-3'

      READ (*,*) C

      WRITE (*,*) 'HOW MANY LITHOLOGIES IN THIS RUN'
      READ (*,*) NLITHO
      DO 101 I=1,NLITHO
      WRITE (*,*) 'WHAT DEPTH TO EACH LITHOLOGY IN METERS'
      READ (*,*) DISTANCE
      WRITE (*,*) 'WHAT IS THE DENSITY OF EACH LITHOLOGY'
      READ (*,*) RDENSI

      STRESS=(.433*354/(2.54*2.54))*WDENSI*DISTANCE*100
101  CONTINUE

```

```
WCOMPR=STRESS*(C**-.7)/1.45E2
RCOMPR=.6*WCOMPR
WRITE (*,*) RCOMPR

RETURN
END

C-----
C
C SUBROUTINE WVISCOSITY:
C TO CALCULATE WATER VISCOSITY AT AN AVERAGE TEMP.
C-----

SUBROUTINE WATERVISCOSITY (WVISCO,WDENSI)
C-----

WRITE(*,*) 'ENTER THE AVERAGE TEMPERATURE IN KELVINS'
READ (*,*) TEMP

TC=647.3
S=.552
TR=TEMP/TC

C WATER VISCOSITY IN CP UNITS

WVISCO1=(WDENSI**.5)*10**S*(1/TR-1)/8.569

C WATER VISCOSITY IN G/CN.SEC UNITS

WVISCO=WVISCO1/100.

RETURN
END

C-----
```

13.0 APPENDIX 2 - Gas Phase Transport Computer Code

```

C-----
C
C   PROGRAM TO SOLVE VERTICAL MIGRATION OF LIGHT HYDROCARBONS
C   BY DISPLACING WATER IN THE OVERLYING POROUS MEDIA
C-----

```

```

C-----VARIABLES-----

```

```

C   DEPTH:   DEPTH TO RESERVOIR
C   NROW:    NUMBER OF VERTICAL ROWS
C   TMAX:    MAXIMUM SIMULATION TIME
C   TIMIN:   INITIAL TIME
C   DELT:    TIME INCREMENT
C   WPOTN:   INITIAL WATER POTENTIAL
C   GPOTN:   INITIAL HC GAS POTENTIAL
C   ITMAX:   MAXIMUM ITERATIONS
C   WDENSI:  WATER DENSITY
C   GDENSI:  HC GAS DENSITY
C   WVISCO:  WATER VISCOSITY
C   GVISCO:  HC GAS VISCOSITY
C   RPRESS:  RESERVOIR PRESSURE POTENTIAL

```

```

C-----

```

```

      IMPLICIT DOUBLE PRECISION (A-H,P-Z)
      COMMON A,B,C,D
      DIMENSION A(1000),B(1000),C(1000),D(1000)
      DIMENSION E(1000),F(1000),G(1000),P(1000),R(1000),Sw(1000),
& SP(1000),GREL(1000),WREL(1000),QG(1000),QW(1000),GPOT(1000),
& WPOT(1000),POLD(1000),ROLD(1000)

```

```

      DIMENSION GPOTX(1000),WPOTX(1000),QG(1000),QW(1000)
      DIMENSION DISTANCE(1000),DISTANCE1(1000)
      DIMENSION SOLD(1000),Sg(1000)

```

```

      CHARACTER*30 DISPLACEMENT
      WRITE(*,*) 'ENTER NAME OF INPUT FILE'
      READ (*, '(a)') DISPLACEMENT
      OPEN (3, FILE=DISPLACEMENT, STATUS='OLD')

```

```

C-----READ AND WRITE SIMULATION DATA-----

```

```

      READ (3,*)      DEPTH,NROW
      READ (3,*)      WPOTN,GPOTN
      READ (3,*)      WDENSI
      READ (3,*)      GDENSI
      READ (3,*)      IRPRNT,NTSTEP
      READ (3,*)      TMAX,DELT,TZERO
      READ (3,*)      C1,C2,ITMAX
      WRITE (*,*)     'ENTER THE RESERVOIR PRESSURE POTENTIAL'
      READ (*,*)      RPRESS

```

```

C   CALL SUBROUTINES FOR INITIAL DATA AND TO PERFORM CALCULATIONS

```

```

WRITE (*,*) 'PLEASE ENTER NLITHO'
READ (*,*) NLITHO
CALL GASVISCO (TMASS,GDENSI,GVISCO,TEMP)
CALL WVISCOSITY (WDENSI,WDENSI,TEMP)
CALL AVERAGE (NLITHO,PORO,PERM)

```

C COMPUTE CONSTANTS AND CONVERSION FACTORS

```

DX=1.0/(NROW-1)
DXSQ=DX*DX
F1=1.0E-3*3600.0*24.0/((2.54*12.0)**2*14.7)
DTDIM=F1*DELT*PERM*WPOTN/(DEPTH*DEPTH*PORO*WVISCO)
F2=DX*DX/DTDIM
F3=WVISCO/GVISCO
F4=4.0*F2
F5=(NROW-1)**2
F6=F3*F5
F7=(WDENSI-GDENSI)*DEPTH/(WPOTN*144.0*(NROW-1))
F8=WVISCO/WVISCO
C1=C1/WPOTN
C2=C2/WPOTN

```

C-----OUTPUT STATEMENTS-----

```

WRITE (8,1000) PERM,DELT/365.0,TZERO,TMAX/365.0
WRITE (8,2000) NROW
WRITE (8,3000) DEPTH*.3,WPOTN,GPOTN
WRITE (8,4000) ((GDENSI*453)/(30.48*30.48*30.48)),
& ((WDENSI*453)/(30.48*30.48*30.48)),GVISCO*.01,
& WVISCO*.01,PORO

```

C-----FORMAT STATEMENTS-----

```

1000 FORMAT (5X,15HPERMEABILITY = ,F15.10/
& 5X,17HTIME INCREMENT = ,F10.4/
& 5X,17HINITIAL TIME = ,F10.4/
& 5X,26HMAXIMUM SIMULATION TIME = ,F10.4//)

2000 FORMAT (5X,7HNROW = ,I5)

3000 FORMAT (5X,8HDEPTH = ,F10.4/
& 5X,8HWPOTN = ,F10.4/
& 5X,8HGPOTN = ,F10.4/)

4000 FORMAT (5X,14HGAS DENSITY = ,F10.4/
& 5X,16HWATER DENSITY = ,F10.4/
& 5X,16HGAS VISCOSITY = ,F10.4/
& 5X,18HWATER VISCOSITY = ,F10.4/
& 5X,11HPOROSITY = ,F10.4/)

```

C-----INITIALIZE ARRAYS-----

```

C
CALL INPUT (GPOTN,WPOTN,GPOT,WPOT,F7,GPOTX,WPOTX,
& C1,C2,Sw,GREL,WREL,NROW,SOLD,Sg,qg,qgx,qw,qwx)
C-----

DO I=1,NROW-1
P(I)=0.5*(GPOT(I)+WPOT(I))
R(I)=0.5*(GPOT(I)-WPOT(I))
END DO

CALL UPDATE (GPOT,WPOT,F7,C1,C2,Sw,SP,GREL,WREL,NROW,SOLD,Sg)
KPRINT=IRPRINT-1
KPUNCH= -1

```

```

C   START COMPUTING FOR SUCCESSIVE TIME STEPS
      DO 200 T= TZERO,TMAX,DELT
          KPRINT=KPRINT+1
          KPUNCH=KPUNCH+1

C   SAVE P AND R AT START OF TIME STEP
          SAVPHI=GPOT(1)
          DO I=1,NROW-1
              POLD(I)=P(I)
              ROLD(I)=R(I)
          END DO

          DO 100 ITER=1,ITMAX

C   FIND NEW POTENTIALS FROM P AND R
          DO I=1,NROW-1
              GPOTX(I)=P(I)+R(I)
              WPOTX(I)=P(I)-R(I)
          END DO

C   ADJUST HC GAS POTENTIAL
          CALL QTERMS (GPOTX,WPOTX,NROW,OGX,OWX,F5,F6,F8,GREL,WREL)
          CALL NEWP (ITER,NROW,OG,OW,OGX,OWX,GPOT,GPOTX,SAVPHI)

          IF(ITER.NE.2) THEN

          DO I=1,NROW-1
              GPOT(I)=GPOTX(I)
              WPOT(I)=WPOTX(I)
          END DO
          END IF

C   UPDATE Sw, AND OBTAIN GREL,WREL,DS/dPC AND E,F AS A FUNCTION OF SATURATION
          CALL UPDATE (GPOT,WPOT,F7,C1,C2,Sw,SP,GREL,WREL,NROW,SOLD,Sg)
          CALL SOLUTIONEF (E,F,NROW,F3,GREL,WREL)

C   PRINT RESULTS WHEN APPROPRIATE
          IF(KPRINT.EQ.IRPRNT) THEN
              IF(ITER.EQ.1.) KPRINT=0

              WRITE (8,1100) T/365.0
              WRITE (8,1200) OG(1),OG(NROW-1),ITER

              DO I=NROW-1,1,-1
                  DIST=OX
                  DISTANCE(I)= (DIST*I)

                  DISTANCE1(I)=DISTANCE(I)*DEPTH
              END DO

              WRITE (8,1300) I,DEPTH,GPOTENTIAL,WATER SAT,GAS SAT

              WRITE (8,1400) (I,DISTANCE(I),DISTANCE1(I)*.33,GPOTX(I)*WPOTN,
& WPOTX(I)*WPOTN,Sw(I),Sg(I),I=NROW,0,-2)

          END IF

          IF(KPUNCH.EQ.NTSTEP.AND.ITER.EQ.1) THEN
              KPUNCH=0

```

```

      END IF
      IF(T.GT.TMAX) GO TO 25
25    WRITE (*,*) 'PROGRAM IS TERMINATED'

C    SOLVE LEA-FROG 'R' EQUATION
      CALL SOLUTIONP (E,F,F4,SP,QG,QW,G,DXSQ,P,ROLD,NROW)
      CALL TRIDAG (1,NROW-1,R)

C    SOLVE LEAP-FROG 'P' EQUATION
      CALL SOLUTIONR (E,F,QG,QW,DXSQ,R,NROW)
      CALL TRIDAG (1,NROW-2,P)
      P(NROW-1)=0.0

100   CONTINUE

C    FIND GAS WELL POTENTIAL AT END OF TIME INCREMENT
      GPOT(0)=BASE
      GPOTX(0)=GPOT(0)

200   CONTINUE

1100  FORMAT (10X,/F20.6//)
1200  FORMAT (20X,2F20.7,10X,13//)
1300  FORMAT (15,15,3F15.5)

1400  FORMAT (15,2F10.2,2F15.5,5X,F5.4,5X,F6.5/)

      END

C-----
      SUBROUTINE INPUT (GPOTN,WPOTN,GPOT,WPOT,F7,GPOTX,WPOTX,
&                     C1,C2,SW,GREL,WREL,NROW,SOLD,Sg,QG,QGX,QW,QWX)
C-----

C    TO READ INITIAL INPUT DATA
      IMPLICIT DOUBLE PRECISION (A-H,P-Z)

      DIMENSION E(1000),F(1000),G(1000),P(1000),R(1000),SW(1000),
& SP(1000),GREL(1000),WREL(1000),QG(1000),QW(1000),GPOT(1000),
& WPOT(1000),POLD(1000),ROLD(1000)

      DIMENSION GPOTX(1000),WPOTX(1000),QGX(1000),QWX(1000)
      DIMENSION SOLD(1000),Sg(1000)

      DO I=0,NROW
          WPOT(I)=1.0
          WPOTX(I)=1.0
      END DO

      DO I=0,NROW
          GPOT(I)=GPOTN/WPOTN
          GPOTX(I)=GPOTN/WPOTN
      END DO

      DO I=1,NROW-1
          QG(I)=0.0
          QW(I)=0.0
      END DO

```

```

DO I=1,NROW-1
  QGX(I)=0.0
  QWX(I)=0.0
END DO

DO I=1,NROW-1

  PC=GPOT(I)-WPOT(I)+F7*(I-0.5)
  Sw(I)=C1/(PC+C2)
  WREL(I)=Sw(I)**4
  GREL(I)=(1.0-Sw(I))**2

END DO

DO I=1,NROW-1
  SOLD(I)=Sw(I)
END DO

RETURN
END

```

```

C-----
C      SUBROUTINE UPDATE (GPOT,WPOT,F7,C1,C2,Sw,SP,GREL,WREL,NROW,SOLD,Sg)
C-----

```

C UPDATING THE ARRAYS Sw,GREL,WREL,GPOT,WPOT AT EVERY GRID POINT

IMPLICIT DOUBLE PRECISION (A-H,P-Z)

```

DIMENSION E(1000),F(1000),G(1000),P(1000),R(1000),Sw(1000),
& SP(1000),GREL(1000),WREL(1000),QG(1000),QW(1000),GPOT(1000)
& WPOT(1000),POLD(1000),ROLD(1000)

```

DIMENSION SOLD(1000),Sg(1000)

DO I=1,NROW-1

```

  PC=GPOT(I)-WPOT(I)+F7*(I-0.5)
  Sw(I)=C1/(PC+C2)
  Sg(I)=SOLD(I)-Sw(I)
  SP(I)=C1/(PC+C2)**2
  WREL(I)=0.001+Sw(I)**2
  GREL(I)=0.001+(1.0-Sw(I))**2

```

END DO

RETURN

END

```

C-----
C      SUBROUTINE QTERMS (GPOT,WPOT,NROW,QG,QW,F5,F6,F8,GREL,WREL)
C-----

```

C COMPUTING INJECTION AND WITHDRAWAL RATES
C POTENTIALS ARE ADJUSTED BY CONSTANT AMOUNT

IMPLICIT DOUBLE PRECISION (A-H,P-Z)

```

DIMENSION E(1000),F(1000),G(1000),P(1000),R(1000),Sw(1000),
& SP(1000),GREL(1000),WREL(1000),QG(1000),QW(1000),GPOT(1000),
& WPOT(1000),POLD(1000),ROLD(1000)
DIMENSION GPOTX(1000),WPOTX(1000),QGX(1000),QWX(1000)

```

```

ZNUM=GREL(1)*(GPOT(0)-GPOT(1))+GREL(NROW-1)*(GPOT(NROW)-
& GPOT(NROW-1)) +F8*WREL(NROW-1)*(WPOT(NROW)-WPOT(NROW-1))

```

```

DEN=GREL(1)+GREL(NROW-1)+FB*WREL(NROW-1)
W=ZNUM/DEN

DO I=1,NROW-1
  WPOT(I)=WPOT(I)+W
  GPOT(I)=GPOT(I)+W
END DO

QG(1)=F6*GREL(1)*(GPOT(0)-GPOT(1))
QG(NROW-1)=F6*GREL(NROW-1)*(GPOT(NROW)-GPOT(NROW-1))
QW(NROW-1)=F5*WREL(NROW-1)*(WPOT(NROW)-WPOT(NROW-1))

RETURN
END

```

```

C-----
SUBROUTINE NEWO (ITER,NROW,QG,QW,QGX,QWX,GPOT,GPOTX,SAVPHI)
C-----

```

C CALCULATING THE NEW INJECTION RATES USING ITERATIVE SCHEME

IMPLICIT DOUBLE PRECISION (A-H,P-Z)

```

DIMENSION E(1000),F(1000),G(1000),P(1000),R(1000),Sw(1000),
& SP(1000),GREL(1000),WREL(1000),QG(1000),QW(1000),GPOT(1000),
& WPOT(1000),POLD(1000),ROLD(1000)

```

```

DIMENSION GPOTX(1000),WPOTX(1000),QGX(1000),QWX(1000)
DIMENSION QGA1(1000),QGA2(1000),QGB1(1000),QGB2(1000),
& QWA1(1000),QWA2(1000),QWB1(1000),QWB2(1000)

```

IF(ITER.EQ.1) THEN

```

QG(1)=(QGX(1)+QG(1))/2.0
QG(NROW-1)=(QGX(NROW-1)+QG(NROW-1))/2.0
QW(NROW-1)=(QWX(NROW-1)+QW(NROW-1))/2.0

```

RETURN

ELSE IF(ITER.EQ.2) THEN

```

FACTOR=(GPOT(0)-SAVPHI)/(QG(1)*(GPOT(0)-GPOTX(1))/QGX(1)+

```

```

& GPOTX(1)-SAVPHI)
QG(1)=QG(1)*FACTOR
QG(NROW-1)=QG(NROW-1)*FACTOR
QW(NROW-1)=QW(NROW-1)*FACTOR
QGA1(1)=QG(1)
QGA1(NROW-1)=QG(NROW-1)
QWA1(NROW-1)=QW(NROW-1)

```

RETURN

ELSE IF(ITER.EQ.3) THEN

```

QGB1(1)=QGX(1)
QGB1(NROW-1)=QGX(NROW-1)
QWB1(NROW-1)=QWX(NROW-1)
QGA2(1)=(QGA1(1)+QGB1(1))/2.0
QGA2(NROW-1)=(QGA1(NROW-1)+QGB1(NROW-1))/2.0
QWA2(NROW-1)=(QWA1(NROW-1)+QWB1(NROW-1))/2.0
QG(1)=QGA2(1)
QG(NROW-1)=QGA2(NROW-1)
QW(NROW-1)=QWA2(NROW-1)

```

RETURN

```

ELSE
  QGB2(1)=QGX(1)
  QGB2(NROW-1)=QGX(NROW-1)
  QWB2(NROW-1)=QWX(NROW-1)
  QG(1)=(QGB1(1)*(QGA2(1)-QGA1(1))-QGA1(1)*(QGB2(1)-
& QGB1(1)))/(QGA2(1)-QGA1(1)-QGB2(1)+QGB1(1))
  QGA2(1)=QG(1)
  QG(NROW-1)=(QGB1(NROW-1)*(QGA2(NROW-1)-QGA1(NROW-1))
& -QGA1(NROW-1)*(QGB2(NROW-1)-QGB1(NROW-1)))/
& (QGA2(NROW-1)-QGA1(NROW-1)-QGB2(NROW-1)+QGB1(NROW-1))
  QGA2(NROW-1)=QG(NROW-1)
  QW(NROW-1)=(QWB1(NROW-1)*(QWA2(NROW-1)-QWA1(NROW-1))
& -QWA1(NROW-1)*(QWB2(NROW-1)-QWB1(NROW-1)))/
& (QWA2(NROW-1)-QWA1(NROW-1)-QWB2(NROW-1)+QWB1(NROW-1))
  QWA2(NROW-1)=QW(NROW-1)
END IF
RETURN
END

```

```

C-----
SUBROUTINE SOLUTIONEF (E,F,NROW,F3,GREL,WREL)
C-----

```

C COMPUTING COEFF. E AND F VALUES OF THE EQUATIONS

IMPLICIT DOUBLE PRECISION (A-H,P-Z)

```

DIMENSION E(1000),F(1000),G(1000),P(1000),R(1000),Sw(1000),
& SP(1000),GREL(1000),WREL(1000),QG(1000),QW(1000),GPOT(1000),
& WPOT(1000),POLD(1000),ROLD(1000)

```

```

DO I=2,NROW-1
  TEMP=(GREL(I-1)+GREL(I))*F3/2.0
  SAVE=(WREL(I-1)+WREL(I))/2.0
  E(I)=TEMP+SAVE
  F(I)=TEMP-SAVE

```

END DO

```

E(1)=F3*GREL(1)+WREL(1)
F(1)=F3*GREL(1)-WREL(1)
E(NROW)=F3*GREL(NROW-1)+WREL(NROW-1)
F(NROW)=F3*GREL(NROW-1)-WREL(NROW-1)
RETURN
END

```

```

C-----
SUBROUTINE SOLUTIONP (E,F,F4,SP,QG,QW,G,DXSQ,P,R,NROW)
C-----

```

IMPLICIT DOUBLE PRECISION (A-H,P-Z)

```

COMMON A,B,C,D
DIMENSION A(1000),B(1000),C(1000),D(1000)
DIMENSION E(1000),F(1000),G(1000),P(1000),R(1000),Sw(1000),
& SP(1000),GREL(1000),WREL(1000),QG(1000),QW(1000),GPOT(1000),
& WPOT(1000),POLD(1000),ROLD(1000)

```

```

P(0)=P(1)
P(NROW)=P(NROW-1)

```

```

DO I=1,NROW-1
  A(I)=E(I)
  B(I)=F4*SP(I)-E(I)-E(I+1)
  C(I)=E(I+1)
  G(I)=DXSQ*(QW(I)-QG(I))+F(I)*(P(I)-P(I-1))-
& F(I+1)*(P(I+1)-P(I))

  D(I)=F4*SP(I)*R(I)+G(I)

END DO
B(1)=B(1)+A(1)
B(NROW-1)=B(NROW-1)+C(NROW-1)
RETURN
END

```

 SUBROUTINE SOLUTIONR (E,F,GG,QW,DXSQ,R,NROW)

```

IMPLICIT DOUBLE PRECISION (A-H,P-Z)

COMMON A,B,C,D
DIMENSION A(1000),B(1000),C(1000),D(1000)
DIMENSION E(1000),F(1000),G(1000),P(1000),R(1000),Sw(1000),
& SP(1000),GREL(1000),WREL(1000),QG(1000),QW(1000),GPOT(1000),
& WPOT(1000),POLD(1000),ROLD(1000)

R(0)=R(1)
R(NROW)=R(NROW-1)

DO I=1,NROW-2
  A(I)=-E(I)
  B(I)=E(I)+E(I+1)
  C(I)=-E(I+1)
  D(I)=DXSQ*(QG(I)+QW(I))+F(I+1)*(R(I+1)-R(I))
& -F(I)*(R(I)-R(I-1))

END DO

B(1)=B(1)+A(1)

RETURN
END

```

 SUBROUTINE TRIDAG (M,J,V)

```

IMPLICIT DOUBLE PRECISION (A-H,P-Z)

COMMON A,B,C,D
DIMENSION A(1000),B(1000),C(1000),D(1000)
DIMENSION BETA(4000),GAMMA(4000),V(4000)

BETA(M)=B(M)
GAMMA(M)=D(M)/BETA(M)

DO I=M+1,J
  BETA(I)=B(I)-A(I)*C(I-1)/BETA(I-1)
  GAMMA(I)=(D(I)-A(I)*GAMMA(I-1))/BETA(I)

END DO

```

```

V(J)=GAMMA(J)
DO I=J-1,M,-1
  V(I)=GAMMA(I)-C(I)*V(I+1)/BETA(I)
END DO
RETURN
END

```

```

-----
C          SUBROUTINE GMIX (TMASS)
-----

```

```

C  TO CALCULATE THE GAS MIXTURE MASS TO BE USED IN GVISCO
C  SUBROUTINE

```

```

WRITE (*,*) 'ENTER THE METHANE FRACTION'
READ (*,*) X1

WRITE (*,*) 'ENTER THE ETHANE FRACTION'
READ (*,*) X2

WRITE (*,*) 'ENTER THE PROPANE FRACTION'
READ (*,*) X3

WRITE (*,*) 'ENTER THE BUTANE FRACTION'
READ (*,*) X4

M1=16.0
M2=30.0
M3=40.0
M4=50.0
M5=60.0

TMASS=M1*X1+M2*X2+M3*X3+M4*X4
RETURN
END

```

```

-----
C          SUBROUTINE GASVISO (TMASS,GDENSI,GVISO,TEMP)
-----

```

```

C  TO CALCULATE GAS MIXTURE VISCOSITY AS AT A SPECIFIED TEMP.
C  USING LEE'S ET AL RELATION

```

```

WRITE (*,*) 'ENTER THE AVERAGE TEMPERATURE IN KELVIN'
READ (*,*) TEMP

TEMPR=TEMP*1.8
GASDENSI=((GDENSI* 453)/(30*30*30))
CALL GMIX (TMASS)

OK=((9.4+.02*TMASS)*TEMPR**1.5)/(209+19*TMASS+TEMPR)
X=((3.5+(986/TEMPR))+.01*TMASS)
Y=(2.4-(.2*X))

```

```

C  GAS VISCOSITY IS NOW IN THE UNITS OF CENTPOISE

```

```

GVISO= (OK*EXP(X*(GASDENSI**Y)))/1E4
RETURN
END

```

```

C-----
C
C SUBROUTINE WVISCOSITY:
C TO CALCULATE WATER VISCOSITY AT AN AVERAGE TEMP.
C-----

SUBROUTINE WATERVISCOSITY (WVISCO,WDENSI)
C-----

WRITE(*,*) 'ENTER THE AVERAGE TEMPERATURE IN KELVINS'
READ (*,*) TEMP

TC=647.3
S=.552
TR=TEMP/TC

C WATER VISCOSITY IN CP UNITS
WVISCO1=(WDENSI**0.5)*10**S*(1/TR-1)/8.569

C WATER VISCOSITY IN G/CM.SEC UNITS
WVISCO=WVISCO1/100.

RETURN
END

C-----
C SUBROUTINE AVERAGE (NLITNO,PORO,PERM)
C-----

C TO CALCULATE AVERAGE PERMEABILITY AND POROSITY OF THE
C OVERLYING ROCKS

IMPLICIT DOUBLE PRECISION (A-H,P-Z)

PERM=0.0
PORO=0.0

DO J22=1,NLITNO
WRITE (*,*) 'ENTER FRACTION OF LITHOLOGY'
READ (*,*) XJ
WRITE (*,*) 'ENTER PERMEABILIT'
WRITE (*,*) 'ENTER POROSITY'

READ (*,*) TPERM,TPORO

TPERM=TPERM*XJ
PERM=TPERM+PERM

PORO=TPORO+PORO

END DO

AVPERM=PERM/NLITNO
AVPORO=PORO/NLITNO

RETURN
END
C-----

```

14.0 APPENDIX 3 - Equations

$$\bar{A}^{i+1} c_{n-1,j}^{i+1} + \bar{B}^{i+1} c_{n,j-1}^{i+1} + \bar{C}^{i+1} c_{n+1,j}^{i+1} + \bar{D}^{i+1} c_{n,j+1}^{i+1} + \bar{E}^{i+1} c_{n,j}^{i+1} = \text{RHS}$$

$$\bar{A}^{i+1} = \left[(\bar{A}\epsilon)_{n-1/2,j} \left[\frac{D_{r_{xx}}}{1/2(\Delta x_n + \Delta x_{n-1})} + v_{x_{n-1/2,j}} \right] + \bar{G} - \bar{H} \right]^{i+1}$$

$$\bar{B}^{i+1} = \left[(\bar{A}\epsilon)_{n,j-1/2} \left[\frac{D_{r_{zz}}}{1/2(\Delta z_j + \Delta z_{j-1})} + v_{z_{n,j-1/2}} \right] + \bar{F} - \bar{I} \right]^{i+1}$$

$$\bar{C}^{i+1} = \left[(\bar{A}\epsilon)_{n+1/2,j} \left[\frac{D_{r_{xx}}}{1/2(\Delta x_n + \Delta x_{n+1})} - v_{x_{n+1/2,j}} \right] - \bar{G} + \bar{H} \right]^{i+1}$$

$$\bar{D}^{i+1} = \left[(\bar{A}\epsilon)_{n,j+1/2} \left[\frac{D_{r_{zz}}}{1/2(\Delta z_j + \Delta z_{j+1})} - v_{z_{n,j+1/2}} \right] - \bar{F} + \bar{I} \right]^{i+1}$$

$$\bar{E} = -\bar{A} - \bar{B} - \bar{C} - \bar{D} + \left[(\bar{A}\epsilon v_z)_{n,j-1/2} - (\bar{A}\epsilon v_x)_{n+1/2,j} - (\bar{A}\epsilon v_z)_{n,j+1/2} \right] - \frac{v}{\Delta t} (\epsilon)$$

$$\text{RHS} = - \frac{V}{\Delta t} c_{n,j}^i (\epsilon_j^{i+1}) - (F^{i+1} + G^{i+1}) c_{n-1,j-1}^{i+1} + (H^{i+1} + f^{i+1}) c_{n-1,j+1}^{i+1} + \\ (f^{i+1} + G^{i+1}) c_{n+1,j-1}^{i+1} - (H^{i+1} + I^{i+1}) c_{n+1,j+1}^{i+1}$$

$$F = \frac{1}{2} \frac{(A \epsilon D_r)_{n-1/2,j}}{\Delta z_j + 1/2(\Delta z_{j+1} + \Delta z_{j-1})}$$

$$G = \frac{1}{2} \frac{(A \epsilon D_r)_{n,j-1/2}}{\Delta x_n + 1/2(\Delta x_{n-1} + \Delta x_{n+1})}$$

$$H = \frac{1}{2} \frac{(A \epsilon D_r)_{n,j+1/2}}{\Delta x_n + 1/2(\Delta x_{n-1} + \Delta x_{n+1})}$$

$$I = \frac{1}{2} \frac{(A \epsilon D_r)_{n+1/2,j}}{\Delta z_j + 1/2(\Delta z_{j-1} + \Delta z_{j+1})}$$